Development of an Early-Stage Decision Support Tool for Evaluating Building Performance Using I-DIFFER Systems

Master's Thesis

Dean Slatinac

Georgios Semertzakis

Department of the Built Environment

Aalborg University

4 May 2026

BUILD DEPARTMENT OF THE BUILT ENVIRONMENT

AALBORG UNIVERSITY

This document has been typeset using LaTeX with Overleaf as compiler, accessible through Aalborg University (AAU) using the official template (with modifications).

AALBORG UNIVERSITY
STUDENT REPORT

Department of the Built Environment
Aalborg University
https://www.en.build.aau.dk/

Title:
Development of an Early-Stage Decision Support Tool for Optimizing Building Performance Using I-DIFFER Systems

Theme:
Early-Stage Decision Support for Energy-Efficient Building Renovation

Project period:
Autumn 2024 – Spring 2026

Project group:
1

Participant(s):
Dean Slatinac
Georgios Semertzakis

Supervisor(s):
Lasse Rohde
Markus Schaffer
Olena K. Larsen

Pages (excl. appendices):
140

Date of completion:
4 May 2026

Abstract—

Abstract

This thesis develops a simplified hourly calculation framework for early-stage comparison of heating and cooling energy needs in traditional renovation solutions and the novel I-DIFFER concept. The framework is implemented in an Excel spreadsheet and combines heat balance calculations with mode-switching logic for pre-heating, cooling, and transparent insulation operation, supporting structured comparison of design alternatives before detailed simulation is performed.

The framework was validated in two stages: first against measurements from a full-scale double-skin façade test facility at Aalborg University, and second against a modified IDA-ICE reference model using the DRY10 climate dataset. The validation showed good agreement for pre-heating and cooling modes, while larger deviations occurred in transparent insulation mode.

Results indicate that I-DIFFER may reduce annual energy need under the investigated assumptions. However, detailed dynamic simulation remains necessary for final design decisions and system sizing.

The content of this report is available (with login) at `https://projekter.aau.dk/projekter/en/`

Contents

Abstract i

Abbreviations **vii**

Nomenclature **viii**

1 Introduction **1**
1.1 Background and motivation 1
1.2 Integrated facade and ventilation concept 2
1.3 Challenges in early-stage assessment 3
1.4 Problem framing and thesis scope 4

2 Literature Review **6**
2.1 Early-stage decision support in building renovation 6
2.2 Simplified energy calculation methods in early design 7
2.3 Temporal resolution and the case for simplified hourly methods . . 8
2.4 Double-skin facade: Energy behaviour and simplified assessment . . 9
2.4.1 Thermal behaviour of double-skin façades 9
2.4.2 Simplified DSF assessment methods and the BESTFACADE approach 11
2.4.3 Validation and limitations of simplified DSF methods 12
2.5 Diffuse ceiling ventilation 13
2.6 Integrated façade-ventilation renovation concepts: I-DIFFER 14
2.6.1 From separate renovation measures to integrated concepts . 14
2.6.2 I-DIFFER evidence and implications for simplified modelling 14
2.7 Synthesis, research gap, and thesis aim 16
2.7.1 Synthesis 16
2.7.2 Research gap and problem statement 16
2.7.3 Research question and thesis aim 17

3 Methodology and Framework Implementation **18**
3.1 Methodological basis and scope 18

3.2 Framework structure and comparative scenario definition 19
3.2.1 Inputs and boundary conditions 21
3.2.2 Outputs and comparison indicators 21
3.2.3 Comparative scenario definition 22
3.3 Simplified hourly calculation method 22
3.3.1 Transmission heat transfer 23
3.3.2 Ventilation heat transfer 23
3.3.3 Solar gains 25
3.3.4 Cavity temperature and outlet air temperature 26
3.3.5 Total heat gains and losses 28
3.3.6 Heating and cooling energy need 29
3.3.7 Methodological limitations of the calculation approach 31
3.4 Operation modes and control assumptions 31
3.4.1 Transparent insulation mode 33
3.4.2 Pre-heating mode 34
3.4.3 Cooling mode 34
3.4.4 Control assumptions in the framework 35
3.5 Spreadsheet implementation 38
3.6 Validation approach 39
3.7 Summary of methodological assumptions 41

4 Validation of the simplified hourly framework 44
4.1 Validation purpose and reference sources 44
4.2 Validation metrics and variables 45
4.3 Experimental validation 47
4.3.1 Pre-heating mode 50
4.3.2 Cooling mode 59
4.4 Dynamic simulation validation 69
4.4.1 Validation purpose and reference case 69
4.4.2 Validation variables, metrics, and period 70
4.4.3 Pre-heating mode 71
4.4.4 Cooling mode 79
4.4.5 Transparent insulation 88

5 Case Scenario 96
5.1 Case study building 96
5.2 Renovation scenarios 98
5.2.1 Baseline-unrenovated building 98
5.2.2 Traditional renovation 99
5.2.3 I-DIFFER concept 99
5.3 Framework input parameters 101
5.4 Operating mode assumptions - I-DIFFER 102

5.4.1 Pre-heating mode . . . 104
5.4.2 Transparent insulation mode . . . 104
5.4.3 Cooling mode . . . 104
5.5 Control parameter selection . . . 105
5.5.1 Sensitivity configurations . . . 105
5.5.2 Sensitivity results . . . 106
5.5.3 Final configuration selection . . . 109
5.6 Comparison indicators . . . 109
5.7 Framework simplifications . . . 110

6 Results 112
6.1 Overview . . . 112
6.2 Annual energy demand - south orientation . . . 113
6.3 Scenario comparison - south orientation . . . 115
6.3.1 Sensitivity of scenario comparison to control assumptions . . . 116
6.4 Monthly energy distribution . . . 119
6.5 I-DIFFER operating mode analysis . . . 121
6.6 Cooling season thermal analysis . . . 122
6.7 Cavity temperature behaviour . . . 123
6.8 Sensitivity analysis - DSF glazing properties and cavity depth . . . 124
6.9 Orientation sensitivity - east facade . . . 128

7 Discussion 131
7.1 Framework suitability for early-stage comparison . . . 131
7.2 Heating and cooling trade-off . . . 132
7.3 Role of solar shading . . . 133
7.4 Orientation sensitivity . . . 133
7.5 Delimitation . . . 134

8 Conclusion 135

Bibliography 137

A Supplementary experimental validation summary tables 141

B Calculation equations used in the simplified framework 143
B.1 Transmission heat transfer . . . 143
B.2 Ventilation heat transfer . . . 144
B.3 Natural ventilation in the DSF cavity . . . 144
B.4 Infiltration heat transfer . . . 145
B.5 Heat recovery in mechanical ventilation . . . 146
B.6 Total heat losses . . . 146
B.7 Solar radiation entering the DSF cavity . . . 146

B.8 Direct solar gains to the room 147
B.9 Heat gains affecting the DSF cavity 147
B.10 Mean DSF cavity temperature 148
B.11 Outlet temperature from the DSF cavity 148
B.12 Total heat gains 148
B.13 Heating energy need 149
B.14 Cooling energy need 150
B.15 Building time constant 151
B.16 Annual energy indicators 151

C Detail input parameters for all scenarios 153

Abbreviations

AAU	Aalborg University
BESTFACADE	Best Practice for Double Skin Facades
BR18	Danish Building Regulations 2018
DCV	Diffuse ceiling ventilation
DSF	Double-skin facade
DRY10	Danish Design Reference Year 2010
HVAC	Heating, ventilation, and air conditioning
I-DIFFER	Integrated double-skin facade and diffuse ceiling ventilation concept
IDA-ICE	IDA Indoor Climate and Energy
MAE	Mean absolute error
ORM30	30-day running mean outdoor temperature
RMSE	Root mean square error
SCM	Simple Calculation Method
SCM-CL	Simple Calculation Method - Cooling mode
SCM-PH	Simple Calculation Method - Pre-heating mode
SCM-TI	Simple Calculation Method - Transparent insulation mode

Nomenclature

Symbol	Description	Unit
A_i	Area of element i	m^2
U_i	Thermal transmittance of element i	$W/(m^2K)$
H_T	Transmission heat transfer coefficient	W/K
H_v	Ventilation heat transfer coefficient	W/K
ρ_a	Air density	kg/m^3
c_a	Specific heat capacity of air	J/(kg K)
q_v	Ventilation airflow rate	m^3/s
$H_{V,ue}$	Ventilation heat transfer coefficient between cavity and outdoor air	W/K
h_v	Hellström ventilation coefficient	$W/(K^{1.5})$
$T_{c,\text{mean}}$	Mean cavity temperature	°C
T_e	Outdoor air temperature	°C
$T_{e,\text{abs}}$	Absolute outdoor air temperature	K
T_i	Indoor air temperature	°C
$T_{c,\text{in}}$	Cavity inlet temperature	°C
$T_{c,\text{out}}$	Cavity outlet temperature	°C
g	Gravitational acceleration	m/s^2
H_{cav}	Cavity height	m
ξ_{tot}	Total pressure-loss coefficient	-
ρ_u	Air density in the cavity	kg/m^3
c_p	Specific heat capacity of air	J/(kg K)
ΔT_{rel}	Relative temperature rise	-
A_{cav}	Characteristic cavity flow area	m^2
$H_{V,iu}$	Ventilation heat transfer coefficient between room and cavity	W/K
q_{50}	Air permeability at 50 Pa	$m^3/(h\ m^2)$
A_{env}	Exposed envelope area	m^2
$\dot{V}_{\text{inf}}$	Infiltration airflow rate	m^3/s
H_{inf}	Infiltration heat transfer coefficient	W/K
$H_{v,\text{eff}}$	Effective ventilation heat transfer coefficient after heat recovery	W/K
η_{hr}	Heat recovery efficiency	-
$F_{F,ue}$	Frame correction factor for external glazing	-
A_{ue}	External glazed area	m^2
$g_{\text{eff},ue}$	Effective solar transmittance of the external transparent component	-
I_s	Solar radiation	W/m^2
$g_{\text{eff},iu}$	Effective solar transmittance of the internal transparent component	-
$\tau_{e,ue}$	Solar transmittance of external glazing	-
t	Time step	h
ϕ_s^{total}	Total solar radiation entering the DSF	W
ϕ_s^{room}	Direct solar heat gains to the room	W
ϕ_s^c	Heat flow affecting the cavity	W
ϕ_h^c	Internal gains assigned to the cavity	W
H_t^{r-c}	Transmission heat transfer coefficient between room and cavity	W/K

Symbol	Description	Unit
H_v^{r-c}	Ventilation heat transfer coefficient between room and cavity	W/K
H_i^{r-c}	Additional heat transfer coefficient between room and cavity	W/K
H_t^{c-o}	Transmission heat transfer coefficient between cavity and outdoor environment	W/K
H_v^{c-o}	Ventilation heat transfer coefficient between cavity and outdoor environment	W/K
H_i^{c-o}	Additional heat transfer coefficient between cavity and outdoor environment	W/K
Q_{ls}	Total heat losses	W
Q_{tr}	Transmission losses	W
Q_v	Ventilation-related losses	W
Q_{gn}	Total heat gains	W
Q_{int}	Internal gains	W
Q_{sol}	Solar gains	W
τ	Time constant	h
C_m	Effective internal heat capacity	J/K
H_m	Total heat loss coefficient	W/K
$Q_{h,\text{nd}}$	Heating energy need	kWh
$Q_{c,\text{nd}}$	Cooling energy need	kWh
E_{base}	Total annual energy demand of baseline	kWh/m^2
E_{scen}	Total annual energy demand of scenario	kWh/m^2
E_{ref}	Total annual energy demand of reference scenario	kWh/m^2
ΔE	Energy difference between scenarios	kWh/m^2
θ_{rm}	Running mean outdoor temperature	°C
$\theta_{\text{ed}-1}$	Daily mean outdoor temperature of previous day	°C
$\theta_{\text{ed}-2}$	Daily mean outdoor temperature two days before	°C
$\theta_{\text{ed}-3}$	Daily mean outdoor temperature three days before	°C
α	Weighting constant for running mean temperature	-
ORM30$_t$	30-day running mean outdoor temperature at timestep t	°C
$T_{e,t-k}$	Outdoor air temperature k hours before timestep t	°C

Chapter 1

Introduction

1.1 Background and motivation

Buildings are closely linked to the global energy and climate challenge, since their operation requires substantial energy and contributes to greenhouse gas emissions. Improving the existing building stock is therefore an important step towards a more sustainable built environment (European Commission, 2020; IEA, 2023). As a result, engineers and architects are increasingly exploring innovative technologies and design strategies to improve energy efficiency, occupant comfort, and environmental sustainability in buildings.

In Europe, building renovation is increasingly important for reducing energy demand, limiting emissions, and improving the quality of existing buildings. Many buildings were constructed before today's energy requirements were introduced, which means that a large part of the building stock still has limited energy performance and indoor environmental quality (European Commission, 2020). Renovation is therefore expected to remain an important focus in the transition towards a more efficient and sustainable built environment.

Within this context, school and office buildings are especially relevant. These building types are strongly affected by occupancy patterns, internal heat gains, ventilation demand, and solar gains through the facade. Renovation decisions in such buildings, therefore, affect not only energy performance, but also indoor environmental quality and the conditions in which people learn and work. These decisions are often made during the early design stage, when information is limited, and several alternatives must be assessed within a short time frame (Attia et al., 2012; Nielsen et al., 2016; Thuvander et al., 2012).

At this stage, the objective is usually not to predict final building performance in

detail, but to compare alternatives in a transparent and consistent way (Nielsen et al., 2016). This creates a methodological challenge. Detailed building performance simulation can represent complex thermal behaviour, airflow, and control strategies, but it requires extensive input data, considerable modelling effort, and specialist knowledge. Simpler methods are easier to use in early-stage design, but they may overlook important interactions when performance depends on time-varying and coupled processes (Kalema et al., 2008; Negendahl & Nielsen, 2015).

1.2 Integrated facade and ventilation concept

A limitation of many conventional renovation strategies is that facade improvements and ventilation upgrades are often treated as separate measures, even though their thermal effects are closely related. In response, greater attention has been paid to integrated approaches in which facade and ventilation systems are designed and assessed together.

One such concept is the integration of a double-skin facade and diffuse ceiling ventilation, referred to in this thesis as the I-DIFFER concept. A double-skin facade consists of two facade layers separated by a cavity. Depending on the façade configuration and operating mode, this cavity influences solar gains, heat transfer, and airflow behaviour (Kalyanova, 2008; Saelens et al., 2003). Diffuse ceiling ventilation is a ventilation principle in which supply air enters the room through a permeable ceiling surface at low velocity. This can support good thermal comfort and effective heat removal, particularly in spaces with relatively high internal loads such as classrooms and offices (Zhang, 2016; Zhang et al., 2014).

In the I-DIFFER concept, these two systems are combined into one integrated façade-ventilation solution. This means that facade and ventilation behaviour cannot be assessed independently. Solar gains and heat exchange in the façade affect the thermal condition of the air supplied to the room, while the ventilation strategy affects how heat is distributed and removed inside the space. The performance of the concept, therefore, depends on the interaction between the two subsystems rather than on the isolated performance of each subsystem alone (Bugenings et al., 2022; Schaffer et al., 2023).

Figure 1.1 illustrates the main operating principles of the I-DIFFER concept is considered in this thesis. In transparent insulation mode, all openings in the DSF cavity and bypass are closed, and the ventilation system is off. In this mode, the closed cavity creates an intermediate thermal zone between the outdoor and indoor environments. When solar radiation enters the cavity, the air temperature in this zone can increase, thereby reducing the temperature difference between the cavity and the indoor space during cold periods.

In pre-heating mode, the ventilation system is on, and the airflow through the DSF cavity and diffuse ceiling plenum is mechanically driven by the exhaust ventilation system. Outdoor air enters the DSF cavity at the bottom, is warmed as it passes through the cavity, and then enters the diffuse ceiling plenum before being supplied to the classroom. In cooling mode, the supply air is mechanically driven through the bypass opening and into the diffuse ceiling plenum. At the same time, the DSF cavity is naturally ventilated through its external openings by wind and buoyancy, which helps remove solar heat from the facade cavity before it is transferred to the classroom (Bugenings et al., 2022; Zhang et al., 2023).

Because of this coupling between facade and ventilation processes, integrated concepts such as I-DIFFER are not well suited to methods that treat the two subsystems separately. Their assessment, therefore, requires an approach that can represent both their individual behaviour and their interaction.

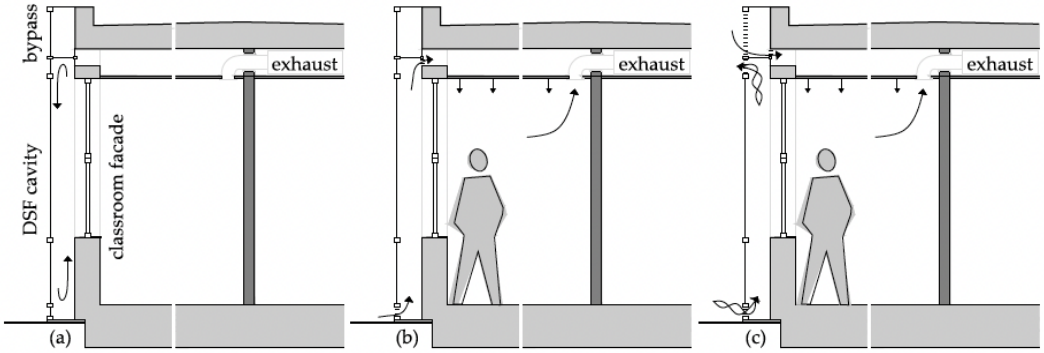

Figure 1.1: Illustration of the integrated DSF-DCV solution: (a) transparent insulation mode, (b) pre-heating mode, and (c) cooling mode. Adapted from Schaffer et al., 2023.

1.3 Challenges in early-stage assessment

Despite the potential of integrated facade-ventilation concepts, their early-stage assessment remains difficult. At this point in the design process, decisions often need to be made before system details, control strategies, and exact boundary conditions are fully defined. This creates a tension between the need for rapid comparative assessment and the complexity of the underlying physical processes.

Detailed building performance simulation tools are commonly used to analyse complex systems such as double-skin facades and integrated ventilation strategies. These tools can represent dynamic interactions among thermal zones, airflow, and control strategies with relatively high accuracy (Hu et al., 2023). However, they typically require extensive input data, specialised expertise, and significant modelling effort. This limits their applicability in early-stage design, where rapid comparison

of multiple design options is often required.

Simplified energy calculation methods are therefore widely used in early design. These methods reduce modelling effort by relying on simplified representations of heat transfer, solar gains, and ventilation processes. For many conventional renovation scenarios, such simplifications can support transparent comparison between alternatives. However, simplified methods often rely on steady-state or low-resolution assumptions and may not adequately represent time-dependent effects such as variable solar radiation, airflow-driven heat exchange, and short-term thermal interactions (Kalema et al., 2008; Negendahl & Nielsen, 2015).

This limitation becomes particularly important in integrated concepts such as I-DIFFER, where performance depends on the coupling between facade behaviour and ventilation processes. Methods that treat these subsystems separately may not capture the dominant interactions affecting heating and cooling energy needs. At the same time, detailed simulation approaches may be too complex for early-stage applications. This creates a methodological gap between available detailed models and the practical needs of early-stage design.

1.4 Problem framing and thesis scope

The assessment of integrated facade-ventilation concepts remains challenging in early-stage renovation design, where key decisions must often be made with limited input data and without detailed knowledge of system operation, control strategies, or exact boundary conditions. In this context, approaches are needed that can support comparison between alternatives while remaining transparent and manageable in terms of input requirements.

This challenge is particularly relevant for the I-DIFFER concept, where the interaction between the double-skin facade and diffuse ceiling ventilation plays an important role in heating and cooling performance. Approaches that treat facade and ventilation systems separately may therefore be insufficient for early-stage comparison of integrated concepts and conventional renovation solutions.

The thesis does not aim to replace detailed building performance simulation or to provide a precise prediction of full building performance. Instead, it focuses on whether a simplified hourly calculation framework can support transparent early-stage comparison of heating and cooling energy needs between traditional renovation solutions and the I-DIFFER concept.

The following chapter reviews the literature on early-stage decision support, simplified energy calculation methods, double-skin facades, diffuse ceiling ventilation, and integrated facade-ventilation concepts. Based on this review, the research gap,

problem statement, research question, and thesis aim are defined.

Chapter 2

Literature Review

2.1 Early-stage decision support in building renovation

Decisions made during the early stages of building renovation projects have a major influence on long-term energy performance, environmental impact, and economic feasibility. Research has shown that many parameters affecting building performance are determined during the early phases of design, even though only limited information is typically available at that stage (Attia et al., 2012). This challenge is particularly relevant in renovation projects, where incomplete documentation of the existing building, uncertain building conditions, and practical constraints increase the complexity of evaluating design alternatives. Renovation processes are therefore often characterised by greater uncertainty than new construction and require careful assessment during the preliminary investigation phase (Thuvander et al., 2012).

In this context, early-stage design support is less concerned with producing highly detailed predictions and more focused on enabling comparison between alternative renovation concepts. Decision-support approaches applied in early-stage renovation must therefore be capable of operating with limited input data while still providing useful insights for decision-makers. Reviews of renovation decision-support methods highlight that such approaches should support the generation and evaluation of alternative strategies and assist stakeholders in assessing the potential effects of renovation measures (Nielsen et al., 2016).

Despite the availability of different sustainability assessment frameworks and design methods, relatively few approaches have been developed specifically to support decision-making in renovation projects during the early design stages (Jensen et al., 2018). As a result, there remains a need for simplified approaches that can

support comparison between alternative renovation concepts while working with the limited information typically available during concept design.

Based on the literature, several requirements can be identified for approaches intended for early-stage renovation design. First, they should rely on input data that are typically available during the early design phase. Second, they should enable rapid iteration across multiple renovation options to support exploration of alternatives. Third, the assumptions underlying the calculations should remain transparent so that results can be interpreted appropriately. Finally, outputs should allow consistent comparison between conventional renovation solutions and more integrated or innovative approaches (Nielsen et al., 2016).

In this thesis, the primary focus is on indicators of heating and cooling performance, which are strongly influenced by facade design, solar gains, and ventilation-related heat removal. These indicators enable examination of whether integrated facade-ventilation concepts, such as I-DIFFER, may offer advantages over representative conventional renovation solutions under comparable boundary conditions. Consequently, the objective of simplified modelling in this thesis is not precise prediction, but transparent and consistent comparison between competing renovation strategies.

2.2 Simplified energy calculation methods in early design

Simplified energy calculation methods are widely used in early design because they require less modelling effort and fewer input data than detailed building performance simulation tools. Their purpose is not to describe all physical processes in full detail, but to estimate energy-related behaviour using a reduced number of variables and assumptions. In early-stage design, this is often appropriate because the main objective is to compare alternatives, identify trends, and screen concepts rather than to produce precise final-design predictions (Negendahl & Nielsen, 2015).

Among the most common simplified approaches are steady-state and monthly energy balance methods. These methods estimate heating and cooling demand using averaged climatic conditions and simplified descriptions of heat transfer, solar gains, internal loads, and ventilation heat exchange. Such approaches are widely used in regulatory calculations and early-stage design because of their limited input requirements and computational simplicity (DS EN ISO 13790, 2008; Kalema et al., 2008).

Studies show that simplified methods can provide acceptable estimates for relatively simple buildings and conventional renovation scenarios. However, their reliability decreases when buildings are strongly affected by solar gains, thermal

mass, or complex ventilation behaviour. In such cases, simplified methods may not adequately capture the dynamic interactions among solar radiation, internal heat gains, thermal storage, and ventilation heat exchange (Kalema et al., 2008).

For the present thesis, the key question is therefore not whether simplified methods are generally feasible, but whether they can preserve the dominant physical mechanisms governing the I-DIFFER concept's performance while remaining suitable for early-stage comparison. The literature suggests that this depends on several issues, including the temporal resolution of the calculation method, the simplified representation of double-skin façade behaviour, the simplified representation of ventilation-related heat removal, and the coupling of facade and ventilation processes within a single framework.

2.3 Temporal resolution and the case for simplified hourly methods

Temporal resolution is important in building energy modelling because many thermal processes vary significantly over short time scales. Solar radiation, internal heat gains, and ventilation-related heat exchange can vary substantially throughout the day, directly affecting heating and cooling demand. Simplified methods based on monthly or seasonal averages may therefore overlook short-term effects that contribute to the risk of overheating and cooling load peaks (Negendahl & Nielsen, 2015).

Comparisons between simplified methods and more detailed simulation approaches show that the accuracy of simplified calculations depends strongly on temporal resolution. Monthly methods can provide reasonable estimates of annual heating demand in relatively simple cases, but their performance decreases when dynamic effects such as solar gains, thermal mass, and variable ventilation become important (Kalema et al., 2008).

This limitation becomes especially relevant in buildings with large glazed facades or adaptive envelope systems. In such cases, solar gains may vary substantially during the day depending on weather conditions, facade orientation, and shading behaviour. Because solar radiation can cause rapid changes in surface temperatures and internal heat gains, methods based on monthly averages may underestimate peak cooling demand and short-term overheating conditions. Research on double-skin façades has also shown that highly glazed façade systems can experience summer overheating due to the combined effect of outdoor temperature, solar gains, and internal loads (Gratia & De Herde, 2007; Saelens et al., 2008).

For these reasons, simplified hourly or quasi-hourly calculation methods can be

understood as a practical compromise between steady-state approaches and detailed dynamic simulation. They allow short-term variations in solar gains, ventilation behaviour, and internal loads to be represented while keeping the modelling structure relatively simple and the input requirements limited. This makes them suitable for early-stage decision support, where transparency and rapid comparison are important (Negendahl & Nielsen, 2015).

In the context of the I-DIFFER concept, temporal resolution is especially relevant because the system relies on the interaction between facade behaviour and ventilation-driven heat removal. Solar gains influence the thermal conditions within the double-skin facade cavity, while diffuse ceiling ventilation affects the removal and distribution of internal heat loads (Bugenings et al., 2022; Hu et al., 2023). Simplified hourly modelling may therefore provide a useful balance between representing these dynamic processes and maintaining the simplicity required for early-stage comparison.

2.4 Double-skin facade: Energy behaviour and simplified assessment

2.4.1 Thermal behaviour of double-skin façades

Double-skin facades are facade systems comprising two glazing layers separated by an air cavity. The cavity may be naturally or mechanically ventilated and can influence the thermal interaction between the outdoor environment and the indoor space. Because of their ability to regulate solar gains, ventilation, and heat transfer through the building envelope, DSFs have been widely investigated in office and educational buildings, where facade performance strongly influences overall energy use and indoor comfort (Kalyanova, 2008; Poirazis, 2006).

Several DSF typologies have been identified in the literature, mainly distinguished by the configuration of the cavity and the airflow path within the facade system. Common typologies include box-window, corridor, shaft-box, and multi-storey facades. These typologies differ in cavity segmentation, airflow connectivity, and ventilation strategies, which significantly influence thermal behaviour and energy performance (Kalyanova, 2008). Figure 2.1 summarises common DSF typologies and principal ventilation modes reported in the literature. These variations are important because cavity configuration and airflow path strongly influence the thermal behaviour of the façade system.

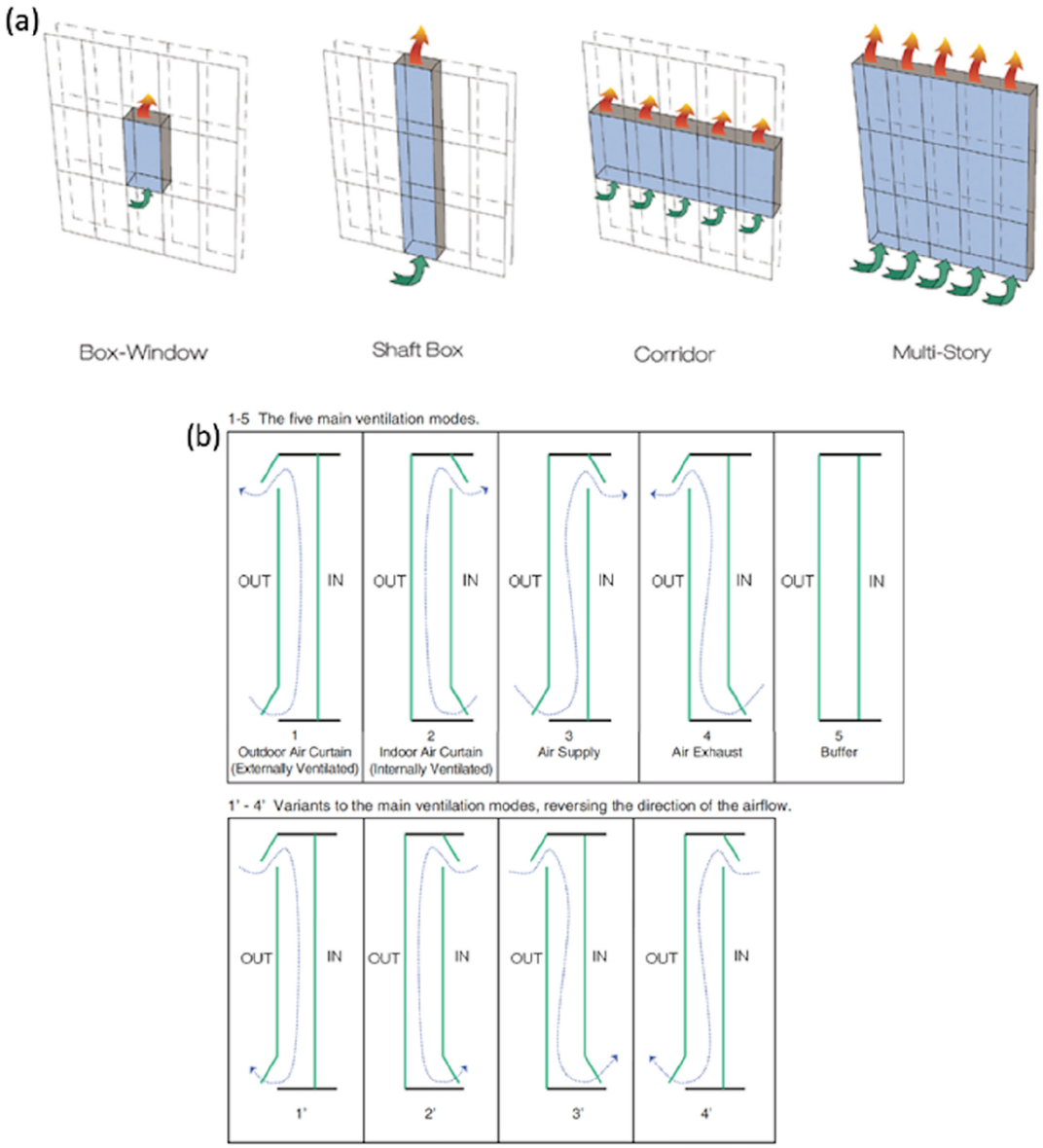

Figure 2.1: Overview of common double-skin facade typologies (a) and principal ventilation modes (b) reported in the literature. The figure illustrates how cavity configuration and airflow path may vary between DSF systems, which in turn influences thermal behaviour and energy performance. Adapted from Pelletier et al., 2023.

The energy performance of DSFs is governed by the interaction between solar radiation, heat transfer through the facade layers, and airflow within the cavity. Solar gains absorbed in the cavity can raise the air temperature, which may reduce heat losses during winter but increase cooling demand during summer, depending on the ventilation strategy and operating mode. Consequently, DSF thermal behaviour

depends strongly on climate conditions, façade orientation, glazing properties, and cavity airflow patterns (Kalyanova, 2008; Saelens et al., 2003).

Because of these interacting processes, DSF performance cannot be evaluated solely by transmission heat losses through the facade. The enthalpy change of the air flowing through the cavity and its interaction with solar gains must also be considered. Previous research has shown that certain DSF configurations can improve heating performance in winter but may increase cooling demand in summer if solar gains are not adequately controlled (Saelens et al., 2008).

Investigations of naturally ventilated DSFs further highlight that facade performance is highly sensitive to environmental conditions such as solar radiation, wind exposure, and façade orientation, which can strongly influence cavity temperatures and the risk of summer overheating (Gratia & De Herde, 2004a, 2004b).

More recent review studies emphasise that DSF performance also depends strongly on design parameters, including cavity geometry, glazing properties, ventilation openings, and operational strategies. Because these parameters vary widely between building designs and climatic contexts, DSF performance cannot be generalised without considering the specific facade configuration and operating conditions (Jankovic & Goia, 2021; Preet et al., 2022).

Taken together, these findings show that DSF behaviour is governed by complex interactions between solar gains, airflow dynamics, and heat transfer processes. As a result, assessing the energy performance of DSFs requires modelling approaches that preserve the dominant physical mechanisms while remaining practical enough for design use.

2.4.2 Simplified DSF assessment methods and the BESTFACADE approach

Although detailed building performance simulation models can represent DSF behaviour with relatively high accuracy, they typically require complex airflow modelling, detailed facade geometry, and extensive input data. Such modelling effort is often impractical in early-stage design, when facade properties, operating strategies, and boundary conditions remain uncertain. As a result, simplified calculation methods have been developed to support preliminary assessment of DSF performance.

One of the most relevant simplified approaches is the Simple Calculation Method (SCM) developed within the BESTFACADE project. The purpose of this method was to provide designers with a practical approach for evaluating the energy performance of buildings with double-skin facades during early design stages without requiring detailed simulation models (BESTFACADE, 2007).

In the SCM approach, the facade cavity is represented using simplified assumptions about cavity temperature and airflow behaviour. The cavity is treated as an intermediate thermal zone, or unheated glazed space, and the thermal interaction between the cavity and the conditioned indoor zone is estimated through simplified heat-balance relationships. Airflow in the cavity is represented through approximate air-change rates depending on facade typology and operating conditions (BESTFACADE, 2007; Marszal et al., 2009).

This simplified representation reduces modelling complexity while still capturing the dominant drivers of façade performance. Instead of modelling detailed airflow dynamics, the method focuses on effective cavity temperature, solar gains, and simplified ventilation behaviour as the main factors influencing heating and cooling demand. As such, the SCM provides an important methodological basis for early-stage DSF assessment and is particularly relevant for the present thesis.

2.4.3 Validation and limitations of simplified DSF methods

The validity of simplified DSF calculation methods has been examined in several studies. Marszal et al., 2009 evaluated the SCM approach by comparing its predictions with measurements from a DSF test facility. Their results showed that the simplified method can provide reasonable estimates of façade performance under many conditions, which supports its use as an early-stage assessment method.

However, the validation study also revealed important limitations. In particular, the method may produce significant deviations under strong solar radiation, where simplified assumptions about the cavity temperature distribution can lead to overestimation of cooling loads. This suggests that solar-driven cavity behaviour is one of the most sensitive aspects of simplified DSF modelling (Marszal et al., 2009).

More recent validation and inter-software comparison studies reinforce this conclusion. Research shows that cavity air temperature remains one of the most difficult DSF variables to predict accurately and that results are highly sensitive to assumptions regarding glazing heat capacity, airflow openings, and convective heat transfer within the cavity (Catto Lucchino et al., 2021; Gennaro et al., 2023).

For the present thesis, the BESTFACADE SCM approach provides an important methodological basis for simplified DSF modelling. Nevertheless, existing simplified methods primarily address the façade subsystem in isolation and do not explicitly model its interaction with indoor ventilation strategies such as diffuse ceiling ventilation. Consequently, additional modelling considerations are required when evaluating integrated façade-ventilation concepts such as I-DIFFER.

2.5 Diffuse ceiling ventilation

Diffuse ceiling ventilation (DCV) is a concept in which supply air is introduced through a suspended ceiling with low supply momentum. Because air enters the room over a large ceiling area rather than through a concentrated diffuser, the resulting airflow is strongly influenced by buoyancy generated by internal heat sources. As a result, DCV differs from conventional mixing ventilation in both air distribution and heat-removal behaviour (Zhang et al., 2014). Figure 2.2 illustrates the principle of diffuse ceiling ventilation, in which supply air enters the room through the ceiling and is distributed at low velocity over a large surface area. This airflow pattern is central to the thermal and ventilation behaviour of DCV systems.

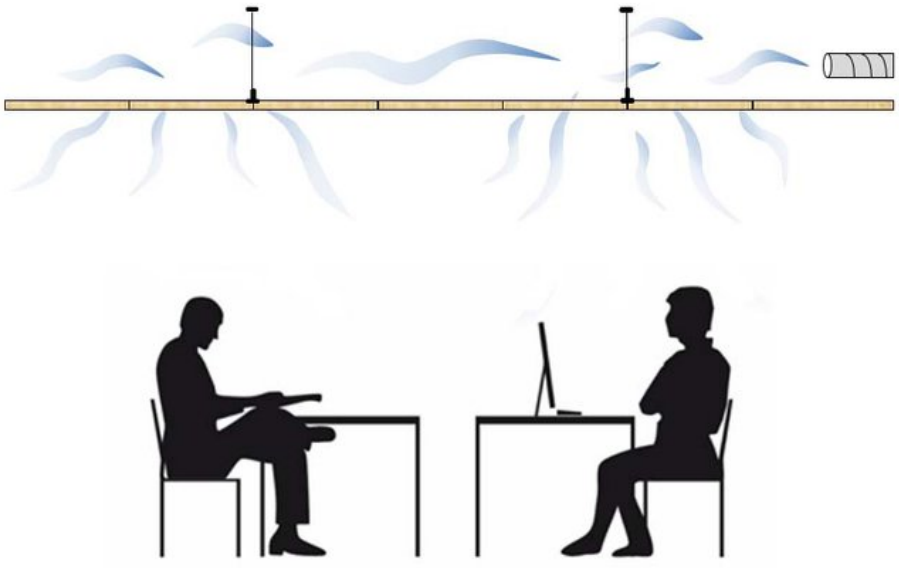

Figure 2.2: Schematic illustration of diffuse ceiling ventilation, showing supply air entering through the ceiling and diffusing into the occupied zone at low velocity. Adapted from Zhang, 2016.

Review studies show that DCV can provide good thermal comfort, low draught risk, low pressure drop, and reduced fan energy use, while also offering potential advantages in spaces with relatively high internal heat loads, such as offices and classrooms (Zhang et al., 2014).

The energy relevance of DCV lies in the fact that its performance is determined not only by ventilation rate but also by the effectiveness with which heat is removed from the occupied space. Because the system depends on low-momentum supply and buoyancy-driven transport, room-air temperatures may not always be well represented by a single, fully mixed-zone temperature. Internal heat sources, ceil-

ing configuration, and plenum design can all affect airflow pattern, temperature distribution, and the removal of sensible heat from the room (Zhang, 2016; Zhang et al., 2014).

For early-stage decision-support approaches, the objective is not to simulate detailed indoor airflow patterns but to capture the main thermal effects of ventilation on heating and cooling demand. In this context, DCV can be represented through simplified parameters that reflect heat removal, air distribution, or non-uniform indoor temperature behaviour. However, simplified approaches often treat ventilation and facade behaviour as separate processes. In integrated facade-ventilation concepts such as I-DIFFER, this is a limitation because the interaction between the double-skin facade and the ventilation system plays an important role in overall heating and cooling performance. Simplified modelling therefore needs to represent not only the individual behaviour of DSF and DCV systems, but also their interaction within the building energy balance (Bugenings et al., 2022; Hu et al., 2023).

2.6 Integrated façade-ventilation renovation concepts: I-DIFFER

2.6.1 From separate renovation measures to integrated concepts

Traditional renovation strategies often treat facade improvement and ventilation upgrading as separate interventions, for example, through insulation, glazing replacement, or HVAC modernisation. Although these measures can improve building performance, they are typically not designed or assessed as a coupled facade-ventilation concept in which facade heat transfer, solar gains, and indoor heat removal are explicitly coordinated. Integrated renovation concepts such as I-DIFFER take a different approach by treating the facade and ventilation systems as interacting subsystems whose combined operation influences overall performance.

In such systems, solar gains through the facade influence indoor heat loads, while indoor airflow and ventilation strategy influence how those loads are distributed and removed. As a result, façade and ventilation behaviour cannot be assessed independently without losing important aspects of system performance. In I-DIFFER, the double-skin facade and diffuse ceiling ventilation are intentionally combined so that facade heat transfer and solar control work together with indoor air distribution and heat removal (Bugenings et al., 2022).

2.6.2 I-DIFFER evidence and implications for simplified modelling

The I-DIFFER concept is described in the literature as an integrated renovation solution in which the double-skin façade acts as an adaptive solar and thermal

buffer, while the diffuse ceiling ventilation system manages the remaining indoor heat loads through low-velocity ceiling supply. Bugenings et al., 2022 provide a simulation-based comparison between I-DIFFER and a traditional renovation package in a school classroom case. Their results indicate that the integrated concept can reduce primary energy demand while maintaining acceptable indoor environmental quality. However, the assessment is based on a detailed IDA-ICE simulation that includes facade zones, openings, leakage paths, and ventilation behaviour, making it a valuable benchmark but less directly applicable as an early-stage design method.

Schaffer et al., 2023 extend this work by examining the robustness of the concept under different orientations, facade properties, and climate conditions. Their results show that the relative performance of I-DIFFER and traditional renovation strategies varies significantly with orientation, facade properties, and climate. This suggests that an early-stage framework would benefit from supporting scenario-based comparison rather than relying on a single fixed prediction.

Hu et al., 2023 further shows how the concept can be represented in EnergyPlus using multiple thermal zones, inter-zone airflow exchanges, and EMS-based control logic. This study is important because it illustrates how the coupling between facade and ventilation is treated in detailed simulation practice.

Experimental work also supports the physical basis of the concept. Studies on integrated DSF-DCV operation report winter heat-recovery effects, summer heat-removal behaviour in the facade cavity, and the importance of thermal mass and operating mode (Zhang et al., 2023). Together, these studies form an evidence chain consisting of comparative simulation, robustness analysis, detailed implementation, and experimental investigation. They also identify the main thermal processes that should be preserved in a simplified representation of I-DIFFER, namely solar-driven DSF behaviour, cavity airflow and heat exchange, and simplified control logic for heating and cooling operation.

At the same time, the current literature evaluates these processes mainly through detailed multi-zone building performance simulation models and experimental setups, which require extensive input data and modelling expertise (Bugenings et al., 2022; Hu et al., 2023; Schaffer et al., 2023; Zhang et al., 2023). No published early-stage decision-support method identified in the reviewed literature appears to assess I-DIFFER with limited input data while explicitly representing the dynamic interaction between the facade and ventilation subsystems. This is the key limitation that motivates the present study.

2.7 Synthesis, research gap, and thesis aim

2.7.1 Synthesis

Based on the reviewed studies, early-stage renovation design requires approaches that can support comparison between alternative concepts under conditions of limited input data and uncertainty. Simplified modelling is therefore important, but its usefulness depends on whether the dominant thermal processes influencing heating and cooling performance are preserved. Traditional steady-state and monthly methods are often suitable for conventional renovation measures, but they are less effective in capturing dynamic behaviour such as time-varying solar gains (Kalema et al., 2008; Negendahl & Nielsen, 2015).

At the same time, the literature indicates that both double-skin facades and diffuse ceiling ventilation can improve building performance. Research on DSF, particularly the BESTFACADE/SCM method, shows that facade behaviour can be simplified into effective thermal variables suitable for early-stage assessment (BESTFACADE, 2007; Marszal et al., 2009). The literature on I-DIFFER further shows how DSF and DCV may operate as an integrated renovation concept. However, the available studies are primarily based on detailed simulations and experiments and do not provide a practical approach for early-stage comparative assessment (Bugenings et al., 2022; Hu et al., 2023; Schaffer et al., 2023; Zhang et al., 2023).

Taken together, the reviewed literature provides knowledge about the individual subsystems and detailed benchmark studies of their combined operation, but it does not identify a simplified coupled framework for early-stage comparison between the I-DIFFER concept and traditional renovation solutions.

2.7.2 Research gap and problem statement

Based on this synthesis, the main gap in the literature is the lack of a simplified early-stage framework for comparing heating and cooling energy needs between traditional renovation solutions and the I-DIFFER concept, while explicitly representing the interaction between facade behaviour and ventilation-related heat removal.

This gap is particularly relevant in early-stage design, where designers and engineers need approaches that can support comparison between alternatives without requiring the level of detail associated with full building performance simulation. Existing simplified methods are generally not designed for integrated facade–ventilation concepts, whereas existing studies on I-DIFFER rely primarily on detailed simulations and experiments. As a result, designers currently lack a transparent, early-stage method to compare integrated facade–ventilation concepts

with traditional renovation solutions under consistent assumptions and comparable boundary conditions.

2.7.3 Research question and thesis aim

Based on the research gap identified above, the thesis addresses the following research question:

How can a simplified hourly calculation framework be developed for early-stage comparison of heating and cooling energy needs in traditional renovation solutions and the I-DIFFER concept?

To address this question, this thesis aims to develop and examine a simplified hourly calculation framework for early-stage comparisons of heating and cooling energy needs between traditional renovation solutions and the I-DIFFER concept.

The contribution of the thesis is a simplified comparative framework intended for early-stage use, rather than a detailed predictive model of full building performance. The framework is intended to operate with limited input data while representing the dominant thermal processes that influence comparative performance. Implemented as a spreadsheet-based prototype, it is used to explore whether transparent and consistent comparison between traditional renovation solutions and the I-DIFFER concept can be supported during early-stage design without relying on detailed building performance simulation.

Chapter 3

Methodology and Framework Implementation

3.1 Methodological basis and scope

This chapter describes the development and implementation of the simplified hourly calculation framework proposed in this thesis. The framework is intended for early-stage comparison of heating and cooling energy needs in traditional renovation solutions and the I-DIFFER concept. Rather than aiming to provide a detailed prediction of full building performance, the chapter describes how a simplified representation of the dominant thermal processes was developed and implemented to support transparent and consistent comparisons under limited input conditions.

The methodological basis of the framework is derived from the BESTFACADE WP4 (BESTFACADE, 2007) method for double-skin facades. BESTFACADE WP4 itself builds on EN ISO 13790, EN ISO 13789, and DIN V 18599. In this context, EN ISO 13790 provides the general heat-balance and utilisation-factor approach for calculating heating and cooling demand, EN ISO 13789 provides the treatment of transmission and ventilation heat transfer through unconditioned spaces, and DIN V 18599 provides the simplified treatment of solar gains and temperature effects in unheated glazed zones. These relationships are not applied unchanged, but are adapted and combined in an hourly structure suited to the comparative aim of the thesis. The resulting framework is implemented as a spreadsheet-based prototype in order to make the assumptions, calculation logic, and outputs traceable throughout the assessment process.

A main methodological choice in this thesis is the use of hourly calculation steps. The original simplified DSF approaches provide a basis for early-stage assessment,

but the hourly adaptation introduced here is intended to more accurately represent short-term variations in solar gains, heat transfer, and ventilation-related heat removal. This is particularly relevant to the I-DIFFER concept, where performance depends on the interaction between solar-driven facade behaviour and ventilation operation throughout the day.

The scope of the framework is limited to room-level comparison of heating and cooling energy needs. The conditioned room and, where relevant, the adjacent facade cavity are represented in simplified form, together with basic climatic inputs, facade properties, ventilation assumptions, and internal gains. The framework is not intended to replace detailed building performance simulation or to provide a precise prediction of full building performance. Instead, it is used to explore the extent to which a simplified hourly approach can support early-stage comparison between traditional renovation solutions and the I-DIFFER concept.

The chapter is structured as follows. Section 3.2 presents the overall framework structure and the comparative scenario definition. Section 3.3 describes the simplified hourly calculation method. Section 3.4 explains the operating modes and control assumptions used in the framework. Section 3.5 presents the spreadsheet-based implementation. Section 3.6 outlines the validation approach, and Section 3.7 summarises the main methodological assumptions.

3.2 Framework structure and comparative scenario definition

The methodological framework developed in this thesis is based on a simplified hourly calculation approach designed for comparative assessment of renovation strategies. The framework links input parameters, scenario definitions, calculation procedures, and resulting energy performance indicators within a consistent analytical structure.

Figure 3.1 presents the structure of the simplified hourly calculation framework used in this study, including inputs, scenario definitions, calculation steps, and resulting outputs.

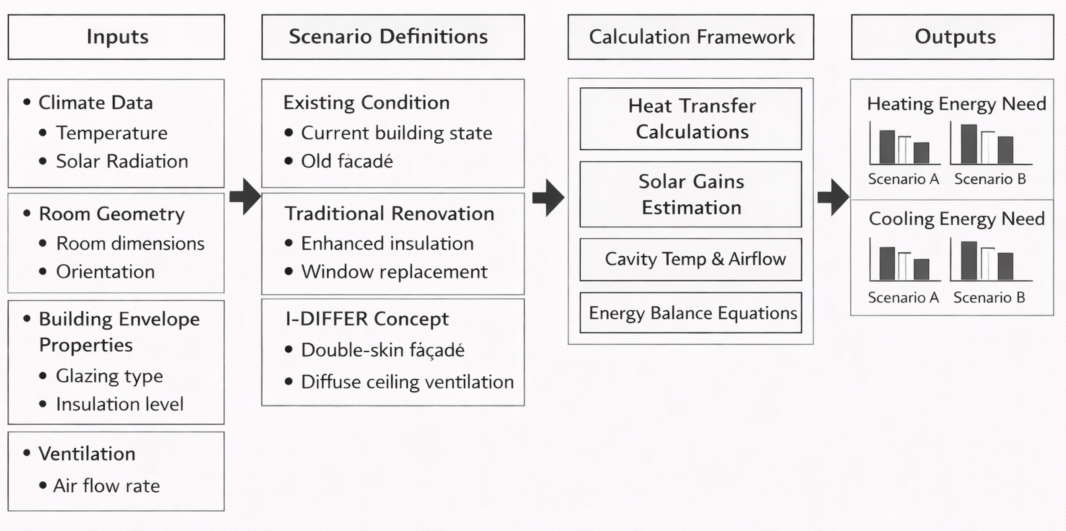

Figure 3.1: Overview of the simplified hourly calculation framework used for comparative analysis. The framework links input parameters, scenario definitions, calculation procedures, and resulting heating and cooling energy needs.

The input parameters include climate data, room geometry, building envelope properties, and ventilation assumptions. Climate data consist of outdoor temperature and solar radiation, which are used to represent external boundary conditions. Room geometry includes the dimensions and orientation of the analysed space. Building envelope properties describe the thermal characteristics of the facade, including glazing type and insulation level. Ventilation is represented through simplified airflow rate assumptions.

Based on these inputs, three renovation scenarios are defined: the existing condition, a traditional renovation solution, and the I-DIFFER concept. The existing condition represents the current state of the building, including the original facade configuration. The traditional renovation scenario includes improvements such as enhanced insulation and window replacement. The I-DIFFER concept is represented through the integration of a double-skin façade and diffuse ceiling ventilation.

The calculation framework applies simplified heat-balance relationships to estimate the thermal performance of each scenario. This includes transmission heat transfer, solar gains, cavity temperature and airflow behaviour, and overall energy balance equations. The framework is structured to maintain consistency across scenarios while allowing differences in facade and ventilation configurations to be reflected in the calculations.

The outputs of the framework are the heating and cooling energy needs of the

analysed space. These results are used to compare the performance of the different renovation scenarios under the same boundary conditions. The framework, therefore, provides a structured basis for evaluating the relative effectiveness of the I-DIFFER concept in comparison with traditional renovation approaches.

The individual components of the calculation framework illustrated in Figure 3.1 are described in detail in the following sections.

3.2.1 Inputs and boundary conditions

The framework requires a set of inputs intended to reflect information that may be available during early-stage design. These inputs include climatic data, building geometry, facade properties, ventilation assumptions, and internal heat gains.

Climatic inputs include hourly outdoor temperature and solar radiation data. Geometric inputs define the room and facade dimensions relevant to transmission, solar gain, and ventilation-related calculations. Facade inputs include thermal transmittance values, glazing properties, and, where relevant, cavity-related assumptions. Ventilation inputs describe airflow assumptions used in the simplified heat-transfer calculations. Internal gains are represented in simplified form through occupants, lighting, and equipment.

The same general climatic basis and room geometry are used across scenarios. This ensures that differences in calculated heating and cooling energy needs are interpreted as differences in renovation strategy rather than in external conditions or case definition.

The full set of input parameters used to define the scenarios is provided in Appendix C

3.2.2 Outputs and comparison indicators

The main outputs of the framework are monthly and annual estimates of heating and cooling energy needs for the investigated renovation scenarios. These outputs are used as comparative indicators rather than as exact predictions of real operational performance.

In this thesis, the outputs are used to compare the existing condition, traditional renovation solutions, and the I-DIFFER concept under a common set of assumptions. Where relevant, the results are also compared across facade orientations and operating modes. The purpose of the outputs is therefore to support transparent and consistent comparison between scenarios at an early design stage.

3.2.3 Comparative scenario definition

The framework is used to compare three main scenario types: the existing condition, a representative traditional renovation solution, and the I-DIFFER concept. The existing condition provides a reference case against which renovation-related changes can be interpreted. The traditional renovation case represents a more conventional improvement strategy, while the I-DIFFER case represents the integrated facade-ventilation concept examined in this thesis.

All three scenarios are evaluated using the same climatic basis, room geometry, and general heat-balance structure. This means that differences in results arise from changes in facade properties, ventilation assumptions, and operational representation rather than from changes in the underlying framework.

In the traditional renovation scenario, the facade and ventilation system are represented as separate measures without the coupled DSF-DCV interaction used in the I-DIFFER case. In the I-DIFFER scenario, by contrast, the cavity and operation-mode logic are included in the calculation structure. This makes it possible to compare a conventional renovation pathway with an integrated concept under consistent assumptions and comparable boundary conditions.

3.3 Simplified hourly calculation method

The simplified hourly calculation method combines established heat-balance relationships with a simplified representation of the double-skin facade cavity as an intermediate thermal zone. The purpose of the method is to estimate heating and cooling energy needs at room level while preserving the main thermal interactions relevant to comparison between the I-DIFFER concept and traditional renovation solutions.

The method is organised into six main calculation groups. First, transmission heat transfer is calculated for the relevant envelope elements. Second, ventilation-related heat transfer is represented through simplified airflow assumptions and corresponding heat transfer coefficients. Third, solar gains are estimated for both the conditioned room and, the DSF cavity. Fourth, the mean cavity temperature and outlet air temperature are estimated in simplified form in the I-DIFFER case. Fifth, total heat gains and losses are combined using simplified balance relationships. Finally, hourly heating and cooling energy needs are estimated using utilisation-factor relationships derived from standard energy-balance methods. The equations implemented in the framework are adopted from the BESTFACADE report(BESTFACADE, 2007) and are based on EN ISO 13790, EN ISO 13789, and DIN V 18599.

3.3.1 Transmission heat transfer

Transmission heat transfer is used to represent conductive heat exchange through the building envelope and, in the I-DIFFER scenario, between the conditioned room and the façade cavity. Following (DS/EN ISO 13789, 2017), the transmission heat transfer coefficient is calculated as:

$$H_T = \sum_i A_i \cdot U_i \tag{3.1}$$

where A_i is the area of element i and U_i is the thermal transmittance of element i.

In the traditional renovation scenario, this coefficient is calculated for the relevant envelope elements of the conventional renovated facade. In the I-DIFFER scenario, transmission heat transfer is divided between the internal skin separating the conditioned room and the cavity and the external skin separating the cavity and the outdoor environment. This distinction allows the cavity to be represented as a separate thermal zone rather than as part of a single facade element.

The purpose of this calculation is not to represent full multidimensional heat flow in detail, but to preserve the dominant conductive heat-transfer pathways relevant to comparative assessment.

3.3.2 Ventilation heat transfer

Ventilation heat transfer is represented through simplified airflow assumptions and corresponding heat-transfer coefficients. Following EN ISO 13789, the general ventilation heat-transfer coefficient is expressed as

$$H_v = \rho_a \cdot c_a \cdot q_v \tag{3.2}$$

where ρ_a is the air density, c_a is the specific heat capacity of air, and q_v is the airflow rate.

In the traditional renovation scenario, this term represents the heat exchange associated with the conventional ventilation system. In the I-DIFFER scenario, ventilation heat transfer may occur both in the conditioned room and in the facade cavity, depending on the operating mode. The same general expression is therefore used across scenarios, but the interpretation of the airflow path depends on the system configuration.

Because the framework is intended for early-stage comparison, airflow is simplified through fixed or mode-dependent assumptions. This makes it possible to compare

the thermal effect of different renovation concepts without detailed airflow modelling.

In cooling mode, cavity ventilation was not represented by a fixed airflow rate, as in pre-heating mode. Instead, the framework adopted the approximation proposed by Hellström in the (BESTFACADE, 2007)report for naturally ventilated double-skin facade cavities. In this approach, the cavity is treated as an unheated intermediate zone, and the ventilation heat-transfer coefficient between the cavity and the outdoor environment, $H_{V,ue}$, depends on cavity height, air properties, pressure losses, and the temperature difference between the outdoor air and the cavity. This means that ventilation heat transfer is temperature-dependent and can therefore, in simplified form, reflect buoyancy-driven heat removal.

Following Hellström, the ventilation heat-transfer coefficient is expressed as

$$H_{V,ue} = h_v \cdot |T_{c,\text{mean}} - T_e|^{0.5} \tag{3.3}$$

where $T_{c,\text{mean}}$ is the mean cavity temperature and T_e is the outdoor air temperature. The coefficient h_v is written as

$$h_v = \left(\frac{2gH_{\text{cav}}}{T_{e,\text{abs}}\,\xi_{\text{tot}}} \right)^{0.5} \rho_u c_p \Delta T_{\text{rel}} A_{\text{cav}} \tag{3.4}$$

and the relative temperature rise is

$$\Delta T_{\text{rel}} = \frac{T_{c,\text{out}} - T_e}{T_{c,\text{mean}} - T_e} \tag{3.5}$$

where g is the gravitational acceleration, H_{cav} is the cavity height, $T_{e,\text{abs}}$ is the absolute outdoor air temperature, ξ_{tot} is the total pressure-loss coefficient, ρ_u is the air density in the cavity, c_p is the specific heat capacity of air, ΔT_{rel} is the relative temperature rise, and A_{cav} is the characteristic cavity flow area.

In simple terms, this means that when the cavity becomes warmer than the outdoor air, the buoyancy effect becomes stronger and more heat is removed by ventilation.

A key simplification of the Hellström approach is that ventilation heat transfer between the room and the façade cavity is assumed to be zero:

$$H_{V,iu} = 0 \tag{3.6}$$

The method, therefore, focuses on the main ventilation exchange between the cavity and the outside. In this thesis, the Hellström-based approach was used to approximate buoyancy-driven cavity ventilation on an hourly basis in cooling mode. This supports a simplified hourly representation of cavity behaviour while remaining suitable for early-stage design assessment.

In addition to mechanical and cavity ventilation, infiltration was also included in the framework following (DS/EN ISO 13789, 2017). Infiltration describes air leaking into and out of the room through gaps and cracks in the building envelope without passing through the ventilation system. The framework estimates infiltration from a pressurisation test value q_{50}, which gives the air permeability of the envelope at 50 Pa. Since real operating pressure differences are much lower, a reduction factor of 1/20 was applied:

$$\dot{V}_{\text{inf}} = \frac{q_{50}}{20} \cdot A_{\text{env}} \tag{3.7}$$

where q_{50} is the air permeability at 50 Pa in $\text{m}^3/(\text{h}\cdot\text{m}^2)$, and A_{env} is the exposed envelope area, including the external wall and roof. The corresponding infiltration heat-transfer coefficient is then

$$H_{\text{inf}} = \rho_a \cdot c_a \cdot \dot{V}_{\text{inf}} \tag{3.8}$$

The same q_{50} value was used in all scenarios as a simplifying assumption.

For the traditional renovation scenario, heat recovery was included in the balanced mechanical ventilation system following (DS/EN ISO 13789, 2017). The heat exchanger preheats the incoming air using heat from the exhaust air and therefore reduces the ventilation heat loss. The effective ventilation heat-transfer coefficient after recovery is

$$H_{v,\text{eff}} = \rho_a \cdot c_a \cdot q_v \cdot (1 - \eta_{\text{hr}}) \tag{3.9}$$

where q_v is the ventilation airflow rate and η_{hr} is the heat recovery efficiency. A value of 73% was used, corresponding to the minimum requirement for fully replaced mechanical ventilation systems under BR18 (Danish Building Regulations, 2018).

3.3.3 Solar gains

Solar gains are represented separately for the conditioned room and, where relevant, the DSF cavity. This distinction is especially important in the I-DIFFER

scenario, where part of the incident solar radiation contributes directly to gains in the room, while another part influences the thermal state of the facade cavity, thereby indirectly affecting heating and cooling performance.

Following DIN V 18599, the total solar radiation entering the DSF is expressed in simplified form as

$$\varphi_s^{\text{total}} = F_{F,ue} \cdot A_{ue} \cdot g_{\text{eff},ue} \cdot I_s \tag{3.10}$$

where $F_{F,ue}$ is the frame correction factor for the external glazing, A_{ue} is the glazed area, $g_{\text{eff},ue}$ is the effective solar transmittance of the external transparent component, and I_s is the solar radiation.

Direct solar heat gains to the conditioned room are represented as

$$\varphi_s^{\text{room}} = F_{F,ui} \cdot A \cdot g_{\text{eff},iu} \cdot F_{F,ue} \cdot \tau_{e,ue} \cdot I_s \cdot t \tag{3.11}$$

where the corresponding factors describe the internal transparent section, external glazing transmittance, and time step.

The remaining solar gains are assumed to affect the cavity and are represented as part of the cavity heat flow:

$$\varphi_s^c = \sum \varphi_s^{\text{total}} - \frac{\sum \varphi_s^{\text{room}}}{t} + \sum \varphi_h^c \tag{3.12}$$

where φ_s^c is the heat flow affecting the unconditioned cavity and φ_h^c represents any internal gains assigned to that zone.

In the traditional renovation scenario, solar gains are represented directly in relation to the room through the conventional facade configuration, without the intermediate cavity state considered in the I-DIFFER case.

3.3.4 Cavity temperature and outlet air temperature

An important part of the I-DIFFER representation is that the facade cavity is treated as an intermediate thermal zone. Instead of modelling it as a fully conditioned space, it is represented as an unheated buffer zone between the room and the outdoor environment. Its temperature depends on solar gains in the cavity, heat exchange with the room, heat exchange with the outdoor air, and ventilation-related heat removal.

In the general formulation, the mean cavity temperature $T_{c,\text{mean}}$ can be written as a steady-state balance between heat gains and heat-transfer coefficients:

$$T_{c,\text{mean}} = \frac{\varphi_s^c + T_i \left(H_t^{r-c} + H_v^{r-c} + H_i^{r-c}\right) + T_e \left(H_t^{c-o} + H_v^{c-o} + H_i^{c-o}\right)}{H_t^{r-c} + H_v^{r-c} + H_i^{r-c} + H_t^{c-o} + H_v^{c-o} + H_i^{c-o}} \tag{3.13}$$

where φ_s^c is the heat flow into the cavity, T_i is the indoor temperature, T_e is the outdoor temperature, and the H-terms represent heat transfer between the room, cavity, and outdoor environment.

This equation shows that the cavity temperature is influenced by both the indoor and outdoor sides. The purpose is not to describe the cavity in full detail, but to preserve its main thermal effect in the simplified framework.

For cooling mode, the cavity balance is coupled with the Hellström formulation for naturally ventilated cavities. In this case, it is more convenient to solve the problem in terms of the cavity temperature rise above outdoor conditions, that is,

$$T_{c,\text{mean}} - T_e \tag{3.14}$$

rather than solving directly for the mean cavity temperature.

When the Hellström ventilation term is inserted into the cavity balance, the following nonlinear equation is obtained:

$$h_v \left(T_{c,\text{mean}} - T_e\right)^{1.5} + \left(H_t^{r-c} + H_t^{c-o}\right)\left(T_{c,\text{mean}} - T_e\right) - \left[H_t^{r-c}\left(T_i - T_e\right) + \varphi_s^c\right] = 0 \tag{3.15}$$

This equation means that cavity temperature and ventilation heat removal affect each other. If the cavity becomes warmer, buoyancy-driven ventilation becomes stronger, which in turn removes more heat from the cavity. The equation is therefore nonlinear.

In the spreadsheet implementation, this equation was rearranged and solved directly for the cavity excess temperature. The implemented solution was written as

$$T_{c,\text{mean}} - T_e = \begin{cases} 0, & \text{if the balance term is } \leq 0 \\ \left(\dfrac{H_t^{r-c}(T_i - T_e) + \varphi_s^c}{H_t^{c-o} + \dfrac{h_v + H_v^{c-o}}{\sqrt{\Delta T_{\text{rel}}}}} \right)^{2/3}, & \text{if the balance term is } > 0 \end{cases} \tag{3.16}$$

This means that when the balance term is zero or negative, the cavity does not become warmer than the outdoor air, and the cavity excess temperature is set to zero. In that case, the mean cavity temperature is equal to the outdoor temperature.

Once the excess temperature has been found, the mean cavity temperature is obtained as

$$T_{c,\text{mean}} = T_e + (T_{c,\text{mean}} - T_e) \tag{3.17}$$

In addition to the mean cavity temperature, the outlet cavity temperature was also estimated. In cooling mode, the inlet air was assumed to be outdoor air, so that

$$T_{c,\text{in}} = T_e \tag{3.18}$$

The outlet temperature was then calculated as

$$T_{c,\text{out}} = T_e + 2\,(T_{c,\text{mean}} - T_e) \tag{3.19}$$

This means that the outlet temperature rise was taken as twice the mean cavity excess temperature above outdoor conditions. If the cavity excess temperature is zero, the mean cavity temperature and the outlet cavity temperature are both equal to the outdoor air temperature.

These cavity temperatures are used only in the I-DIFFER case, since no façade cavity is represented in the traditional renovation scenario. In the present framework, the mean cavity temperature and outlet temperature are used to represent how the DSF affects transmission and ventilation-related heat exchange. Because cavity temperature is one of the most sensitive variables in simplified DSF modelling, the calculated values should be understood as approximate indicators for comparison rather than exact predictions of façade operation.

The Hellström method is therefore used here as a simplified way to represent buoyancy-driven cavity heat removal within an hourly early-stage framework. It does not describe all airflow details, wind effects, or transient behaviour, but it preserves the main physical mechanism needed for comparative analysis.

3.3.5 Total heat gains and losses

Once transmission heat transfer, ventilation-related heat transfer, solar gains, and cavity conditions have been estimated, the framework combines these terms into

total hourly heat gains and total hourly heat losses for the conditioned room. Following the simplified energy-balance structure of EN ISO 13790, total heat losses are expressed as:

$$Q_{ls} = Q_{tr} + Q_v \tag{3.20}$$

where Q_{tr} represents transmission losses and Q_v represents ventilation-related losses.

Total heat gains are expressed as:

$$Q_{gn} = Q_{int} + Q_{sol} \tag{3.21}$$

where Q_{int} represents internal gains and Q_{sol} represents solar gains.

The internal heat gain term Q_{int} represents the combined heat released by occupants, lighting, and equipment within the conditioned room. In the framework, internal gains are represented as a single combined heat input that is either active or zero, depending on the occupancy state of the room. A constant value is applied during occupied hours and zero during unoccupied hours. The occupied value and the definition of occupied hours are specified as part of the case scenario input parameters in Chapter 5.

These relationships are used in both the traditional renovation and I-DIFFER scenarios. The difference lies not in the overall form of the heat balance, but in how the individual transmission, ventilation, and solar-gain terms are defined for each scenario. In this way both conventional and integrated renovation concepts can be compared within the same overall analytical structure.

3.3.6 Heating and cooling energy need

Heating and cooling energy needs are estimated using utilisation-factor relationships derived from (DS/EN ISO 13790, 2008). These relationships are used to account for the fact that not all gains and losses are immediately and fully effective. In this way, the framework includes a simplified representation of thermal response without requiring detailed dynamic simulation.

The utilisation factors depend on the thermal response of the zone, represented in simplified form by the time constant. Following the simplified calculation procedure used in this thesis, the time constant is expressed as:

$$\tau = \frac{C_m/3,6}{H_m} \tag{3.22}$$

where τ is the time constant of the zone, C_m is the effective internal heat capacity, and H_m is the total heat loss coefficient.

For heating mode, the gain utilisation factor is expressed as:

$$\eta_{H,gn} = \frac{1 - \gamma_H^{a_H}}{1 - \gamma_H^{a_H+1}} \tag{3.23}$$

where

$$\gamma_H = \frac{Q_{H,gn}}{Q_{H,ls}} \quad \text{and} \quad a_H = a_{0,H} + \frac{\tau_H}{\tau_{0,H}} \tag{3.24}$$

In these expressions, $\eta_{H,gn}$ is the gain utilisation factor for heating, γ_H is the gain/loss ratio in heating mode, and a_H is a numerical parameter that depends on the time constant of the zone.

For cooling mode, the loss utilisation factor is expressed as:

$$\eta_{C,ls} = \frac{1 - \lambda_C^{a_C}}{1 - \lambda_C^{a_C+1}} \tag{3.25}$$

where

$$\lambda_C = \frac{Q_{C,gn}}{Q_{C,ls}} \quad \text{and} \quad a_C = a_{0,C} + \frac{\tau_C}{\tau_{0,C}} \tag{3.26}$$

Here, $\eta_{C,ls}$ is the loss utilisation factor for cooling, λ_C is the gain/loss ratio in cooling mode, and a_C is a numerical parameter that depends on the time constant of the zone.

The heating energy need is then calculated as:

$$Q_{H,nd} = Q_{H,ls} - \eta_{H,gn} \cdot Q_{H,gn} \tag{3.27}$$

where $Q_{H,nd}$ is the heating energy need, $Q_{H,ls}$ is the total heat loss in heating mode, $Q_{H,gn}$ is the total heat gain in heating mode, and $\eta_{H,gn}$ is the gain utilisation factor for heating.

The cooling energy need is calculated as:

$$Q_{C,nd} = Q_{C,gn} - \eta_{C,ls} \cdot Q_{C,ls} \tag{3.28}$$

where $Q_{C,nd}$ is the cooling energy need, $Q_{C,gn}$ is the total heat gain in cooling mode, $Q_{C,ls}$ is the total heat loss in cooling mode, and $\eta_{C,ls}$ is the loss utilisation factor for cooling.

Within the present framework, these calculated values are used as comparative indicators across scenarios. Their role is therefore not to provide exact operational

prediction, but to support transparent comparison between traditional renovation solutions and the I-DIFFER concept under a common set of assumptions.

3.3.7 Methodological limitations of the calculation approach

Although the method builds on established simplified relationships, it also relies on several assumptions that influence the interpretation of results. These include assumptions regarding airflow rates, cavity temperature, outlet temperature, mode-dependent operation, and the simplified representation of ventilation-related heat removal. In addition, the adaptation of the method to hourly resolution is a methodological choice introduced in this thesis to improve representation of short-term variation, but it does not provide the level of detail associated with full dynamic simulation.

The method should therefore be understood as a comparative framework for early-stage design rather than as a predictive substitute for detailed building performance simulation. Its value depends on whether it can preserve the dominant thermal interactions relevant to comparison between renovation concepts while remaining simple enough to operate under limited input conditions.

3.4 Operation modes and control assumptions

The I-DIFFER concept operates through three distinct modes that adapt the thermal behaviour of the DSF cavity and ventilation system to seasonal and occupancy conditions. In the framework these modes are represented as simplified thermal states: transparent insulation mode, pre-heating mode, and cooling mode. The three modes and their assumed heat transfer paths are illustrated in Figure 3.2

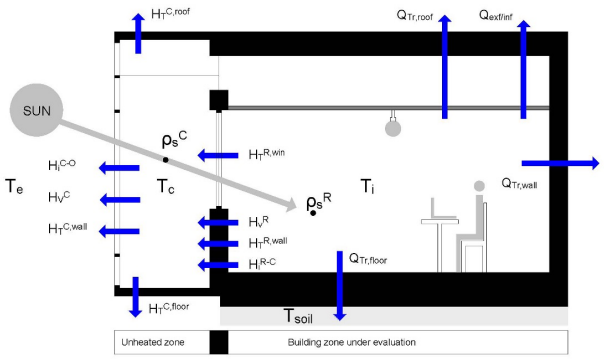

(a) Transparent insulation mode

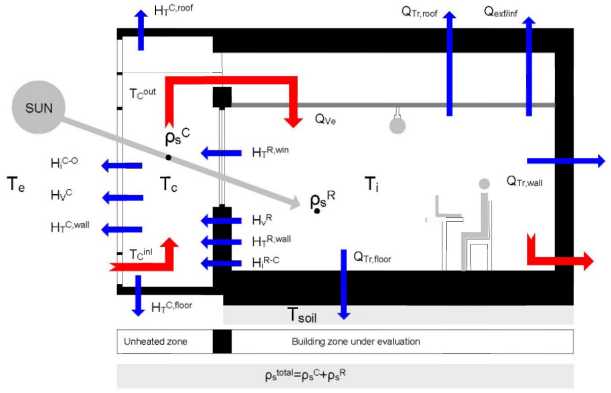

(b) Preheating mode

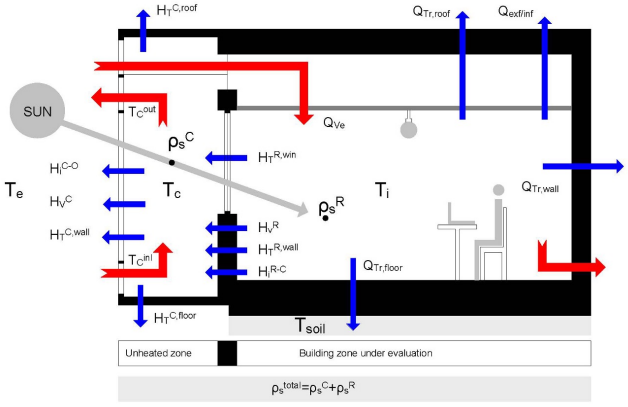

(c) Cooling mode

Figure 3.2: Simplified thermal representation of the operating modes used in the framework: (a) transparent insulation mode, (b) preheating mode, and (c) cooling mode. The figures illustrate the assumed heat-transfer and airflow relationships between the outdoor environment, the DSF cavity, and the conditioned room.

3.4.1 Transparent insulation mode

In transparent insulation mode, the facade cavity is represented primarily as a solar-thermal buffer. The main purpose of this operating mode is to utilise solar gains within the double-skin facade to improve its thermal performance and reduce heat losses under heating-oriented conditions. In this mode, the cavity is not primarily used to preheat supply air or to remove excess heat, but to represent the thermal effect of a solar-responsive facade layer located between the outdoor environment and the conditioned room.

The thermal behaviour of the cavity in transparent insulation mode is governed mainly by the balance between incident solar radiation, conductive heat exchange through the inner and outer facade layers, and simplified ventilation-related heat transfer. Solar gains entering the facade system increase the cavity temperature, and this elevated cavity temperature modifies the heat flow between the room and the exterior. In this way, the cavity acts as an intermediate thermal zone that reduces the direct exposure of the conditioned room to outdoor conditions while making partial use of solar energy. The simplified framework therefore treats the cavity as a buffered space whose temperature affects the overall transmission and energy balance of the room.

Within the framework, transparent insulation mode was implemented as a separate modular calculation pathway with mode-specific assumptions for cavity behaviour and heat exchange. At the same time, it remained part of the integrated tool through the simplified control strategy described later in this chapter. This means that transparent insulation mode was not treated as an unrelated standalone case, but as one operational module of the complete I-DIFFER framework. Such a modular representation makes it possible to preserve the distinct physical logic of transparent insulation operation while maintaining a transparent and comparable overall method.

The simplified framework does not represent detailed optical effects, transient thermal storage in all facade components, or detailed air behaviour within the cavity. Instead, the mode is intended to preserve the main thermal function of the façade cavity as a solar-thermal buffer under transparent insulation operation. This is consistent with the early-stage objective of the thesis, where the aim is to support transparent comparison of renovation concepts rather than to reproduce the full operational detail of a dynamic simulation model. In this way, transparent insulation mode contributes to the framework by representing one of the key thermal operating principles of the I-DIFFER concept in a simplified but physically interpretable form.

3.4.2 Pre-heating mode

In pre-heating mode, the facade cavity is represented as a solar-assisted and mechanically air-driven preconditioning element for incoming air. The main purpose of this operating mode is to use solar gains absorbed in the cavity to increase the temperature of the ventilation air before it enters the room or the diffuse ceiling ventilation plenum.

The thermal logic of pre-heating mode is based on the coupling between facade behaviour and ventilation-related heat transfer. Solar gains increase the cavity air temperature, and the warmed air is then assumed to influence the supply conditions to the room. As a result, the cavity not only affects heat transfer through the facade layers but also contributes to the ventilation-related energy balance of the conditioned zone. This makes pre-heating mode particularly important in the context of the I-DIFFER concept, since it explicitly represents the interaction between the double-skin facade and the diffuse ceiling ventilation principle.

Within the framework, pre-heating mode was implemented as a separate modular calculation pathway with its own assumptions for airflow path, cavity behaviour, and thermal interaction with the room. At the same time, it remained part of the integrated tool through the simplified control strategy described later in this chapter. This means that pre-heating mode was not evaluated in isolation, but as an operational module within the complete I-DIFFER framework. Such a modular structure allows the specific thermal role of the pre-heating pathway to be preserved while keeping the overall framework transparent and consistent across modes.

The simplified framework does not attempt to reproduce detailed room-air distribution or transient plenum behaviour. Instead, it represents the dominant thermal effect of using the cavity as a solar-assisted preheating element in an hourly comparative framework. This is consistent with the early-stage objective of the thesis, where the purpose is not to predict exact operational performance, but to examine whether a simplified representation can support transparent comparison of integrated facade-ventilation concepts and more conventional renovation solutions.

3.4.3 Cooling mode

In cooling mode, the facade cavity is represented as a naturally ventilated heat-removal pathway. The thermal role of the cavity in this mode differs from that in transparent insulation and pre-heating operation. Rather than acting mainly as a thermal buffer or as a preheating element, the cavity is used to limit the transfer of unwanted solar heat to the conditioned room and to support heat removal from the facade system under warmer conditions. In the integrated concept, this corre-

sponds to an operating principle in which heat is removed from the façade system while room supply air is introduced through the bypass.

The cooling-mode module was therefore linked to the cavity ventilation formulation described in Section 3.3. In particular, the cavity ventilation heat transfer was approximated using the Hellström-based method from the BESTFACADE WP4 report. This allowed the framework to represent the dominant effect of buoyancy-driven cavity ventilation under cooling conditions without relying on detailed airflow modelling. As the cavity temperature rises above the outdoor temperature, ventilation heat removal increases, which helps capture the façade's cooling-related thermal behaviour in a simplified hourly form.

Within the overall framework, cooling mode was implemented as a separate modular calculation pathway, with mode-specific assumptions for cavity behaviour and heat removal. At the same time, it remained part of the integrated tool through the simplified control strategy described later in this chapter. This means that cooling mode was not treated as an unrelated stand-alone case, but as one operational module of the complete I-DIFFER framework. Such a modular representation makes it possible to preserve the distinct physical logic of cooling operation while maintaining a transparent and comparable overall method.

The simplified framework does not reproduce detailed real-time control airflow behaviour. Instead, it represents the main cooling-related function of the facade cavity and its interaction with the room-level energy balance through a simplified, mode-specific calculation pathway. This is consistent with the early-stage objective of the thesis, where the purpose is a transparent comparison of renovation concepts rather than a detailed prediction of operational control behaviour.

3.4.4 Control assumptions in the framework

The control logic described in this section represents a significant simplification compared to the real I-DIFFER system. In a real concept, the system responds dynamically to indoor operative temperature, occupancy sensors, and weather conditions. The simplified framework instead uses fixed rules to assign modes at each hour. This approach was chosen because detailed control strategies are rarely known at the early design stage and because the simplified rules are transparent and reproducible across different climate datasets and building configurations.

Two control configurations are implemented in the framework and compared in this thesis. The first is ORM30-based seasonal switching, which uses the 30-day outdoor running mean temperature to define a fixed seasonal boundary, cooling mode runs only in summer and pre-heating and transparent insulation run only in winter. The second is instantaneous energy-based switching, which assigns the

operating mode at each hour based on which mode requires the least energy to maintain the room temperature setpoint. The two configurations are compared in terms of mode hour distribution and cooling energy assignment in Chapter 5, and in terms of annual heating and cooling energy demand across all renovation scenarios in Chapter 6.

The real I-DIFFER system operates all three modes throughout the full year, switching between them based on operative temperature thresholds and hysteresis bands at each timestep. The instantaneous energy-based configuration is the closest simplified approximation to this behaviour, since it reacts to current room energy conditions rather than a fixed seasonal boundary. The ORM30 configuration restricts each mode to a specific season, which is a stronger simplification but produces more stable and consistent seasonal energy assignment as discussed in Chapter 5.

Seasonal switching - ORM30 configuration

The seasonal boundary is defined by the 30-day outdoor running mean temperature ORM30, calculated in the framework as the arithmetic mean of the preceding 720 hourly outdoor temperature values:

$$ORM30_t = \frac{1}{720} \sum_{k=1}^{720} T_{e,t-k}$$

where $T_{e,t-k}$ is the outdoor air temperature k hours before the current timestep t. This is a simplification of the exponentially weighted daily formulation defined in (DS/EN 16798, 2019), where recent days are weighted more strongly than older days. The arithmetic hourly mean is used here for practical implementation in the hourly spreadsheet framework. The effect of this simplification on the seasonal boundary dates has not been assessed in this study.

A threshold of 10°C is applied to the ORM30 value following (DS/EN 16798, 2019), which defines this as the boundary between the winter and summer season. When ORM30 is below 10°C, the heating season is active, and either pre-heating or transparent insulation mode is assigned depending on occupancy. When ORM30 reaches or exceeds 10°C, the cooling season is active, and cooling mode is assigned for all hours. In the ORM30 configuration, cooling mode runs only in summer, pre-heating and transparent insulation run only in winter; the three modes are strictly separated by season.

Instantaneous energy-based switching configuration

In the instantaneous configuration, no fixed seasonal boundary is applied. At each hour the framework calculates the total energy need for each mode available at that hour, and assigns the mode that requires the least energy to keep the room at

the heating setpoint. Occupied hours compare pre-heating mode against cooling mode. Unoccupied hours compare transparent insulation mode against cooling mode. The mode with the lower combined heating and cooling energy need is assigned based on both the energy comparison and the occupancy schedule. All three modes can operate throughout the year, pre-heating during occupied hours, transparent insulation during unoccupied hours, and cooling mode whenever it is more energy efficient than the other available mode under the occupancy schedule.

This configuration is the closest simplified approximation to the real I-DIFFER operating logic, where all three modes are available throughout the year rather than being restricted to fixed seasonal boundaries.

Shading control

Solar shading is represented through a threshold-based control logic following (Bugenings et al., 2022) and (Karlsen et al., 2016). The shading activation threshold is a user-adjustable input parameter in the framework. When active, the effective solar heat gain coefficient is reduced from the unshaded value to g = 0.10, consistent with Class 4 solar shading performance as defined in (DS/EN 14501, 2021). The framework implements shading for both the I-DIFFER scenario, and the traditional renovation scenario, allowing direct comparison between the two renovation strategies with and without shading active.

Two shading limitations apply in the framework. First, in transparent insulation mode (Bugenings et al., 2022) use shading at low solar radiation levels as an additional insulation layer to reduce thermal radiation losses between cavity surfaces. The simplified framework does not calculate long-wave radiation exchange between cavity surfaces and therefore does not implement this shading function in transparent insulation mode. Second, when shading is active in cooling mode, the venetian blinds reflect a portion of solar radiation back into the cavity. The framework does not calculate the additional energy that accumulates in the cavity from this reflection.

Both control configurations use the same shading logic. The sensitivity analysis in Chapter 5. additionally compares both configurations with shading removed to isolate the individual contributions of seasonal switching and shading to the annual energy results.

Summary of control configurations

The two configurations are summarised in Table 3.1. The key difference is that the ORM30 configuration restricts each mode to a specific season while the instantaneous configuration allows all three modes to operate throughout the year based on the hourly energy comparison and occupancy schedule. Both configurations use the same occupancy schedule and shading logic.

Table 3.1: Control configurations

Parameters	ORM30 configuration	Instantaneous configuration
Season definition	ORM30 threshold 10°C	No fixed boundary
Summer	Cooling mode only	Cooling when most efficient
Winter occupied	Pre-heating only	Pre-heating or cooling
Winter unoccupied	Transparent insulation only	Transparent insulation or cooling
Shading	Cooling mode above threshold	Cooling mode above threshold
All three modes full year	No	Yes

3.5 Spreadsheet implementation

The simplified hourly calculation framework was implemented as a spreadsheet. The purpose of the implementation is not to present a software product but to provide a transparent and accessible environment in which the calculation logic can be structured, tested, and compared across scenarios. A spreadsheet format was selected because it allows the explicit representation of equations, inputs, intermediate variables, and outputs, consistent with the early-stage purpose of the framework.

The spreadsheet is organised so that inputs, intermediate calculations, and outputs are separated into distinct sections. This structure is intended to improve transparency and reduce the risk of confusion between user-defined assumptions and calculated results. Input sections contain climatic data, building geometry, envelope properties, ventilation assumptions, internal gains, and control-related mode assignments. Calculation sections implement the simplified hourly relationships described in the previous sections, including transmission heat transfer, ventilation-related heat transfer, solar gains, mean cavity temperature, outlet temperature, total gains and losses, and heating and cooling energy needs. Output sections summarise hourly and comparative results for the evaluated renovation scenarios.

The spreadsheet is structured so that the same base equations apply to all renovation scenarios; transmission heat losses, ventilation heat losses, solar gains, and room heat balance are calculated using the same methods across all three scenarios. This ensures that the comparison between the unrenovated condition, traditional renovation, and I-DIFFER is carried out on a consistent basis, making the results directly comparable. Each scenario uses its own set of input values reflecting the specific envelope properties, glazing, and ventilation assumptions of that scenario.

The I-DIFFER scenario additionally includes a set of equations specific to the DSF cavity: mean cavity and outlet cavity temperature calculation. The room heat balance uses mode-specific boundary conditions, meaning the cavity temperature and ventilation contribution to the room differ between pre-heating, transparent insu-

lation, and cooling mode, and the room heat balance is calculated separately for each mode at each hour. This additional equation set covers the physical behaviour introduced by the addition of the DSF cavity to the facade.

The framework supports comparison across different facade orientations by changing the solar radiation input for the relevant orientation. No separate model is needed for each case; the same calculation structure produces results for all orientations within the same spreadsheet.

Because the framework is implemented as a spreadsheet, certain simplifications are introduced at the implementation level. These include predefined calculation sequences and sequential dependencies between variables where each hourly result depends on the inputs and intermediate values calculated for that same hour. Such implementation choices support transparency and repeatability but they also mean that the spreadsheet should be understood as an analytical aid for comparative assessment rather than a comprehensive simulation environment.

The spreadsheet therefore serves two methodological roles. First it provides the practical structure for applying the simplified hourly calculation framework. Second it makes the assumptions and equations visible in a form that supports scrutiny, testing, and discussion. The Excel spreadsheet is the practical implementation of the simplified hourly calculation framework, providing an early-stage tool for comparing heating and cooling energy needs between traditional renovation and the I-DIFFER concept before detailed dynamic simulation is carried out.applicability.

3.6 Validation approach

Validation in this thesis is carried out at two levels. The first level evaluates the simplified DSF representation against experimental data. The second level compares the overall framework results for the I-DIFFER case scenario with detailed simulation results from the published IDA ICE study by Bugenings et al., 2022. The purpose of validation is not to prove full predictive accuracy but to examine whether the framework produces results that are sufficiently reasonable and physically consistent to support early-stage comparison.

The first validation level is based on experimental data from The Cube, a full-scale outdoor DSF test facility at Aalborg University described by Kalyanova and Lund, 2014a, 2014b. Two DSF operating modes were used: pre-heating and cooling, corresponding to the external air-curtain mode described by Kalyanova et al. These modes were selected because they represent the main heating-related and cooling-related DSF behaviours relevant to the framework. The validation focused on facade-related variables calculated by the model, namely cavity temperature, outlet air temperature, and the resulting heating or cooling energy need. The com-

parison assesses whether the simplified DSF representation captures the dominant thermal behaviour of the facade under measured boundary conditions in a physically consistent way.

The second validation level concerns the integrated I-DIFFER case scenario. The framework results are compared with the modified IDA ICE simulation results reported by Bugenings et al., 2022 and provided by Aalborg University. The IDA ICE model was modified to run each operating mode separately throughout the full year under single-mode conditions, allowing direct comparison with the simplified framework under consistent boundary conditions. The comparison focused on the main output variables used in this thesis, namely heating energy need and mean cavity temperature for each operating mode. The full dynamic control logic of the IDA ICE model was not replicated, as the purpose of this validation level was to assess the main thermal and energy behaviour of the framework under comparable boundary conditions rather than to reproduce the detailed control operations of the reference model. The validation was therefore organised by mode, covering transparent insulation, pre-heating, and cooling, consistent with the framework's three-mode structure.

Agreement between the simplified framework and the reference results was assessed using bias, (MAE) mean absolute error, and (RMSE) root mean square error (RMSE), following the definitions used by (Karlsen et al., 2016). Bias is equivalent to the mean bias error and represents the average signed difference between the simplified framework and the reference values. Bias was used to identify systematic over- or underprediction, MAE to indicate the typical magnitude of deviation, and RMSE to emphasise larger errors.

$$\text{Bias} = \text{MBE} = \frac{1}{N}\sum_{i=1}^{N}(x_i - y_i) \tag{3.29}$$

$$\text{MAE} = \frac{1}{N}\sum_{i=1}^{N}|x_i - y_i| \tag{3.30}$$

$$\text{RMSE} = \sqrt{\frac{1}{N}\sum_{i=1}^{N}(x_i - y_i)^2} \tag{3.31}$$

where x_i is the value calculated by the simplified framework, y_i is the corresponding reference value, and N is the total number of compared data points. With this sign convention, a positive bias indicates overprediction by the simplified framework, while a negative bias indicates underprediction. These numerical metrics

were supported by graphical comparison through time-series plots, monthly comparisons, scatter plots, and summary charts.

The validation is selective and aligned with the framework scope. At the subsystem level, it examines whether the DSF model gives reasonable temperature and energy results. At the case-study level, it examines whether the simplified framework produces consistent comparative energy needs and mean cavity temperatures relative to the modified IDA ICE model. In this way, validation serves both to evaluate the framework and to identify its limitations.

The DSF validation is based on experimental data from The Cube, a full-scale outdoor DSF test facility at Aalborg University described by Kalyanova and Lund, 2014a, 2014b. Two DSF operational modes are used: preheating mode and external air curtain mode. These modes were selected because they represent the main heating-related and cooling-related DSF behaviours relevant to the framework. At this level, the validation focuses on the facade-related variables calculated by the model, namely cavity temperature, outlet air temperature, and the resulting heating or cooling energy need. The comparison is used to assess whether the simplified DSF representation captures the dominant thermal behaviour of the facade under measured boundary conditions in a physically consistent way.

The second validation level concerns the integrated I-DIFFER case scenario. Here, the framework results are compared with the modified detailed IDA ICE simulation results reported by Bugenings et al., 2022, and provided by Aalborg University. The comparison focuses on the main output variables used in the thesis, namely, the heating energy need and mean cavity temperature for the I-DIFFER.

The validation is therefore selective and aligned with the framework's scope. At the subsystem level, it examines whether the DSF model gives reasonable temperature and energy results. At the case-study level, it examines whether the simplified framework provides consistent comparative energy needs and mean cavity temperature results relative to the published IDA ICE benchmark.

3.7 Summary of methodological assumptions

Summary of methodological assumptions

The simplified hourly framework developed in this thesis is based on a set of methodological assumptions introduced to support transparent early-stage comparison between traditional renovation solutions and the I-DIFFER concept. These assumptions were necessary to keep the framework manageable and transparent, while still preserving the dominant thermal processes relevant to comparative assessment. The purpose of the framework is therefore not to reproduce the full

physical detail of a dynamic building performance simulation model, but to provide a structured and traceable method for comparing heating and cooling energy needs under consistent boundary conditions.

A first methodological assumption is that the assessment is performed at room level. The conditioned room and, where relevant, the adjacent facade cavity are represented in simplified form, while the wider building context is not modelled in full detail. This means that the framework focuses on the local interaction between facade behaviour, ventilation-related heat transfer, solar gains, and room-level heating and cooling energy need. The resulting outputs are therefore intended as comparative indicators for the analysed space, rather than exact predictions of full-building operational performance.

A second assumption is the use of hourly temporal resolution. The framework adopts hourly calculation steps in order to represent the short-term variation of solar gains, heat transfer, and ventilation-related effects more explicitly than would be possible in a monthly method. This choice was made because the I-DIFFER concept depends strongly on time-varying interaction between solar-driven facade behaviour and ventilation operation. At the same time, the framework remains simplified compared with detailed dynamic simulation, since the hourly calculations are based on reduced physical representations and predefined assumptions rather than full transient multi-zone modelling.

A third assumption concerns the representation of the double-skin facade cavity as an intermediate thermal zone. In the framework, the cavity is treated as an unheated zone whose mean temperature is determined from simplified heat-balance relationships involving solar gains, conductive heat exchange, and ventilation-related heat removal. This representation is based on simplified DSF logic derived from the BESTFACADE approach and related standards, but adapted into an hourly spreadsheet-based form suited to the comparative objective of this thesis. Consequently, the cavity temperature and outlet temperature should be understood as simplified state variables used to preserve the dominant thermal influence of the facade cavity, rather than as exact predictions of local temperature distribution within the cavity. The cavity temperature is calculated instantaneously at each hour without heat storage between timesteps. This means the framework does not account for thermal mass in the cavity construction, which is the dominant source of deviation identified in the validation.

A fourth assumption concerns the representation of ventilation. In the general framework, ventilation heat transfer is simplified through heat-transfer coefficients derived from airflow assumptions. For the cooling-mode module, the cavity ventilation heat transfer is represented using the Hellström-based approximation adopted from the BESTFACADE WP4 report. This means that buoyancy-driven cavity ven-

tilation is represented through a temperature-dependent ventilation heat-transfer coefficient, rather than a fully resolved airflow model. The approach preserves the dominant feedback between cavity overheating and heat removal, but it does not reproduce detailed airflow behaviour and wind-driven ventilation effects.

A fifth assumption is that the integrated concept is represented through three operational mode modules: transparent insulation mode, pre-heating mode, and cooling mode. Each mode is formulated as a separate modular calculation pathway because the airflow path, the thermal role of the cavity, and the dominant heat-transfer mechanisms differ between operating conditions. At the same time, these modules are not treated as unrelated stand-alone cases. Instead, they are combined into one integrated framework through a simplified control strategy. This allows the framework to preserve the physical logic of each operating principle while still representing the I-DIFFER concept as one combined system.

A sixth assumption concerns control representation. The framework does not simulate detailed real-time controller behaviour in the same way as a full building performance simulation model. Instead, simplified control rules are used to determine the active operational mode under given conditions. The purpose of this simplification is to support transparent and consistent early-stage comparison rather than detailed operational prediction. As a result, the mode transitions should be understood as idealised representations of control logic, suitable for comparative analysis but not for precise replication of actual I-DIFFER behaviour.

A seventh assumption concerns the treatment of boundary conditions and comparability. The same climatic basis, room geometry, and general heat-balance structure are applied across the analysed scenarios. This means that differences in calculated heating and cooling energy need arise from differences in facade properties, ventilation assumptions, and operational representation rather than from differences in scenario definition. This assumption is methodologically important because it ensures that the results can be interpreted as differences between renovation strategies under common external conditions.

An eighth assumption concerns the interpretation of the outputs. The calculated heating and cooling energy needs are used in this thesis as comparative performance indicators, not as exact forecasts of real operational energy use. The framework is intended to support screening, interpretation, and comparison of early-stage renovation options. The results should therefore be understood as indicators of relative performance and dominant thermal behaviour under a common simplified framework, rather than as final design values.

Chapter 4

Validation of the simplified hourly framework

4.1 Validation purpose and reference sources

The validation was carried out to assess the reliability of the simplified framework and to support the methodological choices adopted in the thesis. Since the framework is intended for early-stage comparative assessment, the objective was not to reproduce the full level of detail of experiments or dynamic simulation, but to examine whether the selected simplified methods preserved the dominant thermal behaviour of the I-DIFFER concept with acceptable agreement.

The validation had two main purposes. First, it was used to assess agreement for the key outputs of the framework, namely mean cavity temperature, outlet cavity temperature, and heating and cooling energy need, with airflow included where relevant as a supporting variable. Second, it was used to examine whether the selected simplified methods were sufficiently consistent with the reference results to support their use in the final framework.

For consistency, the simplified method was labelled according to operating mode. In this notation, SCM-PH refers to the BESTFACADE-based pre-heating formulation used in the framework, SCM-CL refers to the BESTFACADE-based cooling formulation using the Hellström approach, and SCM-TI refers to the transparent-insulation formulation used in the framework.

Two reference sources were used, both provided by Aalborg University. The first consisted of full-scale experimental reference cases from *'The Cube'* test facility at Aalborg University. In the present thesis, the experimental reference for pre-heating mode was taken from Kalyanova and Lund, 2014b, while the experimental

reference for cooling mode was taken from Kalyanova and Lund, 2014a. These sources provide measured data and boundary conditions for the empirical validation of double-skin façade behaviour. They also clearly distinguish between the two operating modes used in the present experimental validation: in external air curtain mode, the cavity airflow is naturally driven and varies over time, whereas in pre-heating mode, the airflow is constant and mechanically driven. Importantly, these experimental datasets were used only to validate the DSF subsystem, not the diffuse ceiling ventilation system, since the measurements were obtained from a DSF test facility rather than from an integrated DSF-DCV case.

The second reference source consisted of a dynamic-simulation reference case based on the I-DIFFER study by Bugenings et al., 2022, in which the integrated concept was analysed using IDA-ICE. In this thesis, the original IDA-ICE model was modified so that each analysed operating mode was represented by a single constant mode throughout the year, rather than through the original multi-mode control sequence. The resulting simulation outputs were provided by Aalborg University and used as the dynamic references for pre-heating, cooling, and transparent insulation modes. In addition, cooling energy need was excluded from the modified IDA-ICE model setup. The experimental and dynamic references were therefore used as complementary validation levels, providing, on the one hand, measured DSF behaviour and associated energy need for the façade test cases, and, on the other, a detailed reference model for the I-DIFFER concept. Accordingly, the experimental validation addresses only the façade subsystem, whereas the dynamic-simulation validation addresses the integrated concept at room level.

The two reference sources served different validation roles. The experimental reference cases were used to assess agreement with measured DSF behaviour and associated energy need for SCM-PH and SCM-CL, whereas the dynamic-simulation reference case was used to assess agreement with the modified detailed reference model of the I-DIFFER concept. For transparent-insulation mode, validation was limited to dynamic simulation, as no corresponding experimental reference case was included in the present study. Together, these two validation levels form the basis for performance assessment of the framework.

4.2 Validation metrics and variables

The comparison between the simplified framework and the reference results was based on three indicators defined in Section 3.6: Bias, MAE, RMSE. These indicators were used to describe different aspects of model performance rather than relying on a single metric. Bias indicates whether the simplified framework tends to overpredict or underpredict. MAE was considered the most useful overall measure because it expresses the average magnitude of the deviation. RMSE was included

because it responds more strongly to larger deviations.

The validation focused on the variables most important for the thermal behaviour represented by the framework: mean cavity temperature, outlet cavity temperature, heating energy need, and cooling energy need.

The same indicators were used throughout the validation in order to ensure consistent comparison between the simplified framework and the two reference sources. In the experimental validation, they were used to assess how well SCM-PH and SCM-CL reproduced the measured DSF behaviour from *The Cube* test facility. In the dynamic-simulation validation, they were used to compare SCM-PH, SCM-CL, and SCM-TI with the modified IDA-ICE reference model of the I-DIFFER concept.

The numerical indicators were interpreted together with the graphical results. Time-series plots were used to show how the calculated and reference values developed over selected representative periods, while scatter plots were used to show their agreement relative to the line of perfect agreement. The indicators were calculated over the full available validation period, whereas the figures were limited to shorter periods in order to make the behaviour easier to interpret. This combination allowed both the overall magnitude of the deviation and its development over time to be assessed.

4.3 Experimental validation

This section provides the validation of the simplified calculation methods using full-scale experimental measurements from The Cube test facility at Aalborg University. The purpose is to assess how well the simplified methods reproduce the measured thermal behaviour of the double-skin façade in pre-heating mode and in cooling mode operated as an external air curtain. Since the experimental reference cases describe the façade system only, this part of the validation concerns the DSF subsystem rather than the integrated DSF–DCV concept. The pre-heating reference case is based on Kalyanova and Lund, 2014b, while the cooling reference case is based on Kalyanova and Lund, 2014a.

The experimental validation is based on measurements from *The Cube*, a full-scale outdoor test facility developed for double-skin façade research at Aalborg University. The facility consists of a south-facing DSF connected to an adjacent experiment room, together with an instrument room and a plant room. Figure 4.1 illustrates the exterior of the facility, the overall plan layout, and the plan and section of the experiment room and façade geometry used in the present validation.

(a) Exterior view

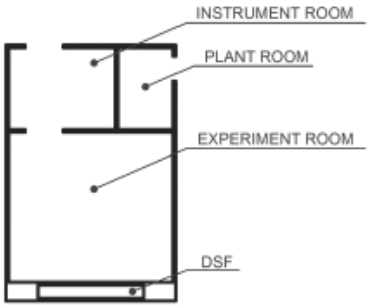

(b) Test facility layout

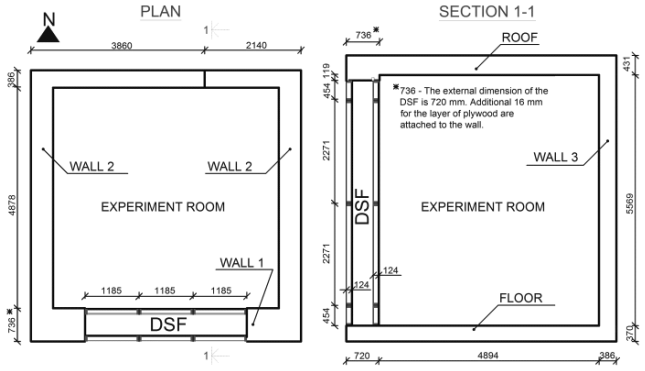

(c) Plan and section of the experiment room and double-skin façade

Figure 4.1: *The Cube* experimental facility used for DSF validation: (a) exterior view, (b) test facility layout, and (c) plan and section of the experiment room and double-skin façade. Adapted from Kalyanova and Lund, 2014a, 2014b.

To define the experimental reference case for both operating modes, the internal dimensions of the DSF cavity and the adjacent experiment room are summarised in Table 4.1. These dimensions describe the shared physical geometry of *The Cube* used in the present validation and provide a common geometric reference for the pre-heating and cooling cases. More detailed information on the façade construction and the experimental setup is given in Kalyanova and Lund, 2014a, 2014b.

Table 4.1: Internal dimensions of *The Cube* used in the experimental validation

Zone	Width [m]	Depth [m]	Height [m]
DSF cavity	3.555	0.580	5.450
Experiment room	5.168	4.959	5.584

Source: Kalyanova and Lund, 2014a, 2014b.

The experimental reference variables used in the pre-heating and cooling cases are summarised in Table 4.2 together with their role in the simplified calculation methods. The table distinguishes between variables used as inputs and variables calculated by the methods for comparison against the measured reference data. The main validation variables are the mean cavity air temperature, outlet cavity air temperature, and heating and cooling energy need, while air flow rate is included as a supporting variable, particularly in cooling mode.

Table 4.2: Experimental reference variables and corresponding SCM inputs and outputs used for pre-heating and cooling mode validation

Parameter	Unit	Exp. ref.-PH	Exp. ref.-CL	SCM-PH	SCM-CL
Input variables					
Period	–	09.11–30.11.2006	01.10–15.10.2006	Applied	Applied
Indoor air temperature, T_i	°C	22 (constant)	22 (constant)	Input	Input
Outdoor air temperature, T_e	°C	Measured	Measured	Input	Input
Solar radiation, I_s	W/m^2	Measured	Measured	Input	Input
Inlet cavity air temperature, $T_{c,in}$	°C	Measured	Measured	Input ($= T_e$)	Input ($= T_e$)
Main validation variables					
Mean cavity air temperature, $T_{c,mean}$	°C	Measured	Measured	Calculated	Calculated
Outlet cavity air temperature, $T_{c,out}$	°C	Measured	Measured	Calculated	Calculated
Heating energy need, $Q_{H,nd}$	kWh	Measured	Measured	Calculated	Calculated
Cooling energy need, $Q_{C,nd}$	kWh	Measured	Measured	Calculated	Calculated
Supporting variable					
Air flow rate, q_v	m^3/h	143 (constant)	Measured	Input	Calculated

Source: Kalyanova and Lund, 2014a, 2014b.
Note: Calculated SCM outputs were compared with measured values from the experimental reference data. In cooling mode, air flow rate was included as a supporting variable for interpreting the thermal behaviour of the DSF rather than as the primary validation target.

The following subsections present the validation results separately for the two operating modes. Section 4.3.1 addresses pre-heating mode, for which airflow is mechanically driven and constant, whereas Section 4.3.2 addresses cooling mode, in which the cavity operates as an external air curtain with naturally driven airflow.

4.3.1 Pre-heating mode

In pre-heating mode, outdoor air enters the DSF cavity through the bottom opening, is preheated while passing through the cavity, and is then supplied to the interior through the top opening. The experimental reference case is based on full-scale measurements from *The Cube* reported in Kalyanova and Lund, 2014b and represents mechanically driven operation with constant airflow. In this subsection, SCM-PH is evaluated against the experimental reference through comparison of the mean cavity temperature, outlet cavity temperature, heating energy need, and cooling energy need.

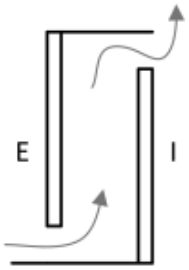

Figure 4.2: Schematic illustration of pre-heating mode.

For the pre-heating reference case, the experimental period extends from 9 to 30 November 2006. The experiment room temperature was maintained at approximately 22 °C, and the airflow through the cavity was kept constant at 143 m^3/h by the mechanical ventilation system. In the present validation, outdoor air temperature and solar radiation were used as inputs to SCM-PH, while the calculated mean cavity temperature, outlet cavity temperature, heating energy need, and cooling energy need were compared with the experimental reference data.

The validation results are presented through summary energy comparisons, time-series plots, scatter plots, and the corresponding validation metrics.

Total energy need

Figure 4.3 compares the measured and calculated total heating and cooling energy need for the pre-heating reference case over the full measurement period.

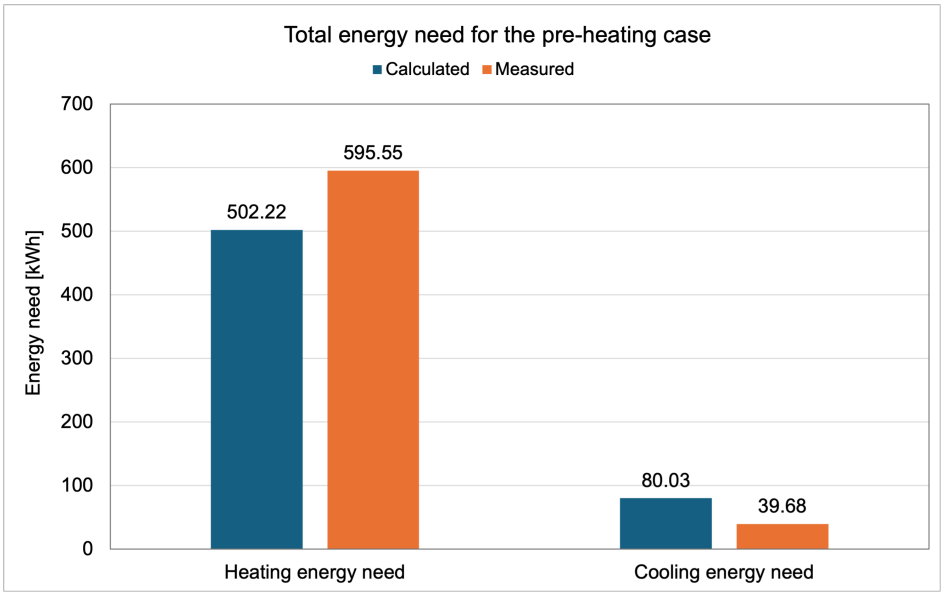

Figure 4.3: Comparison of measured and calculated total heating and cooling energy need for the pre-heating reference case over the full measurement period.

Figure 4.3 shows that SCM-PH reproduces the overall pattern of the pre-heating case, as heating remains the dominant energy requirement. The calculated heating energy need is 502.22 kWh, compared with the measured value of 595.55 kWh, while the calculated cooling energy need is 80.03 kWh, compared with the measured value of 39.68 kWh. This means that the model underestimates heating by about 16% and overestimates cooling by about 102%. In other words, SCM-PH predicts too little heating and too much cooling, which suggests that the simplified calculation overestimates solar gains. As a result, some of the energy that appears as heating need in the measurements instead appears as cooling need in the model. Even when both parts are combined, the calculated total energy need is 582.25 kWh, whereas the measured total is 635.23 kWh, so the overall result is still underestimated by about 8%.

Heating and cooling energy need over time

Figures 4.4 and 4.5 compare the measured and calculated heating and cooling energy need over the pre-heating reference period, including detailed views for 11–15 November.

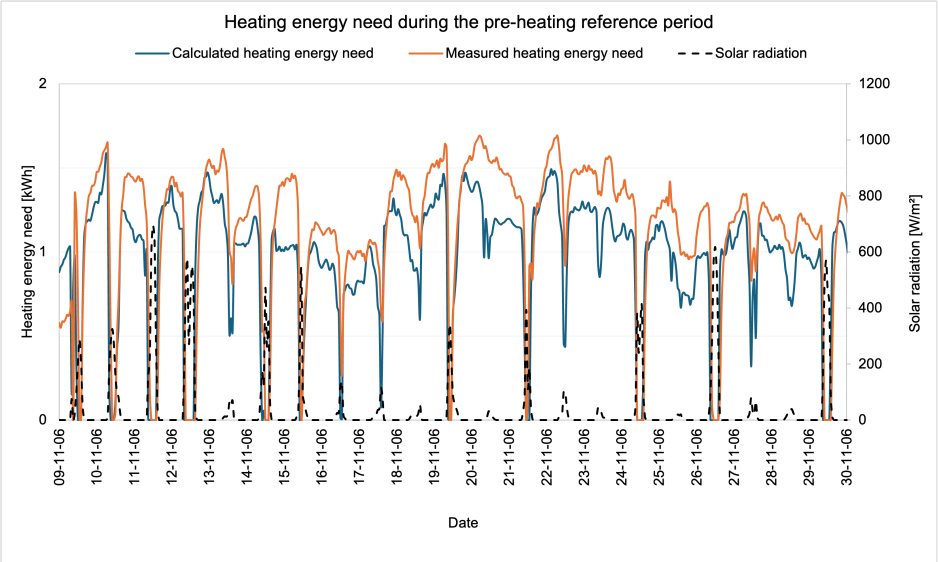

(a) Entire measurement period.

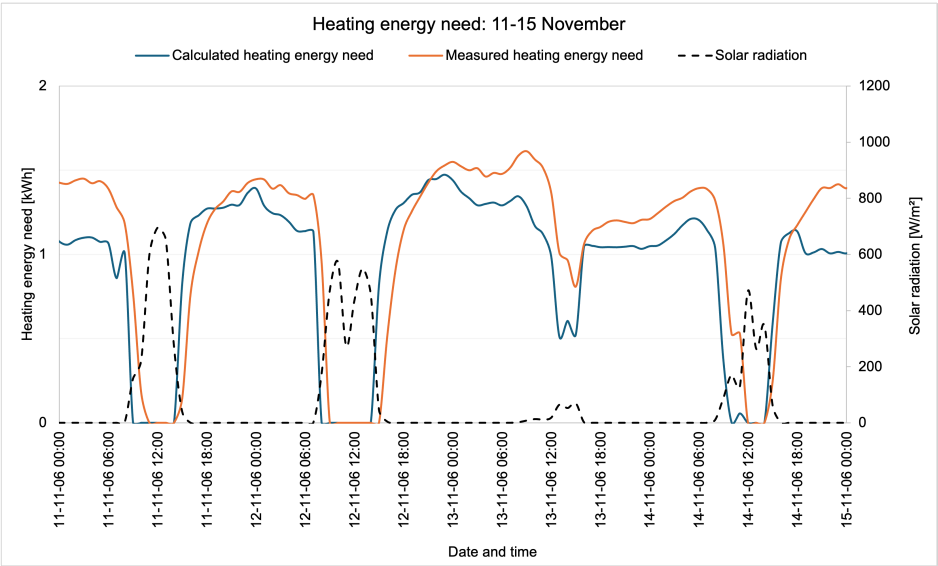

(b) Detailed view for 11-15 November.

Figure 4.4: Comparison of measured and calculated heating energy need during the pre-heating reference period, together with solar radiation.

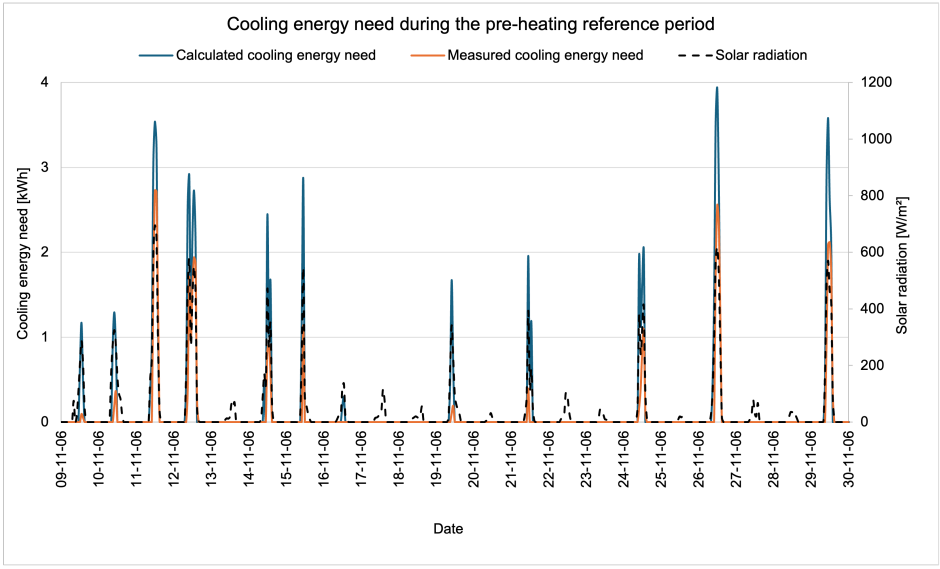

(a) Entire measurement period.

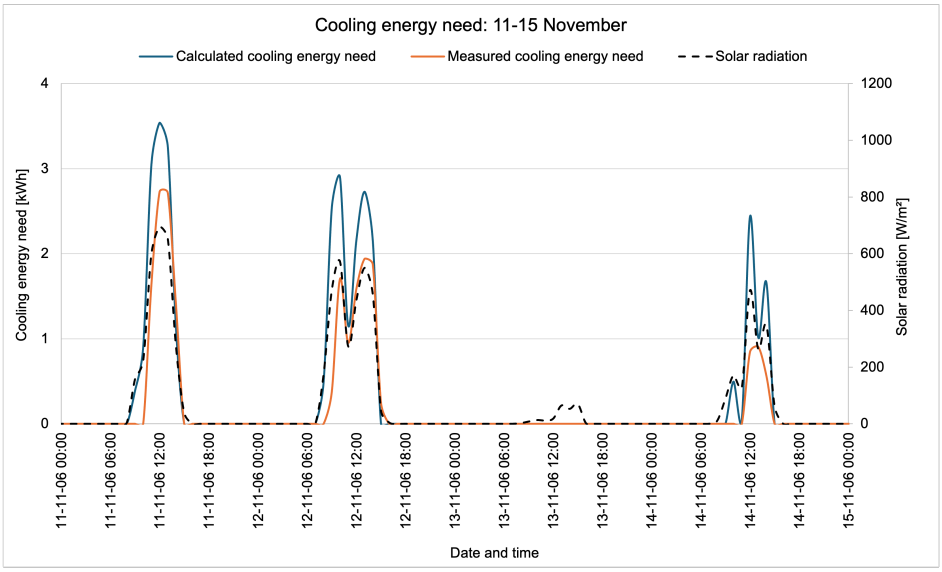

(b) Detailed view for 11-15 November.

Figure 4.5: Comparison of measured and calculated cooling energy need during the pre-heating reference period, together with solar radiation.

Figures 4.4 and 4.5 show that SCM-PH follows the main variation in both heating and cooling energy need over the pre-heating period. For heating, the model generally follows the measured trend, but the calculated values stay lower for most of the period. This matches the underestimation already seen in the total energy

comparison. For cooling, the model captures the main peaks, but they are often larger than in the measurements. This is most evident on days with higher solar radiation. The detailed views for 11-15 November show the same pattern: the model captures the general response over time, but the heating and cooling peak sizes are not reproduced as well. This behaviour becomes clearer in the cavity-temperature comparisons, where the effect of solar radiation on the DSF thermal response can be examined more directly.

The summary values support the same pattern. For heating energy need, the calculated average is 0.95 kWh compared with 1.13 kWh measured, while the maximum value is 1.59 kWh compared with 1.69 kWh measured. For cooling energy need, the calculated average is 0.15 kWh compared with 0.08 kWh measured, and the calculated maximum is 3.93 kWh compared with 2.73 kWh measured. This shows that heating is underestimated on average, whereas cooling is overestimated both on average and at peak conditions. Additional summary values for pre-heating mode are provided in Table A.1 in the appendix.

Cavity temperatures over time

Figures 4.6 and 4.7 compare the measured and calculated mean cavity temperature and outlet cavity temperature over the pre-heating reference period, including detailed views for 26-30 November.

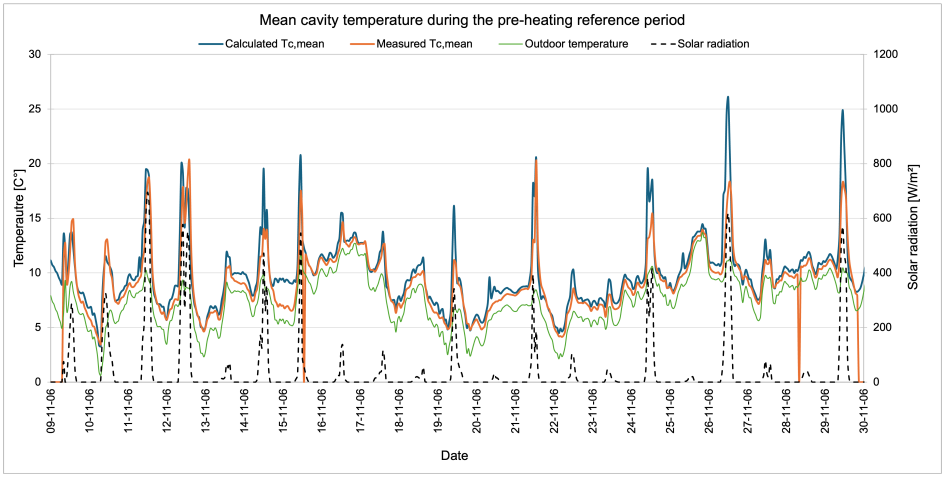

(a) Entire measurement period.

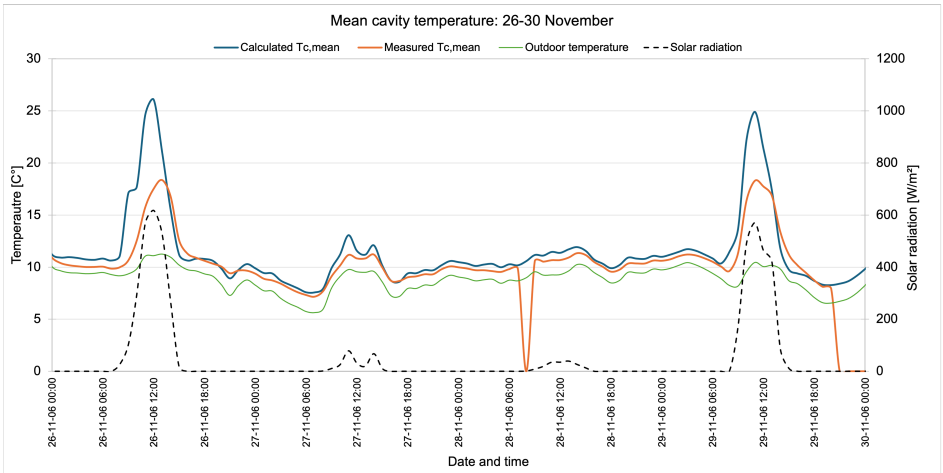

(b) Detailed view for 26-30 November.

Figure 4.6: Comparison of measured and calculated mean cavity temperature during the pre-heating reference period, together with outdoor temperature and solar radiation.

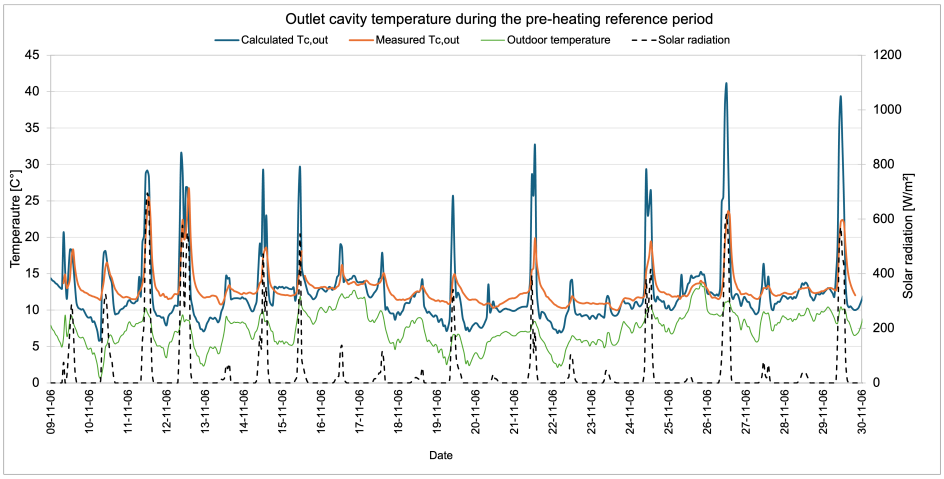

(a) Entire measurement period.

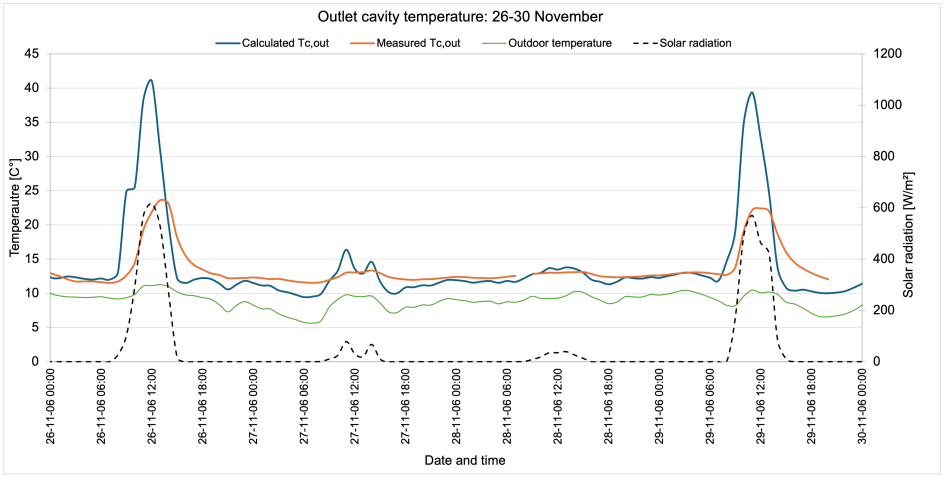

(b) Detailed view for 26-30 November.

Figure 4.7: Comparison of measured and calculated outlet cavity temperature during the pre-heating reference period, together with outdoor temperature and solar radiation.

Figures 4.6 and 4.7 show that SCM-PH follows the main variation in both mean cavity temperature and outlet cavity temperature during the pre-heating period. The timing of the main peaks is generally reproduced well, especially in the detailed views for 26-30 November. Outside the peak periods, the agreement is generally closer, particularly for the mean cavity temperature. For the mean cavity temperature, the agreement is reasonably good over much of the period, though the calculated values tend to increase during stronger peaks. For outlet cavity temperature, the difference is more evident. The calculated peaks are usually higher than the measured ones. This suggests that the model reacts too strongly to solar gains

in the cavity. The same tendency was already seen in the overestimation of the cooling energy need. This becomes clearer in the scatter plots and the validation metrics presented next.

The summary temperature values show a similar tendency. For mean cavity temperature, the calculated average is 9.99 °C compared with 9.30 °C measured, while the calculated maximum is 26.07 °C compared with 20.32 °C measured. For outlet cavity temperature, the calculated average is 12.47 °C compared with 12.95 °C measured, whereas the calculated maximum reaches 41.04 °C compared with 26.66 °C measured. This indicates that the general temperature level is reproduced more closely than the higher solar-driven peaks. Additional summary values for pre-heating mode are provided in Table A.1 in the appendix.

Scatter plots and validation metrics

Figures 4.8 and 4.9 summarise the agreement between SCM-PH and the experimental reference for the main validation variables in pre-heating mode.

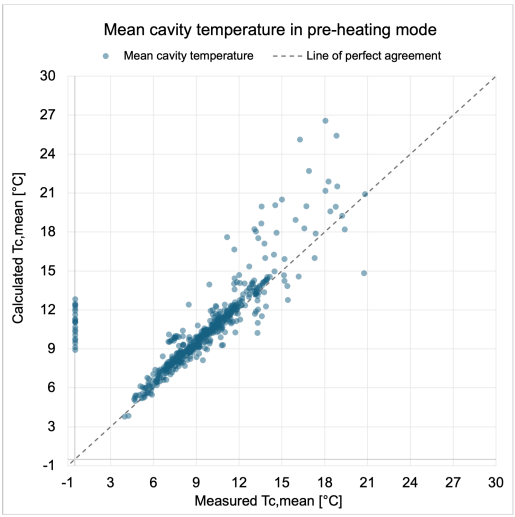

(a) Mean cavity temperature.

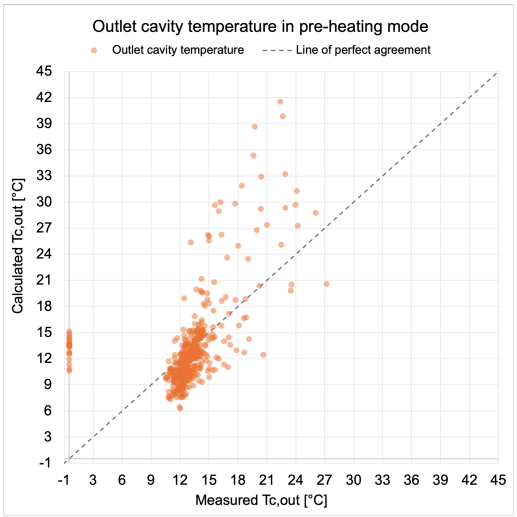

(b) Outlet cavity temperature.

Figure 4.8: Scatter plots comparing measured and calculated cavity temperatures in pre-heating mode.

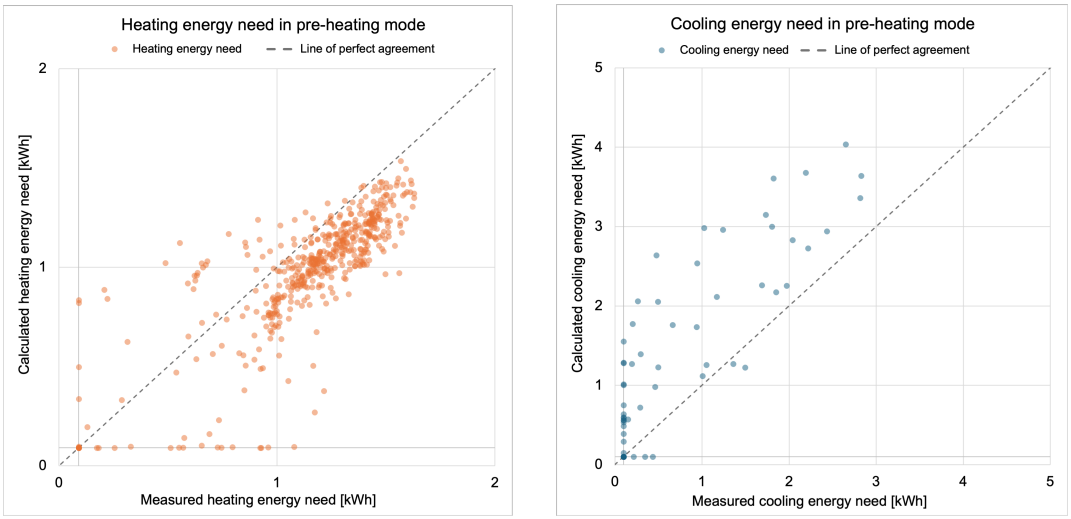

(a) Heating energy need.

(b) Cooling energy need.

Figure 4.9: Scatter plots comparing measured and calculated energy need in pre-heating mode.

Figures 4.8 and 4.9 show the same pattern as the time-series plots. For the mean cavity temperature, most points stay fairly close to the line of perfect agreement, though the model tends to yield higher values at the upper end. For outlet cavity temperature, the spread is wider, and the mismatch is more evident, especially at higher values. The same applies to the energy plots. Heating energy need follows the overall trend reasonably well, but the calculated values are often lower than the measured ones. Cooling energy need is more scattered, and most points lie above the line of perfect agreement, indicating that SCM-PH often overestimates cooling energy need during the pre-heating period. Table 4.3 shows the same pattern, with weaker agreement for outlet cavity temperature and cooling energy need than for mean cavity temperature and heating energy need.

Table 4.3 reports the validation metrics based on hourly values for the main variables in pre-heating mode.

Table 4.3: Validation metrics for pre-heating mode based on experimental reference data

Variable	n	Calculated mean	Measured mean	Bias	MAE	RMSE
Mean cavity temperature [°C]	528	9.990	8.926	1.064	1.247	2.507
Outlet cavity temperature [°C]	528	12.474	12.431	0.043	2.658	4.212
Heating energy need [kWh]	528	0.951	1.128	-0.177	0.224	0.278
Cooling energy need [kWh]	528	0.152	0.075	0.076	0.080	0.310

Table 4.3 confirms the main trends already seen in the figures. The mean cavity temperature shows moderate agreement, with a positive bias of 1.064 °C, indicating that SCM-PH tends to overestimate this variable. Outlet cavity temperature has a much smaller bias, but the larger MAE and RMSE. Heating energy need is underestimated, as indicated by the negative bias of -0.177 kWh, while cooling energy need is overestimated, with a positive bias of 0.076 kWh, which agrees with the results from the time-series and scatter-plot comparisons.

Overall, the experimental validation in pre-heating mode shows that SCM-PH reproduces the overall thermal behaviour of the DSF with reasonable agreement. The strongest agreement is found for mean cavity temperature and heating energy need, while outlet cavity temperature and cooling energy need show larger deviations. This suggests that the simplified method captures the general response of the pre-heating case, but tends to react too strongly under higher solar gains.

4.3.2 Cooling mode

In cooling mode, the DSF operates as an external air curtain, with both cavity openings connected to the outdoor environment. Outdoor air enters at the bottom, is heated while passing through the cavity, and leaves again through the top opening. The experimental reference case is based on full-scale measurements from *The Cube* reported by Kalyanova and Lund, 2014a and represents naturally driven cavity airflow in external air curtain mode.

Figure 4.10 illustrates the airflow path in cooling mode, where the DSF operates as an external air curtain with naturally driven cavity airflow.

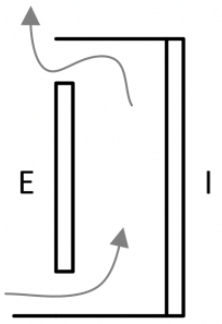

Figure 4.10: Illustration of the airflow path in cooling mode, where the DSF operates as an external air curtain.

For the cooling reference case, the experimental period extends from 1 to 15 October 2006. The experiment room temperature was maintained at approximately 22 °C, while the cavity airflow was naturally driven and varied over time. In

the present validation, outdoor air temperature and solar radiation were used as inputs to SCM-CL. The cavity airflow was not specified as an input, but was predicted within SCM-CL using the Hellström-based approximation. The calculated mean cavity temperature, outlet cavity temperature, heating energy need, cooling energy need, and airflow were then compared with the experimental reference data.

The validation results for cooling mode are presented through total energy comparisons, time-series plots, scatter plots, and the corresponding validation metrics.

Total energy need

Figure 4.11 compares the measured and calculated total heating and cooling energy need for the cooling reference case over the entire measurement period.

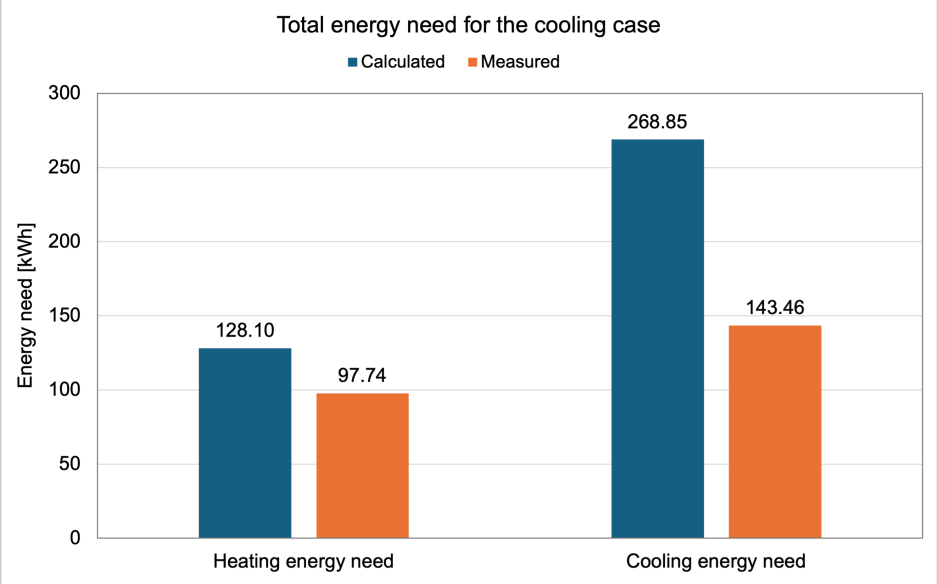

Figure 4.11: Comparison of measured and calculated total heating and cooling energy need for the cooling reference case over the entire measurement period.

Figure 4.11 shows that SCM-CL overestimates both the total heating energy need and the total cooling energy need relative to the experimental reference. The calculated heating energy need is 128.10 kWh, compared with the measured value of 97.74 kWh, which corresponds to an overestimation of about 31%. The calculated cooling energy need is 268.85 kWh, compared with the measured value of 143.46 kWh, which corresponds to an overestimation of about 87%. When heating and cooling are combined, the total calculated energy need is 396.95 kWh, whereas the measured total is 241.20 kWh, giving an overall overestimation of about 65%. This shows that SCM-CL reproduces the cooling-dominated character of the case,

but it overpredicts the magnitude of both heating and cooling energy need, especially cooling.

Heating and cooling energy need over time

Figures 4.12 and 4.13 compare the measured and calculated heating and cooling energy need over the cooling reference period, including detailed views for selected periods.

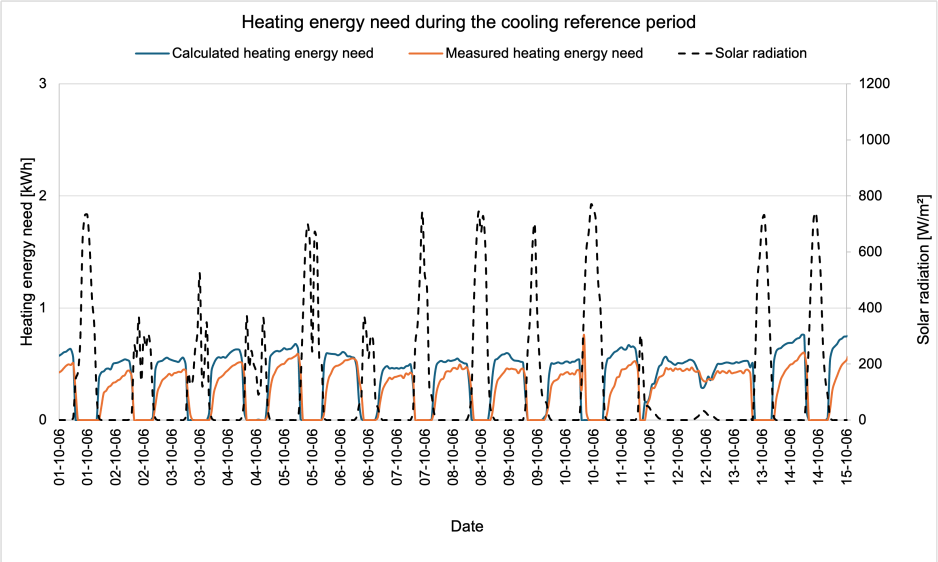

(a) Entire measurement period.

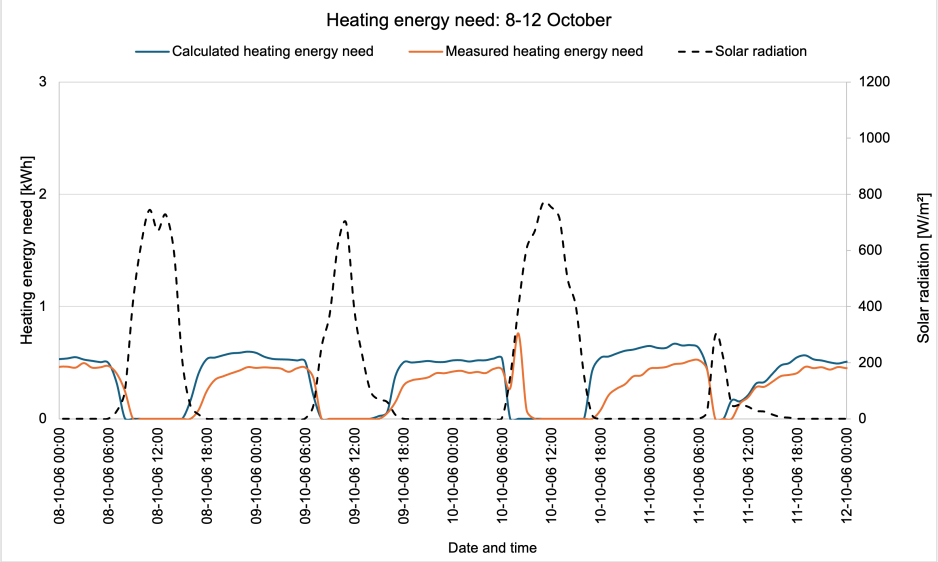

(b) Detailed view for 8-12 October.

Figure 4.12: Comparison of measured and calculated heating energy need during the cooling reference period, together with solar radiation.

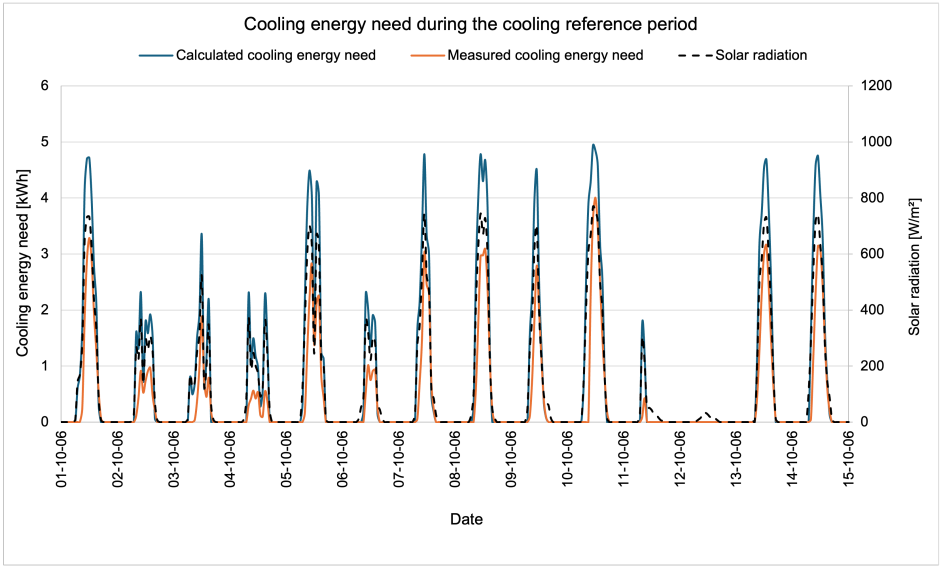

(a) Entire measurement period.

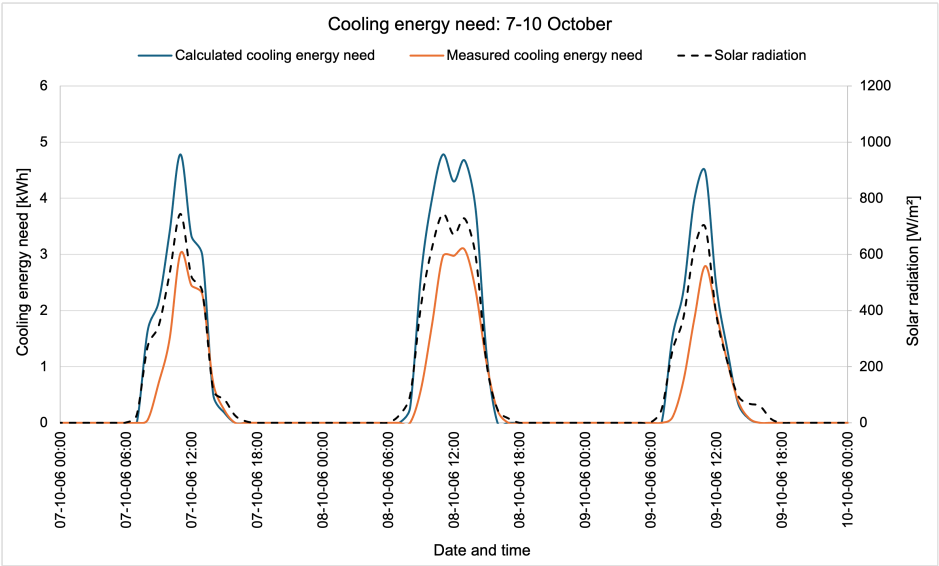

(b) Detailed view for 7-10 October.

Figure 4.13: Comparison of measured and calculated cooling energy need during the cooling reference period, together with solar radiation.

Figures 4.12 and 4.13 show that SCM-CL follows the main variation in both heating and cooling energy need during the cooling reference period. For heating, the model generally follows the measured trend, but the calculated values are often higher than the measured ones over much of the period. For cooling, the timing

of the main peaks is reproduced well, but the calculated peaks are usually larger than the measured ones. This is most evident during periods with stronger solar radiation. The detailed views show the same pattern: SCM-CL follows the general response over time, but the peak heating and cooling values are not reproduced as accurately. This behaviour becomes clearer in the cavity-temperature comparisons, where the effect of solar radiation on the DSF thermal response can be examined more directly.

The summary values show the same pattern. For heating energy need, the calculated average is 0.36 kWh compared with 0.27 kWh measured, while both the calculated and measured maximum are 0.76 kWh. For cooling energy need, the calculated average is 0.75 kWh compared with 0.40 kWh measured, and the calculated maximum is 4.94 kWh compared with 4.00 kWh measured. This confirms that heating is slightly overestimated on average, while cooling is overestimated both on average and at peak conditions. Additional summary values for cooling mode are provided in Table A.2 in the appendix.

Cavity temperatures over time

Figures 4.14 and 4.15 compare the measured and calculated mean cavity temperature and outlet cavity temperature over the cooling reference period, including detailed views for selected periods.

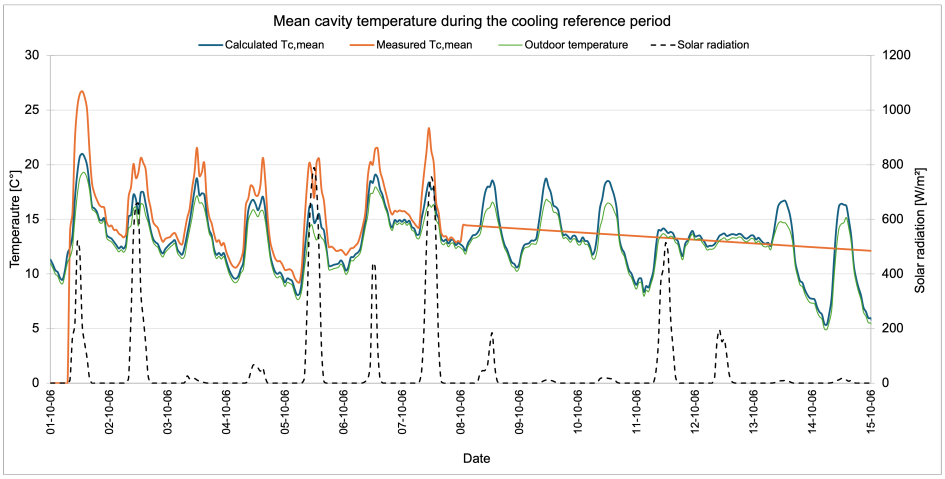

(a) Entire measurement period.

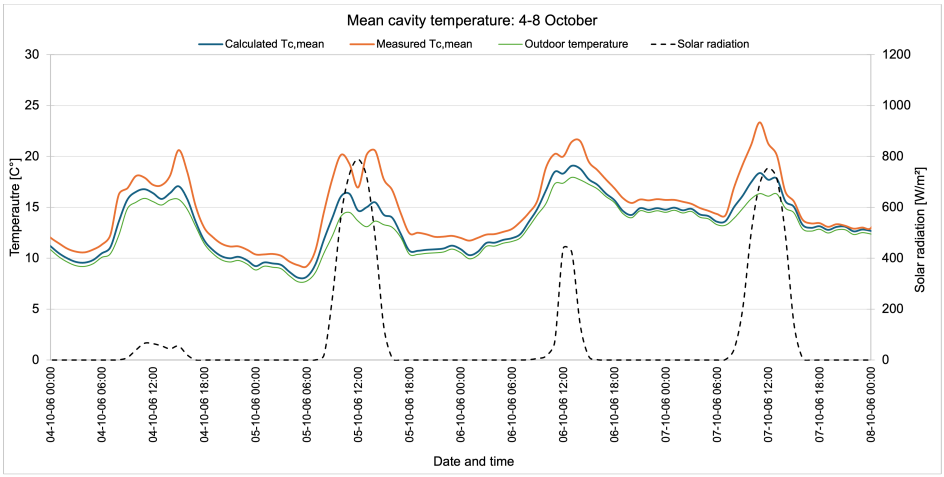

(b) Detailed view for 4-8 October.

Figure 4.14: Comparison of measured and calculated mean cavity temperature during the cooling reference period, together with outdoor temperature and solar radiation.

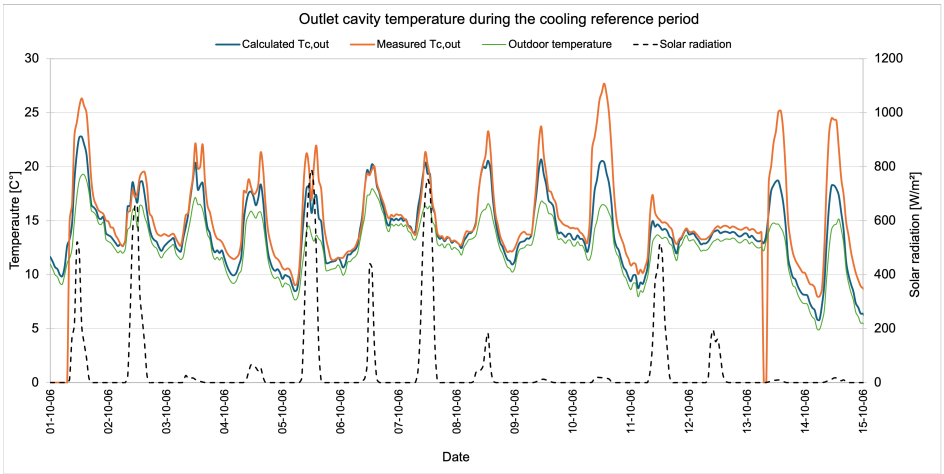

(a) Entire measurement period.

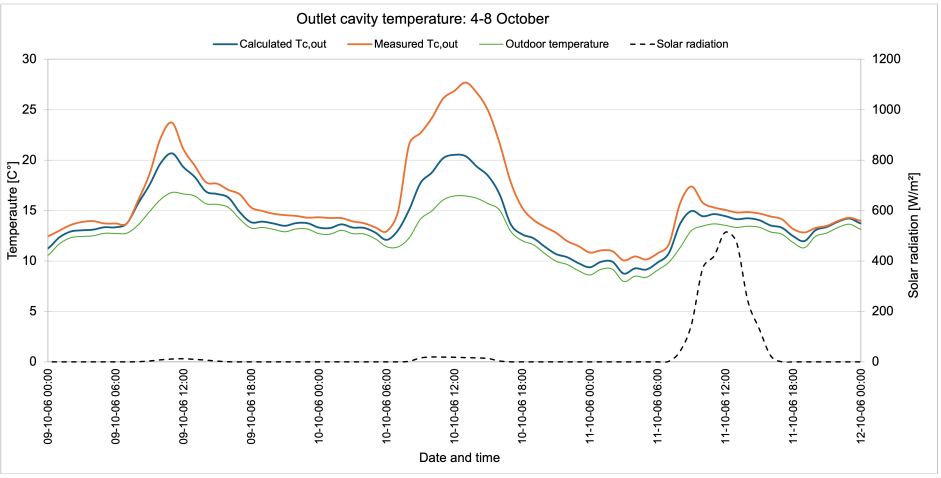

(b) Detailed view for 9-12 October.

Figure 4.15: Comparison of measured and calculated outlet cavity temperature during the cooling reference period, together with outdoor temperature and solar radiation.

Figures 4.14 and 4.15 show that SCM-CL follows the main variation in both mean cavity temperature and outlet cavity temperature during the cooling reference period. The timing of the main peaks is generally reproduced well, especially in the detailed views. For mean cavity temperature, the agreement is reasonably good over much of the period, although the calculated values are often lower than the measured ones during stronger peaks. The same pattern appears for outlet cavity temperature, where the calculated peaks also tend to stay below the measured values. This suggests that SCM-CL captures the overall cavity response, but underestimates the temperature rise in the cavity during periods with stronger solar

gains. The relation between these temperature deviations and the energy results becomes clearer in the scatter plots and validation metrics presented next.

The summary temperature values support the same reading. For mean cavity temperature, the calculated average is 13.15 °C compared with 14.26 °C measured, while the calculated maximum is 21.00 °C compared with 26.73 °C measured. For outlet cavity temperature, the calculated average is 13.80 °C compared with 15.36 °C measured, and the calculated maximum is 22.77 °C compared with 27.69 °C measured. This shows that the model underestimates both the general cavity temperature level and the stronger temperature peaks. Additional summary values for cooling mode are provided in Table A.2 in the appendix.

For airflow, the filtered comparison gives an average of 1864.51 m^3/h calculated versus 1328.23 m^3/h measured. The calculated minimum is 1196.21 m^3/h, whereas the measured minimum is 299.38 m^3/h, while the maximum values are closer at 3516.53 m^3/h calculated and 3754.19 m^3/h measured. This suggests that the model does not reproduce the lower airflow periods well.

Scatter plots and validation metrics

Figures 4.16 and 4.17 summarise the agreement between SCM-CL and the experimental reference for the main validation variables in cooling mode.

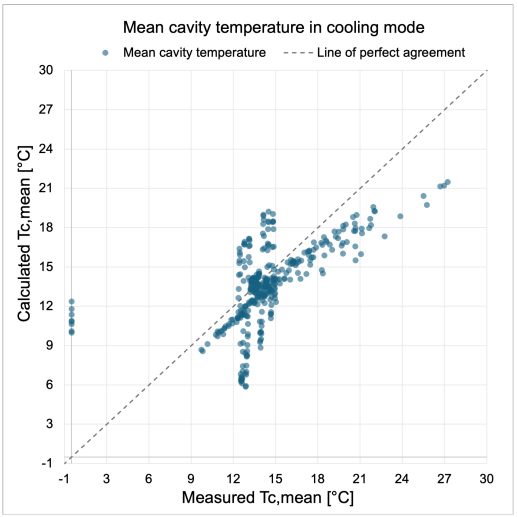

(a) Mean cavity temperature.

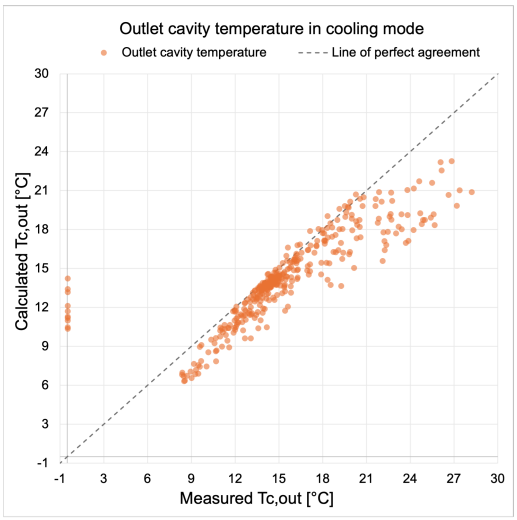

(b) Outlet cavity temperature.

Figure 4.16: Scatter plots comparing measured and calculated cavity temperatures in cooling mode.

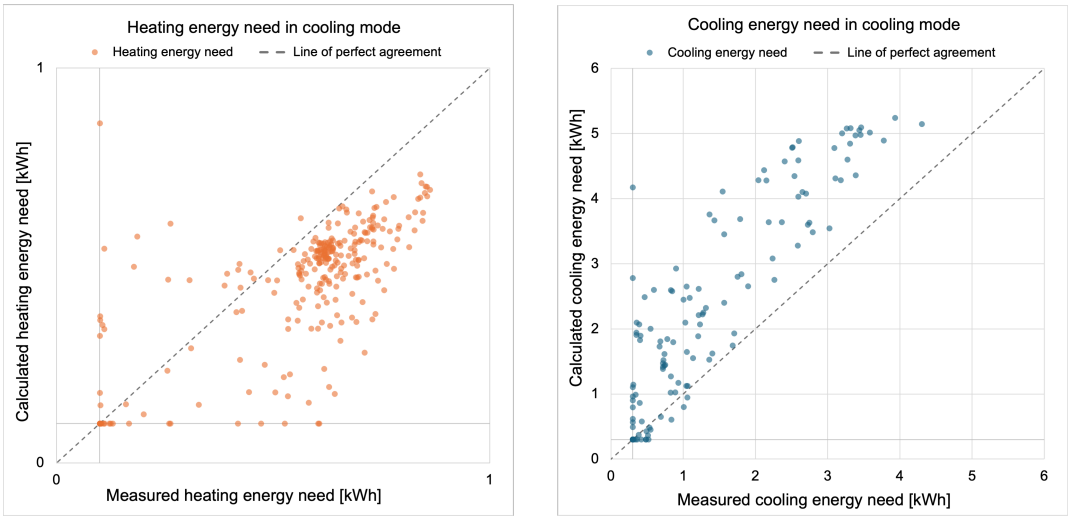

(a) Heating energy need.

(b) Cooling energy need.

Figure 4.17: Scatter plots comparing measured and calculated energy need in cooling mode.

Figures 4.16 and 4.17 show the same pattern as the time-series plots. For mean cavity temperature, many points lie reasonably close to the line of perfect agreement, although the model tends to give lower values at the upper end. For outlet cavity temperature, the spread is smaller, but most of the higher values still fall below the line, which means that the model tends to underestimate the stronger peaks. The same applies to the energy plots. Heating energy need follows the general trend, but the calculated values are often higher than the measured ones. Cooling energy need is more scattered, and most points lie above the line of perfect agreement, showing that SCM-CL tends to overestimate cooling during the cooling reference period. Table 4.4 shows the same pattern in the validation metrics.

Table 4.4 reports the validation metrics based on hourly values for the main variables in cooling mode.

Table 4.4: Validation metrics for cooling mode based on experimental reference data

Variable	n	Calculated mean	Measured mean	Bias	MAE	RMSE
Mean cavity temperature [°C]	360	13.145	13.940	-0.795	2.182	2.991
Outlet cavity temperature [°C]	360	13.796	14.929	-1.133	1.808	2.891
Heating energy need [kWh]	360	0.356	0.272	0.084	0.109	0.157
Cooling energy need [kWh]	360	0.747	0.398	0.348	0.358	0.753
Airflow [m^3/h]	360	1860.2	1092.1	768.1	1080.2	1302.3

Table 4.4 confirms the same pattern seen in the figures. Mean cavity temperature is underestimated overall, as shown by the negative bias of -0.795 °C, and outlet cavity temperature as well, with a negative bias of -1.133 °C. Heating energy need is slightly overestimated, as indicated by the positive bias of 0.084 kWh, while cooling energy need is more strongly overestimated, with a positive bias of 0.348 kWh.

In summary, the experimental validation in cooling mode shows that SCM-CL reproduces the general thermal behaviour of the DSF with mixed agreement. Outlet cavity temperature and the energy variables follow the measured behaviour reasonably well, whereas mean cavity temperature show larger deviations. This indicates that the simplified method is able to represent the main response of the cooling case, but it underestimates the cavity temperature rise and tends to overpredict the resulting energy need.

Taken together, the experimental validation shows that the simplified methods reproduce the main thermal behaviour of the DSF with reasonable agreement, although the accuracy differs across variables and operating modes. In pre-heating mode, the main deviations are linked to stronger predicted solar-driven peaks and higher cooling energy need, while in cooling mode the cavity temperatures are generally lower than measured and the cooling energy need is again overestimated. This provides a basis for the next step of validation against the dynamic simulation reference.

4.4 Dynamic simulation validation

4.4.1 Validation purpose and reference case

Validation is important for several reasons in this context. The simplified framework uses calculation methods that were not originally developed for the I-DIFFER concept. Applying them together in a single hourly tool introduces simplifications whose effect on results is not known in advance. The most significant of these is the absence of thermal mass, which means the framework reacts instantly to changing outdoor conditions without storing heat between hours as a real building would. Comparing the framework against a detailed dynamic simulation that includes thermal mass shows how large this effect is for each operating mode and whether the results are still physically reasonable for early-stage comparison. The goal is not to show that the simplified framework produces the same results as a full simulation. It is to check that the framework captures the dominant thermal behaviour of the I-DIFFER concept well enough to support meaningful and transparent comparison between renovation strategies.

Two validation levels are therefore used. The experimental validation in Section 4.3 addressed the DSF subsystem against full-scale measurements. The dynamic

simulation validation addresses the integrated I-DIFFER concept at room level, including the interaction between the facade cavity and the conditioned room.

The reference for the dynamic simulation validation is a modified version of the IDA-ICE model of the I-DIFFER concept developed by Bugenings et al. (2022) and provided by Aalborg University. The case study building is a south-facing school classroom located in Aalborg, Denmark, with a floor area of 50 m^2 and internal gains of 2500 W applied during occupied hours, representing 21 occupants and equipment. The complete building geometry, envelope properties, glazing specifications, and system parameters are described in detail in Chapter 5.

The original IDA-ICE model of Bugenings et al. (2022) uses a more complex operation logic than the simplified framework. For the purpose of this validation, the model was modified so that each operating mode was represented as a single constant mode running throughout the full year, with no mode switching, no shading control, no ORM30 threshold, and no occupancy-based control applied. This modification was necessary to allow direct mode-by-mode comparison between the simplified framework and the reference model.

Three separate single-mode simulations were produced, one for pre-heating mode, one for cooling mode, and one for transparent insulation mode. In pre-heating and cooling mode the mechanical ventilation system operates at a maximum airflow rate of 900 m^3/h during occupied hours and is turned off during unoccupied hours. In transparent insulation mode no mechanical ventilation is applied. Cooling energy need was excluded from the modified IDA-ICE model setup since the focus of the dynamic validation was on cavity temperature behaviour and heating energy need.

The dynamic simulation reference was run using the Danish Design Reference Year (DRY10). The DRY10 outdoor air temperature and solar radiation on the DSF surface were provided together with the simulation outputs by Aalborg University and used directly as inputs to the simplified framework for the dynamic validation. This differs from the measured hourly weather data, Copenhagen, Denmark, used in the case scenario in Chapters 5 and 6, which means the validation results cannot be directly compared with the case scenario results. They do however provide a consistent basis for checking whether the simplified framework behaves in line with the reference model under the same climate conditions.

4.4.2 Validation variables, metrics, and period

The dynamic simulation validation focused on two main variables: mean DSF cavity air temperature and heating energy need. Mean cavity temperature characterises the thermal state of the DSF cavity and directly influences both the ven-

tilation preheating benefit and the transmission losses through the inner facade. Heating energy need is the primary output used for scenario comparison in Chapter 6.

The validation was carried out separately for each of the three operating modes using the full year of 8760 hourly values as the validation period, giving a consistent and complete basis for statistical comparison.

Agreement between the simplified framework and the dynamic simulation reference was assessed using three statistical metrics defined in Section 3.6, following (Karlsen et al., 2016): Bias, MAE, and RMSE. Bias shows whether the framework tends to calculate values that are consistently higher or lower than the reference. MAE shows the average size of the hourly differences regardless of direction and gives a straightforward sense of how far off the framework is on a typical hour. RMSE is similar to MAE but reacts more strongly to hours where the difference is particularly large. Using all three together gives a clearer picture of framework performance.

The validation results for each mode are presented through a statistical summary table, scatter plots of hourly cavity temperatures, time series comparisons over representative periods, and monthly and weekly heating energy comparisons. The statistical metrics were calculated over the full 8760-hour validation period while the graphical comparisons focus on representative shorter periods to make the behaviour easier to interpret.

4.4.3 Pre-heating mode

In pre-heating mode the DSF cavity openings are open and mechanical ventilation draws outdoor air through the bottom inlet, picks up heat from solar radiation, and supplies it to the room through the top outlet. The simplified framework calculation for this mode follows the BESTFACADE pre-heating formulation described in Section 3.3.

The statistical summary for mean cavity temperature and heating energy need over the full 8760-hour validation period is shown in Table 4.5.

Table 4.5: Statistical summary for pre-heating mode dynamic validation

Variable	SCM-PH	IDA-ICE	Bias	MAE	RMSE
Mean cavity temperature [°C]	20.1	17.4	2.67	6.11	11.51
Max cavity temperature [°C]	121.2	51.7	–	–	–
Min cavity temperature [°C]	-10.4	-6.0	–	–	–
Total heating energy [kWh]	4302	4146	–	–	–
Heating demand [kW mean]	0.49	0.47	0.02	0.28	0.52

The framework overestimates the mean cavity temperature by 2.67°C relative to the IDA-ICE reference. The MAE of 6.11°C and RMSE of 11.51°C indicate that while the mean agreement is reasonable, the hourly deviations can be significant. The large difference between MAE and RMSE confirms that deviations are concentrated in a small number of hours with very large errors. During winter unoccupied hours, without solar radiation, the framework cavity temperature is slightly higher than the reference but follows the same pattern. With high solar radiation and ventilation off the framework produces unrealistic temperature peaks. During occupied hours when ventilation is active the framework cavity temperature is close to the reference and follows the same pattern. The effect of thermal mass becomes most visible in summer: when the reference model has absorbed heat during high-solar-radiation periods, it releases it slowly during the night, while the framework cavity temperature instantly falls toward, but above, the outdoor temperature.

The large difference between the maximum cavity temperatures, 121.23°C for the framework and 51.70°C for the reference, reflects this same limitation. During peak solar radiation hours, when ventilation is off, the framework reacts instantly to high solar input, producing unrealistic temperature peaks that the reference model doesn't show. The minimum cavity temperatures are similar between the two models: -10.36°C for the framework and -6.00°C for the reference, reflecting cold winter nights when both models closely track outdoor temperatures.

For heating energy, the framework provides a total of 4302 kWh, compared to 4146 kWh for the reference, a difference of 156 kWh, or 3.8%. It is important to note that this close overall agreement comes at a cost. The framework calculates heating energy during summer months when the reference shows zero demand, which increases the framework's total, while in winter, it underestimates heating energy because it supplies warmer, preheated air to the room under high solar radiation during occupied hours, compared to the reference. These two effects partially cancel each other, resulting in a close overall total. The MAE of 0.28 kW and RMSE of 0.52 kW indicate that while individual hours show deviations, the overall heating energy pattern is well captured by the framework.

The total annual heating energy comparison is shown in Figure 4.18

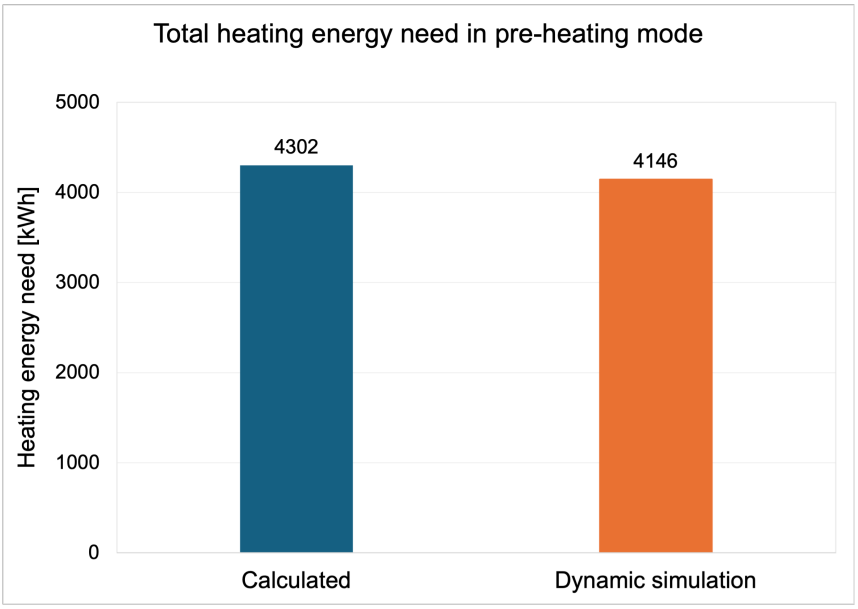

Figure 4.18: Total annual heating energy need for pre-heating mode. SCM-PH compared to IDA-ICE dynamic simulation reference.

The monthly heating energy comparison is shown in Figure 4.19. From January through March and again in November and December the framework underestimates heating energy compared to the reference. On days with high solar radiation the framework calculates a higher mean cavity temperature, meaning it supplies warmer preheated air to the room and calculates smaller ventilation losses. On days with lower solar radiation the framework calculates slightly lower cavity temperatures and slightly higher losses. During the winter months, when high-solar-radiation days dominate, the framework underestimates heating demand. From April through October, the framework overestimates heating energy. During July, August, and September, the IDA-ICE reference shows zero heating demand while the framework continues to calculate heating need. Analysis of the reference model indoor temperature data confirmed that room temperature in the reference did not fall below 20°C from approximately 3 June to 19 October, while the framework calculates heating demand whenever outdoor temperature drops below the setpoint. This occurs during unoccupied summer nights when internal gains are zero and the framework reacts instantly to falling outdoor temperatures without any thermal storage to slow the response. Pre-heating mode is not intended to operate during summer; in the real I-DIFFER system, ORM30 switching would activate cooling mode before this period. The summer heating demand is a direct consequence of the single-mode validation setup.

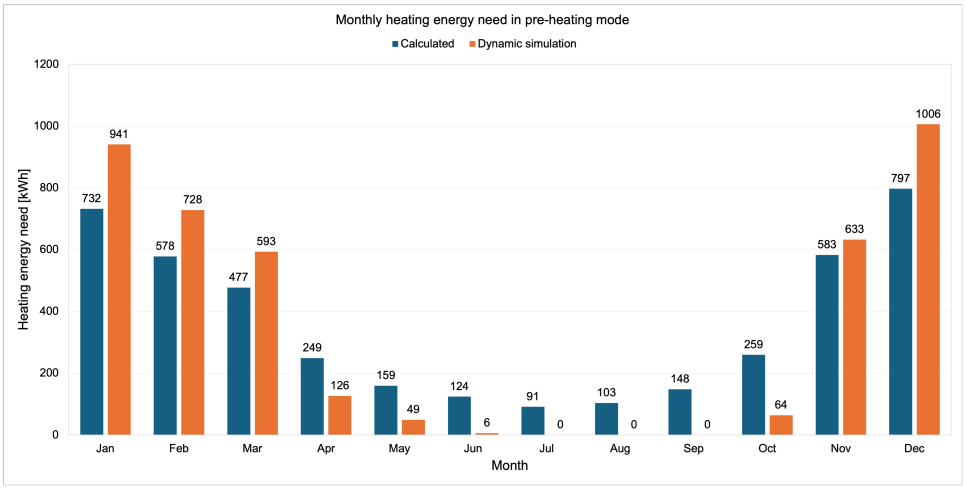

Figure 4.19: Monthly heating energy need for pre-heating mode. SCM-PH compared to IDA-ICE dynamic simulation reference

The average monthly mean cavity temperature comparison is shown in Figure 4.20. The framework consistently overestimates cavity temperature during winter months by approximately 4-5°C on average. This overestimation is most visible during unoccupied hours when ventilation is off. During occupied hours when mechanical ventilation is active, the framework cavity temperature aligns more closely with the reference as the active airflow moderates temperatures in both models. When solar radiation is higher during occupied hours, the alignment is better; on days with lower solar radiation, the framework shows a slight underestimation during occupied hours. The pattern is consistently driven by the combination of solar radiation intensity and ventilation activity.

During July, the framework cavity temperature closely tracks outdoor temperature during unoccupied hours without solar radiation, while the reference model stays above both the framework and outdoor temperature, retaining heat stored during the day. During August and September, the behaviour follows the same pattern but with an important difference. In these months, the framework produces high-temperature peaks during unoccupied hours with strong solar radiation, while also falling more quickly toward outdoor temperatures than the reference during nights and low-radiation periods. This creates a trade-off: high overestimation during solar peaks and underestimation when solar radiation is absent, whereas the reference model with thermal mass maintains a more stable mean cavity temperature. In July and September, the higher solar radiation peaks bring the framework average closer to the reference average, while August shows an underestimation of average cavity temperature because the reference thermal mass keeps the cavity warmer during cool summer nights.

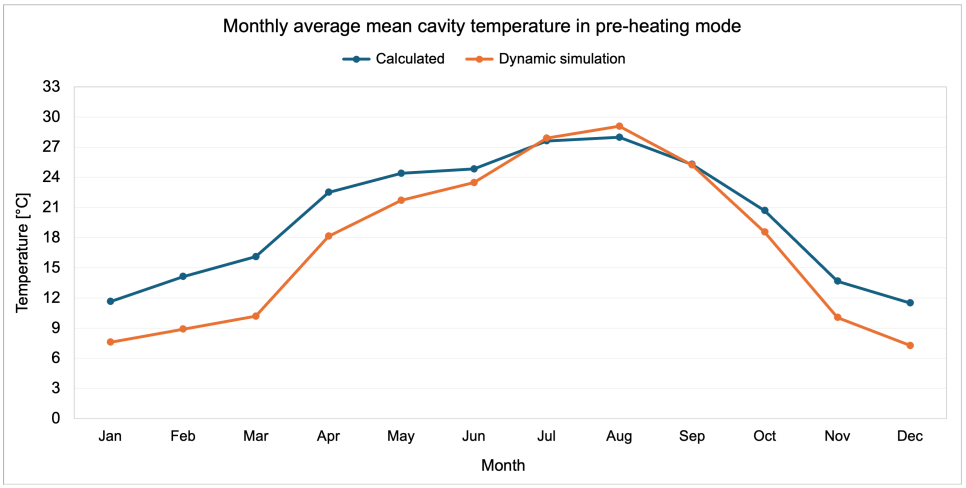

Figure 4.20: Monthly mean cavity temperature for pre-heating mode. SCM-PH compared to IDA-ICE dynamic simulation reference

A detailed view of the heating energy need for the full month of January is shown in Figure 4.21, with a further detailed view of 3-7 January shown in Figure 4.22. January is the most representative period for the pre-heating mode since it is physically active throughout this month in the real I-DIFFER system. The January comparison shows the framework underestimating heating energy on days with high solar radiation, where the warmer calculated cavity temperature reduces ventilation losses, and slightly overestimating on days with low solar radiation and lower cavity temperatures.

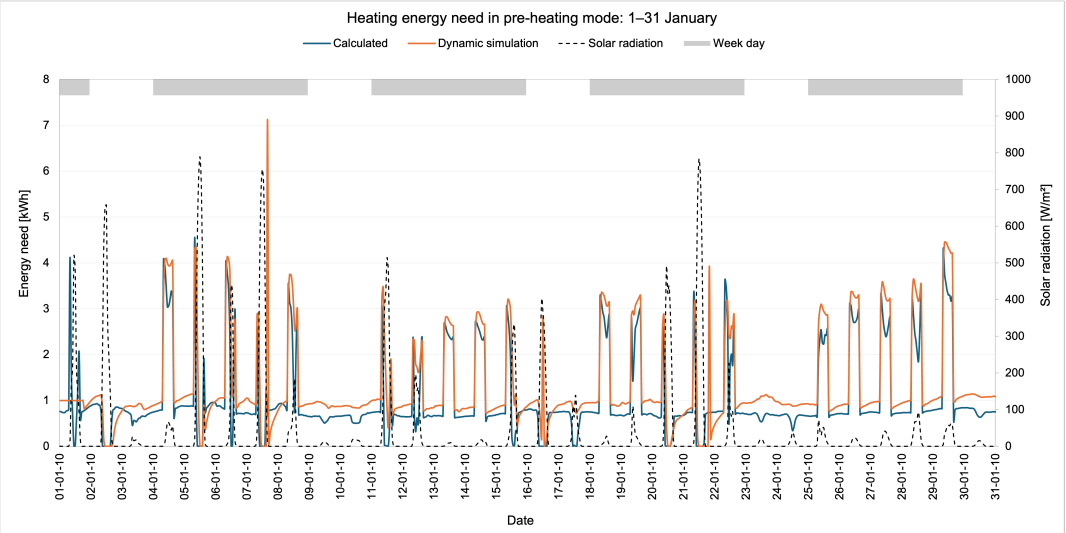

Figure 4.21: Heating energy need for pre-heating mode, January. SCM-PH compared to IDA-ICE dynamic simulation reference

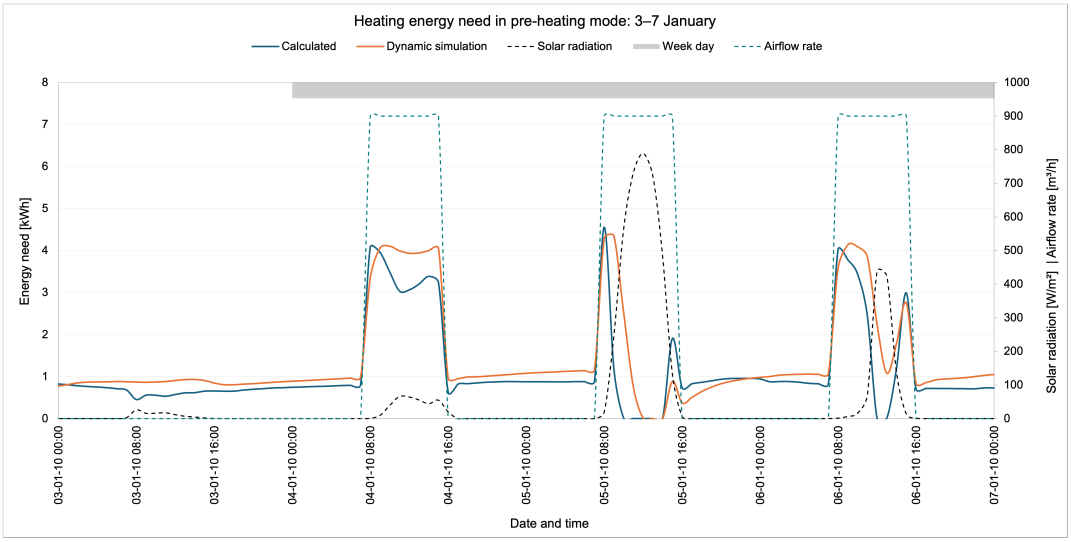

Figure 4.22: Detail of heating energy need for pre-heating mode, 3-7 January. SCM-PH compared to IDA-ICE dynamic simulation reference

A detailed view of mean cavity temperature for the full month of January is shown in Figure 4.23, with a further detailed view of 3-7 January shown in Figure 4.24. During occupied hours when ventilation is active, the framework cavity temperature aligns closely with the reference. During unoccupied hours when ventilation is off, the framework overestimates cavity temperature with larger deviations

on days with higher solar radiation. At the start of each occupied period, when ventilation activates, the framework temperature drops toward the reference level, confirming that active airflow moderates the cavity temperature in both models. On days with low solar radiation during occupied hours, the framework shows a slight underestimation compared to the reference.

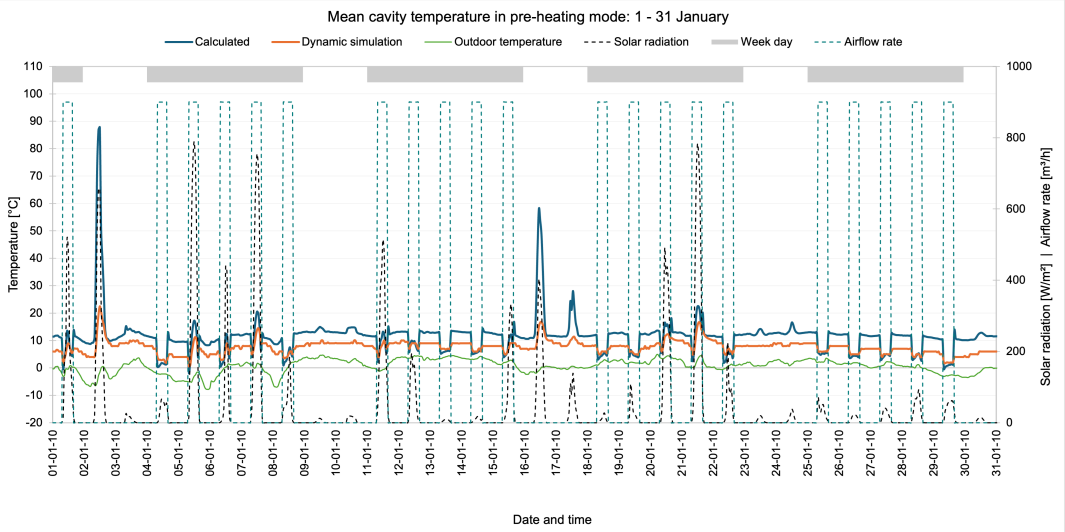

Figure 4.23: Heating energy need for pre-heating mode, January. SCM-PH compared to IDA-ICE dynamic simulation reference.

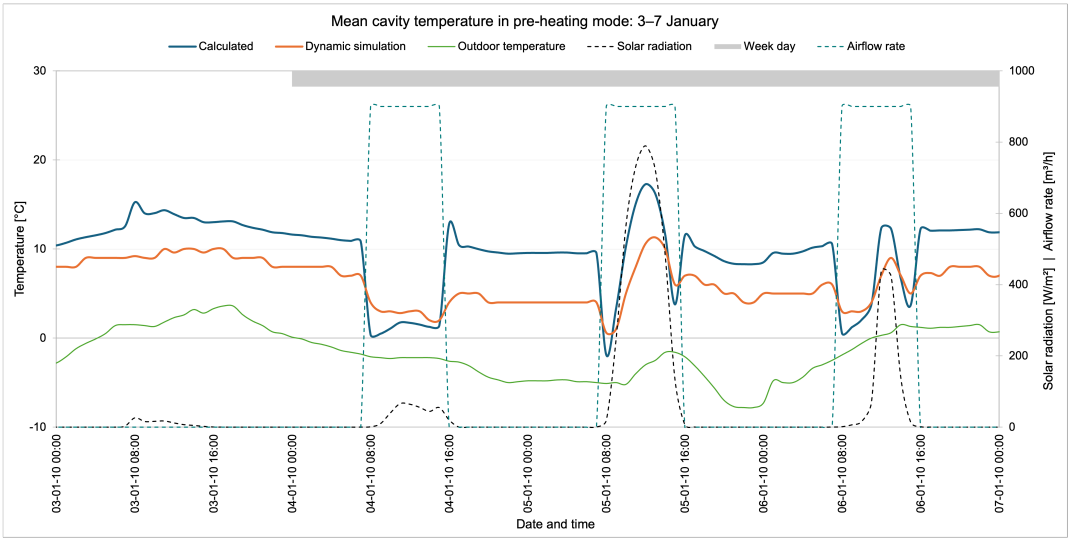

Figure 4.24: Detail of heating energy need for pre-heating mode, 3-7 January. SCM-PH versus IDA-ICE dynamic simulation reference.

The hourly scatter plots for mean cavity temperature and heating energy need are shown in Figure 4.25, with the IDA-ICE reference on the horizontal axis and the framework on the vertical axis. The dashed line shows perfect agreement.

For cavity temperature, the scatter clusters close to the perfect agreement line at low and moderate temperatures, corresponding to cold nights and cloudy days. At higher temperatures, the framework systematically overestimates, with points above the line corresponding to peak solar radiation hours during unoccupied periods when ventilation is off, which causes unrealistic temperature spikes.

For heating energy, most points cluster near the perfect agreement line. Markers on the vertical axis represent summer hours during which the reference calculates zero heating demand, while the framework responds to cool outdoor temperatures. Markers on the horizontal axis represent unoccupied winter weekend hours, during which the framework instantly reduces heating demand to zero in response to solar radiation above approximately 100 W/m², whereas the reference does not respond at this level due to thermal mass. Both models reduce heating demand to zero only when solar radiation exceeds approximately 400 W/m². Heating energy markers reflect the fundamental difference in thermal response between the two models.

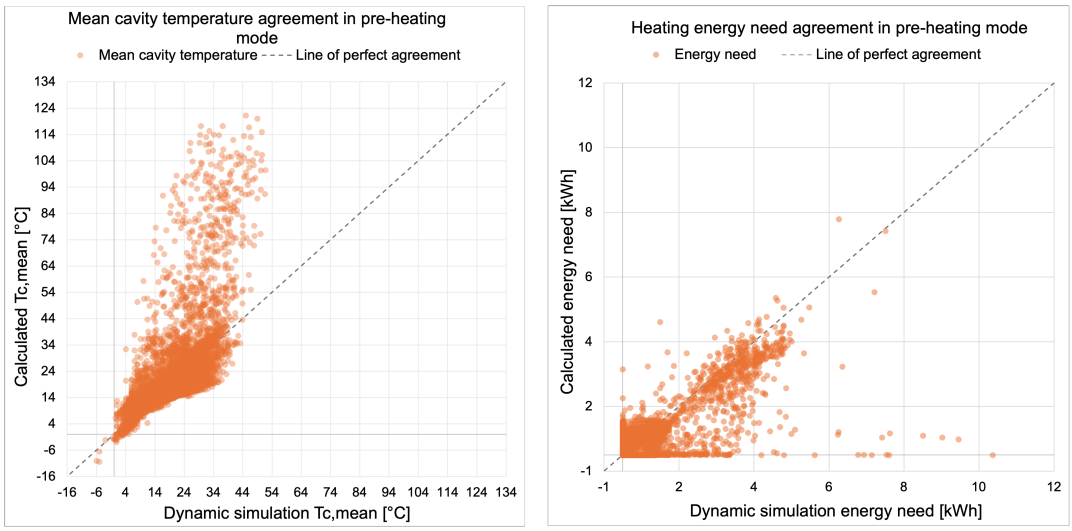

(a) Hourly mean cavity temperature

(b) Heating energy need

Figure 4.25: Scatter plots of hourly mean cavity temperature (a) and heating energy need (b) for pre-heating mode. SCM-PH compared to IDA-ICE dynamic simulation reference. The dashed line shows perfect agreement.

Overall, the pre-heating mode shows acceptable agreement for early-stage comparison purposes. The total heating energy difference of 3.8% is small despite the

opposing seasonal tendencies that partially cancel each other. The main limitation is the overestimation of peak cavity temperatures during unoccupied hours due to the absence of thermal mass. In the real I-DIFFER system, pre-heating mode only operates during occupied hours when mechanical ventilation is active. The unrealistic temperature peaks observed during unoccupied hours in the single-mode validation would therefore not occur in real operation. During occupied hours, the active ventilation airflow moderates the cavity temperature and prevents the extreme spikes seen when ventilation is off. The summer heating demand is a direct consequence of the single-mode validation setup and does not reflect real I-DIFFER operation, where ORM30 switching prevents pre-heating mode from running in summer.

4.4.4 Cooling mode

In cooling mode both DSF cavity openings are fully open and buoyancy-driven natural ventilation removes solar heat from the cavity. Supply air enters the room through the bypass at outdoor temperature. The simplified framework calculation for this mode follows the Hellström buoyancy formulation described in Section 3.3. The statistical summary for mean cavity temperature and heating energy need over the full 8760-hour validation period is shown in Table 4.6.

Table 4.6: Statistical summary for cooling mode dynamic validation

Variable	SCM-CL	IDA-ICE	Bias	MAE	RMSE
Mean cavity temperature [°C]	9.32	10.43	-1.10	1.11	1.21
Max cavity temperature [°C]	30.66	32.56	–	–	–
Min cavity temperature [°C]	-13.68	-11.26	–	–	–
Total heating energy [kWh]	8541	8355	–	–	–
Heating demand [kW mean]	0.97	0.95	0.02	0.28	0.53

The framework underestimates mean cavity temperature by 1.10°C relative to the IDA-ICE reference. The MAE of 1.11°C and the RMSE of 1.21°C indicate good hourly agreement, with small, consistent deviations. The close values of MAE and RMSE confirm that deviations are evenly distributed without large individual outliers, which contrasts with the pre-heating mode, where the RMSE was significantly larger than the MAE due to extreme temperature peaks during unoccupied hours. In cooling mode, the open cavity with active buoyancy-driven ventilation naturally limits temperature extremes, and no unrealistic temperature peaks are observed throughout the year.

The consistent underestimation is likely driven by two combined effects. The Hellström buoyancy formulation removes heat from the cavity more aggressively than the reference model, keeping framework cavity temperatures slightly lower

throughout the year. At the same time the reference model retains heat in the cavity construction through thermal mass, keeping it slightly warmer than the framework particularly during periods of low or no solar radiation. The maximum cavity temperatures show reasonable agreement: 30.66°C for the framework and 32.56°C for the reference, a difference of 1.90°C. The minimum cavity temperatures show a slightly larger difference, the framework minimum of -13.68°C compared to the reference minimum of -11.26°C, occurring during cold winter days with low solar radiation and nights when the single-mode simulation runs in cooling mode, through periods when the real system would have switched to pre-heating or transparent insulation mode.

For heating energy, the framework provides a total of 8541 kWh, compared to 8355 kWh for the reference, a difference of 186 kWh (2.2%). As in pre-heating mode, this close overall agreement comes at a trade-off. The framework calculates heating energy during the summer months when the reference shows zero demand. Analysis of the reference model indoor temperature data confirmed that room temperature did not fall below 20°C from approximately 20 June to 5 September, while the framework calculates heating demand whenever outdoor temperature drops below the room setpoint of 20°C, during unoccupied time, with no internal gains, causing heat losses through the inner facade and roof. During winter, unoccupied hours, when ventilation is off, both models closely follow the same pattern, with the framework slightly underestimating. When solar radiation exceeds approximately 400 W/m^2, the framework reduces heating demand to zero, whereas the reference shows only a minimal reduction. This threshold is higher than in pre-heating mode because in cooling mode, the cavity is actively ventilated. Removing heat and keeping cavity temperatures lower than in pre-heating mode, where ventilation is off, and the cavity retains solar heat, meaning a higher solar radiation level is needed to offset room heat losses and reduce heating demand to zero in cooling mode. During occupied hours when ventilation is active, both models closely align, depending on the fresh air that is supplied through the bypass into the room at outdoor temperature. The mean heating demand bias of 0.02 kW confirms good overall agreement. The MAE of 0.28 kW and RMSE of 0.53 kW indicate that while individual hours show deviations the overall heating energy pattern is well captured by the framework.

The total annual heating energy comparison is shown in Figure 4.26.

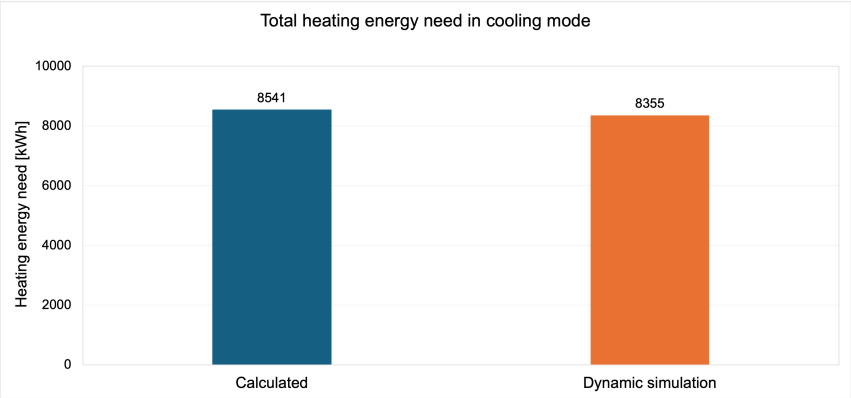

Figure 4.26: Total annual heating energy need for cooling mode. SCM-CL compared to IDA-ICE dynamic simulation reference.

The monthly heating energy comparison is shown in Figure 4.27. From January through April and again in November and December, the framework underestimates heating energy relative to the reference. During occupied hours when ventilation is active, both models closely align, while during unoccupied hours, the energy pattern depends on outdoor temperature and solar radiation. When solar radiation exceeds approximately 400 W/m², the framework reduces heating demand to zero while the reference shows only a minimal reduction. From May through October, the framework overestimates heating energy relative to the reference. During the period from approximately 20 June to 5 September, the reference shows zero heating demand while the framework continues to calculate heating need whenever outdoor temperature drops below the room setpoint. The overall energy pattern is well followed in both models throughout the year.

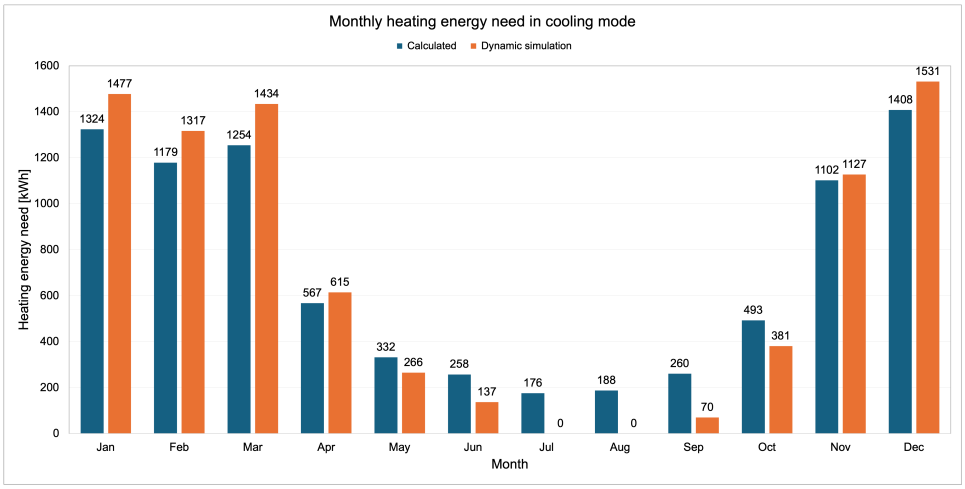

Figure 4.27: Monthly heating energy need for cooling mode. SCM-CL compared to IDA-ICE dynamic simulation reference

The average monthly mean cavity temperature comparison is shown in Figure 4.28. The framework consistently underestimates cavity temperature throughout the year, with a minimum of 0.83°C in December and a maximum of 1.39°C in August. The smaller underestimation in December is consistent with lower solar radiation in winter, when both models produce cavity temperatures closer to outdoor temperature. The larger underestimation in August is driven by periods of low or no solar radiation, when the reference cavity retains heat through its thermal mass while the framework temperature falls more quickly toward the outdoor temperature. The monthly cavity temperature chart shows no unrealistic peaks throughout the full year. The framework follows the reference pattern consistently across all months, confirming that the Hellström buoyancy formulation captures the thermal behaviour of the open naturally ventilated cavity well.

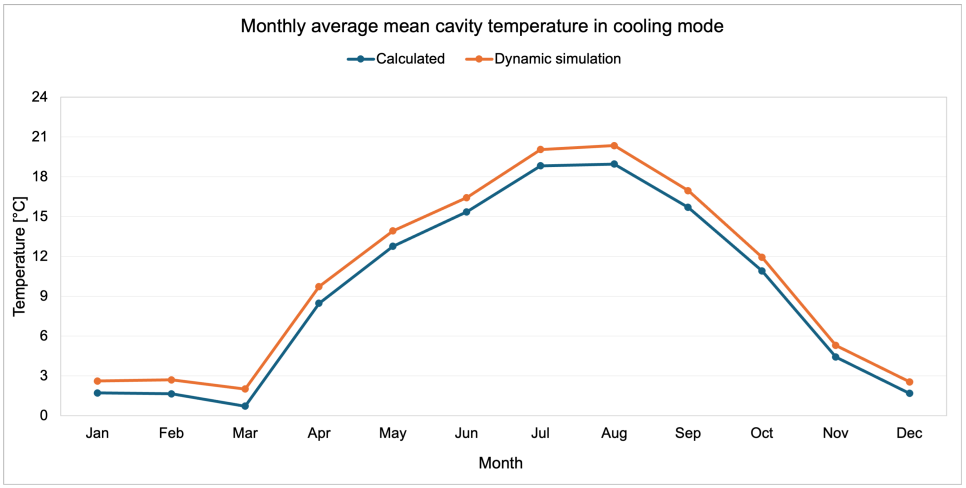

Figure 4.28: Monthly mean cavity temperature for cooling mode. SCM-CL compared to IDA-ICE dynamic simulation reference.

A detailed view of heating energy need for the full month of April is shown in Figure 4.29, with a further detailed view of 22-24 April shown in Figure 4.30. April reveals an interesting pattern where the reference model produces four brief heating demand spikes while the framework stays at or near zero. The observed operative temperature in the reference model at these periods is 20.81°C, just 0.81°C above the heating setpoint. When solar radiation drops from its daily peak and internal gains and ventilation simultaneously switch off, the operative temperature briefly falls below 20°C, triggering heating activation in the reference model. The framework calculates heating demand using a simple instantaneous heat balance rather than an operative temperature, and it does not produce the same response.

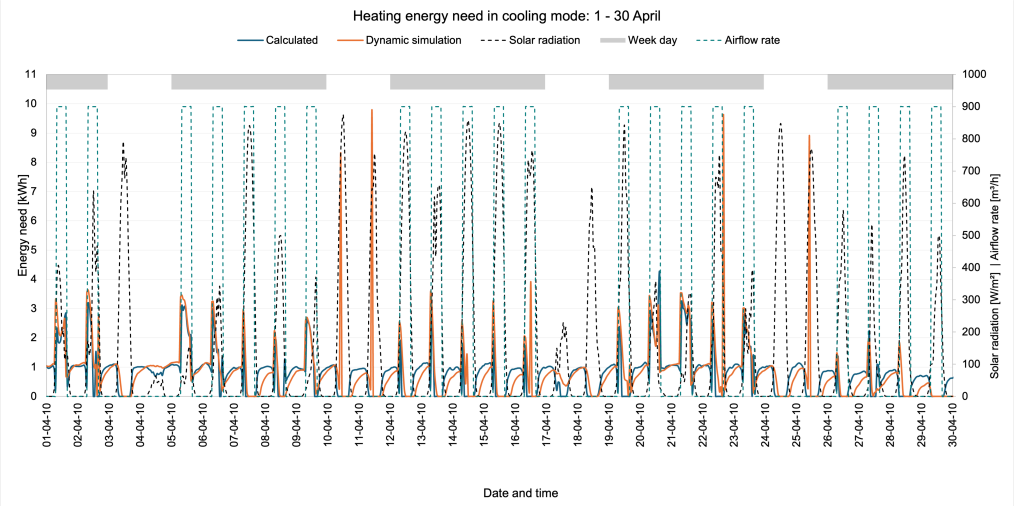

Figure 4.29: Heating energy need for cooling mode, April. SCM-CL compared to IDA-ICE dynamic simulation reference.

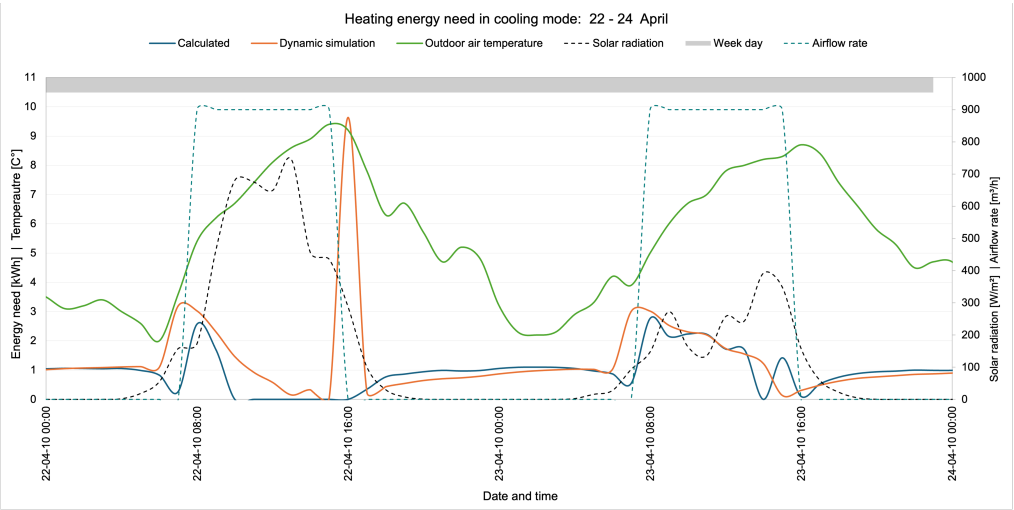

Figure 4.30: Detail of heating energy need for cooling mode, 22-24 April. SCM-CL compared to IDA-ICE dynamic simulation reference.

A detailed view of heating energy need for the full month of August is shown in Figure 4.31. The framework evenly distributes heating demand across unoccupied periods and nights when outdoor temperatures drop below the room setpoint, whereas the reference shows zero heating demand throughout August. This confirms the summer heating consequence of the single-mode validation setup; the framework reacts instantly to cool outdoor temperatures while the reference room temperature remains above 20°C due to thermal mass.

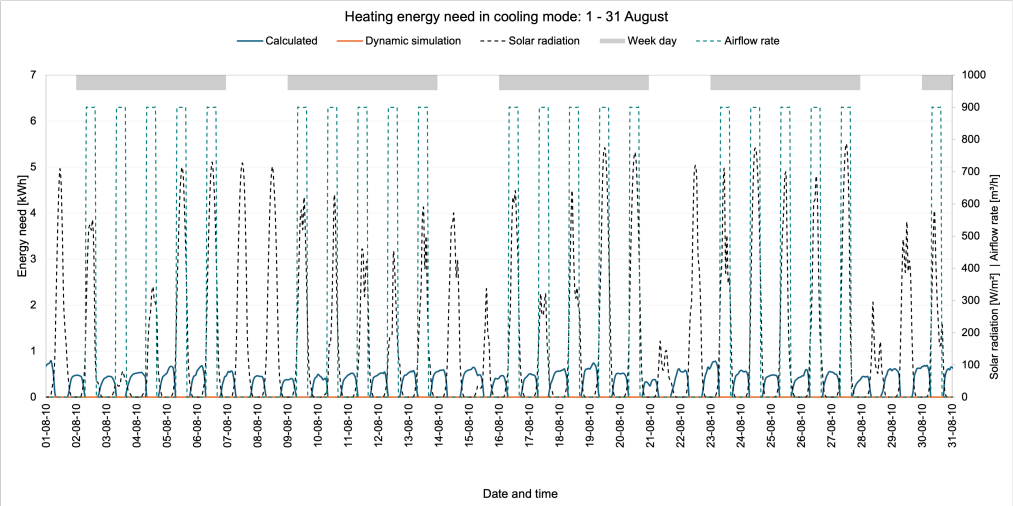

Figure 4.31: Heating energy need for cooling mode, August. SCM-CL compared to IDA-ICE dynamic simulation reference.

The mean cavity temperature for the full month of August is shown in Figure 4.32, and the detailed view of 20-25 August are shown in Figure 4.33. The framework shows a consistent small underestimation throughout the month with no unrealistic peaks. The daily cycle is clearly visible during unoccupied hours, and at night, the framework cavity temperature falls more quickly toward outdoor temperature than the reference, which retains heat through thermal mass and responds more gradually. The overall agreement is very good and the chart confirms that the Hellström buoyancy formulation follows the reference pattern closely throughout August.

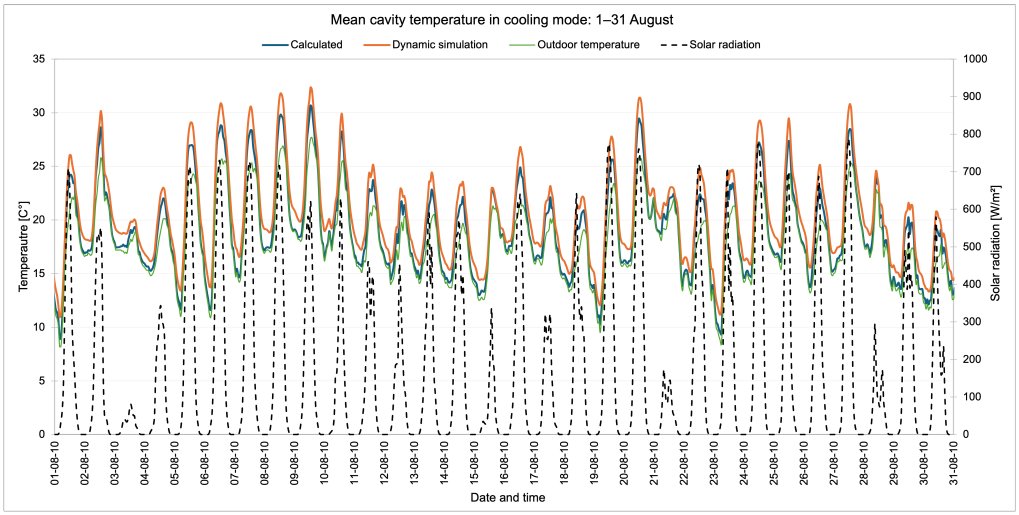

Figure 4.32: Mean cavity temperature for cooling mode, August. SCM-CL compared to IDA-ICE dynamic simulation reference.

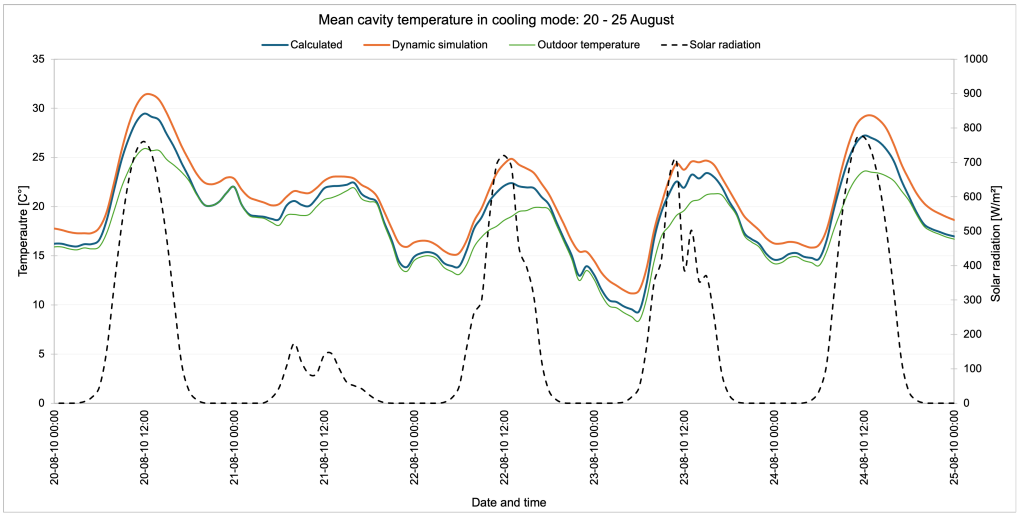

Figure 4.33: Detail of mean cavity temperature for cooling mode, 20-25 August. SCM-CL compared to IDA-ICE dynamic simulation reference.

The hourly scatter plots for mean cavity temperature and heating energy need are shown in Figure 4.34, with the IDA-ICE reference on the horizontal axis and the framework on the vertical axis. The dashed line shows perfect agreement.

For cavity temperature the scatter clusters tightly along the perfect agreement line throughout the full temperature range with points consistently slightly below the line, confirming the systematic underestimation of 1.10°C. The tight clustering and

absence of extreme outliers confirms that cooling mode shows the best cavity temperature agreement of the three operating modes. The even distribution of points along the line is consistent with the close MAE and RMSE values of 1.11°C and 1.21°C.

For heating energy most points cluster near the perfect agreement line. Markers on the vertical axis represent summer hours where the reference calculates zero heating demand, while the framework calculates positive heating need due to cool outdoor temperatures. Markers on the horizontal axis represent unoccupied winter hours, during which the framework reduces heating demand to zero in response to solar radiation above approximately 400 W/m², whereas the reference shows only a minimal reduction. In cooling mode this threshold is higher than in preheating mode because the open naturally ventilated cavity continuously removes heat, keeping cavity temperatures lower and requiring higher solar radiation levels to offset room heat losses.

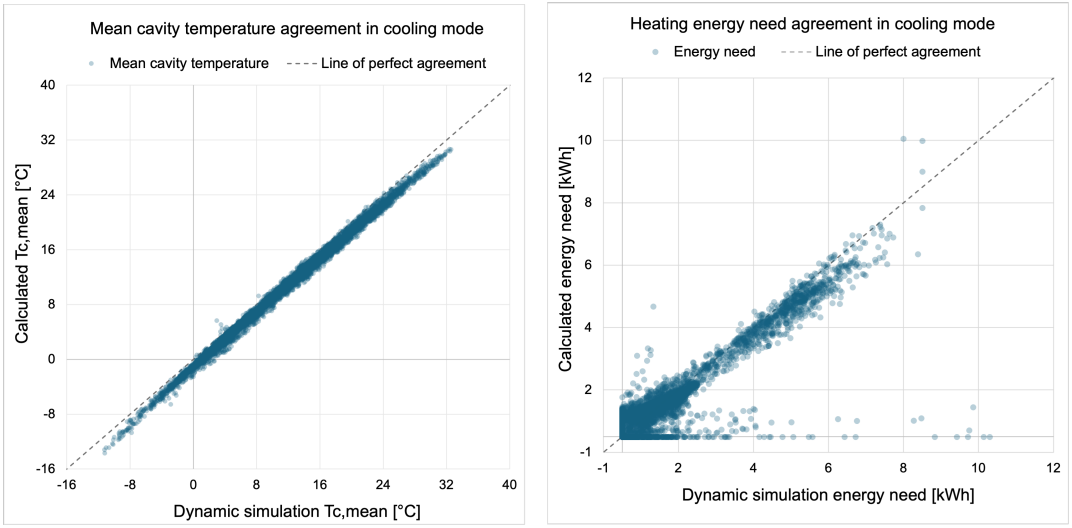

(a) Hourly mean cavity temperature

(b) Heating energy need

Figure 4.34: Scatter plots of hourly mean cavity temperature (a) and heating energy need (b) for cooling mode. SCM-CL compared to IDA-ICE dynamic simulation reference. Dashed line shows perfect agreement.

Cooling mode shows the best agreement of the three operating modes. The mean cavity temperature bias of -1.10°C is small and the MAE of 1.11°C indicates consistent hourly agreement without extreme outliers. The total heating energy difference of 2.2% is good. The Hellström buoyancy formulation successfully captures the thermal behaviour of the open naturally ventilated cavity, confirming its suitability for representing cooling mode in the simplified framework.

4.4.5 Transparent insulation

In transparent insulation mode all DSF cavity openings are closed and the cavity acts as a sealed thermal buffer between the outdoor environment and the inner facade. No mechanical ventilation is active in this mode. In the single-mode validation, the room is set with no internal gains and no ventilation throughout the full year, allowing direct comparison of cavity temperature and heating energy behaviour between the framework and the reference model under consistent boundary conditions.

The statistical summary for mean cavity temperature and heating energy need over the full 8760-hour validation period is shown in Table 4.7.

Table 4.7: Statistical summary for transparent insulation mode dynamic validation

Variable	SCM-TI	IDA-ICE	Bias	MAE	RMSE
Mean cavity temperature [°C]	27.79	29.22	-1.40	12.61	17.43
Max cavity temperature [°C]	121.97	69.34	–	–	–
Min cavity temperature [°C]	5.64	9.97	–	–	–
Total heating energy [kWh]	2813	1141	–	–	–
Heating demand [kW mean]	0.32	0.13	0.19	0.27	0.49

Transparent insulation mode shows the largest deviations of the three operating modes. The mean cavity temperature bias of -1.40°C appears moderate, but the MAE of 12.61°C and RMSE of 17.43°C indicate substantial hourly deviations. The large difference between MAE and RMSE confirms that deviations are concentrated in a small number of hours with very large errors, specifically peak solar radiation hours. When solar radiation is below approximately 100 W/m^2 the framework cavity temperature almost aligns with the reference, following the same pattern closely. When solar radiation is high the framework produces unrealistic temperature peaks due to the high solar radiation, the sealed cavity with no ventilation reacts instantly to the full solar input.

The large difference between maximum cavity temperatures of 121.97°C for the framework and 69.34°C for the reference reflects this limitation directly. The minimum cavity temperatures show the opposite pattern, a framework minimum of 5.64°C compared to the reference minimum of 9.97°C, because the reference thermal mass retains heat overnight, preventing the cavity from falling as quickly as the framework toward outdoor temperatures.

For heating energy the framework gives a total of 2813 kWh compared to 1141 kWh for the reference, a difference of 1672 kWh or 146.5%. This large overestimation mostly comes from the summer months; from 7 April to 3 November, the reference model shows zero heating demand, while the framework continues to calcu-

late heating need. The framework overestimates cavity temperature during winter hours with high solar radiation, reducing heating demand during peak solar hours, while during hours without solar radiation the framework cavity is cooler than the reference, producing higher heating demand. The reference model shows nine distinct heating demand spikes in January reaching from 2 to 7.5 kW. These spikes occur when solar radiation drops from its peak and the reference room temperature briefly falls toward the heating setpoint. The reference activates heating briefly to maintain the setpoint. The framework shows a constant heating demand of approximately 0.7 to 0.9 kWh during hours without solar radiation. When solar radiation is present, the framework heating demand drops toward zero while the reference continues to show heating demand, confirming that the framework reacts more strongly to solar radiation than the reference.

The mean heating demand bias of 0.19 kW confirms systematic overestimation throughout the year. The MAE of 0.27 kW is similar to the other two modes, indicating that the overestimation is spread evenly across many hours at a low level. The RMSE of 0.49 kW is nearly double the MAE, reflecting larger deviations at specific hours.

The total annual heating energy comparison is shown in Figure 4.35.

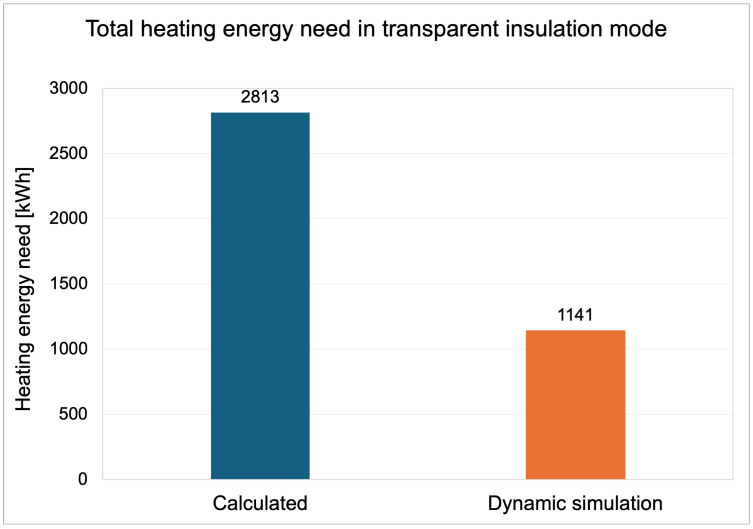

Figure 4.35: Total annual heating energy need for transparent insulation mode. SCM-TI compared to IDA-ICE dynamic simulation reference.

The monthly heating energy comparison is shown in Figure 4.36. From January through April and again in November and December the framework overestimates heating energy relative to the reference. From May through October the reference shows zero heating demand while the framework continues to calculate heating

need ,a direct consequence of the single-mode validation setup where no internal gains and no ventilation are applied throughout the full year.

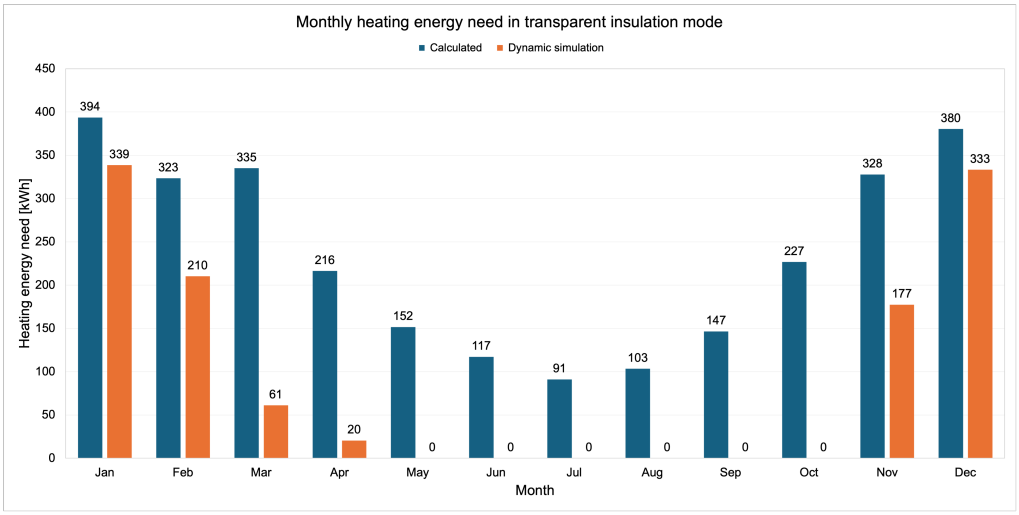

Figure 4.36: Monthly heating energy need for transparent insulation mode. SCM-TI compared to IDA-ICE dynamic simulation reference.

The average monthly mean cavity temperature comparison is shown in Figure 4.37. From January through March and again in November and December, the framework overestimates cavity temperature with a minimum overestimation of 1.01°C in November and a maximum of 2.15°C in February. During summer, the framework underestimates cavity temperature with the largest underestimation of 6.48°C in August and the smallest of 0.1°C in March. The large summer underestimation occurs because the reference sealed cavity retains heat stored during warm summer periods through thermal mass, keeping cavity temperatures much higher during cool summer nights than the framework which falls instantly toward outdoor temperature.

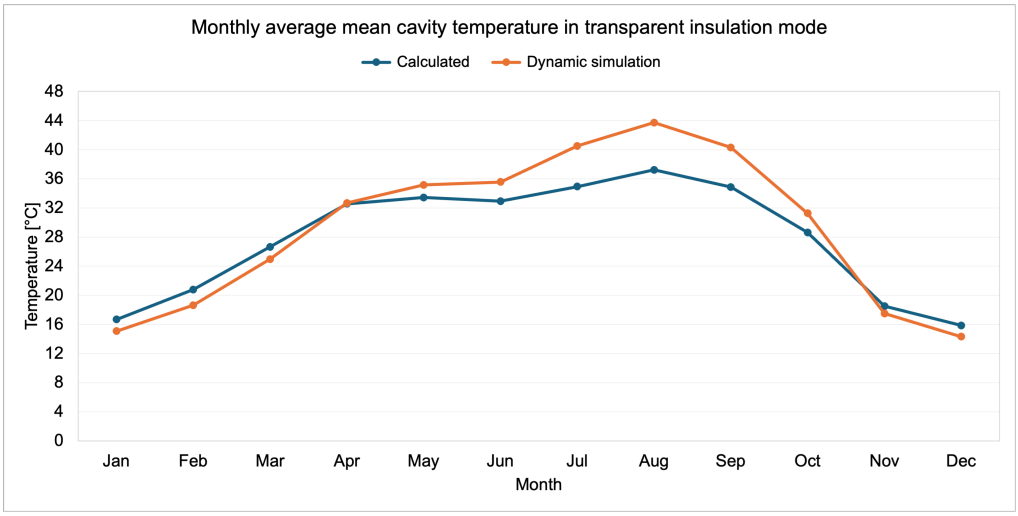

Figure 4.37: Monthly mean cavity temperature for transparent insulation mode. SCM-TI versus IDA-ICE dynamic simulation reference.

A detailed view of heating energy need for the full month of January is shown in Figure 4.38, with a further detailed view of 1-7 January shown in Figure 4.39. The full January comparison shows the framework producing a constant heating demand of approximately 0.7 to 0.9 kWh during hours without solar radiation, while the reference shows nine distinct spikes reaching from 2 to 7.5 kW. When solar radiation is present the framework heating demand drops toward zero. The detail view of 1-7 January clearly shows this pattern at hourly resolution, the framework reacts instantly to solar radiation while the reference responds more gradually with larger but shorter heating demand spikes driven by operative temperature falling briefly below the setpoint when solar radiation drops.

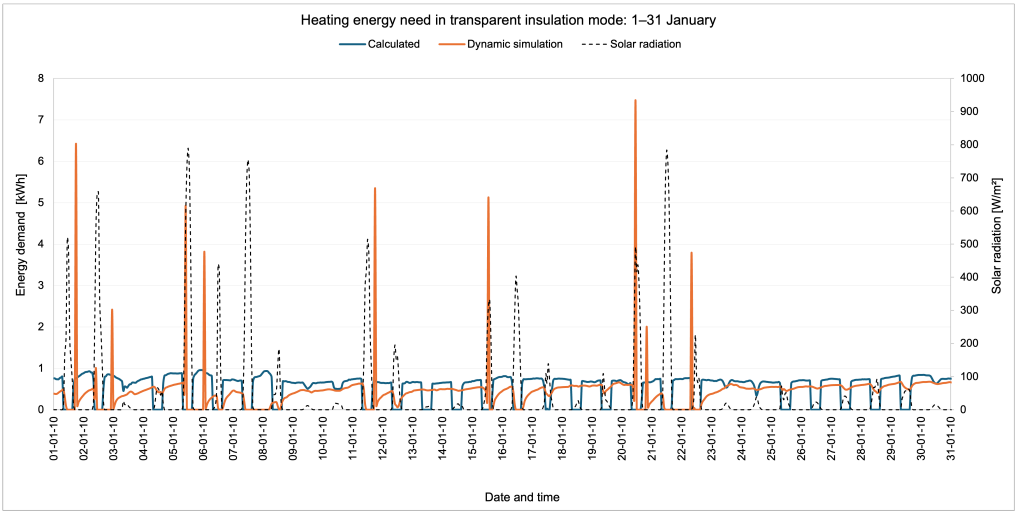

Figure 4.38: Heating energy need for transparent insulation mode, January. SCM-TI compared to IDA-ICE dynamic simulation reference.

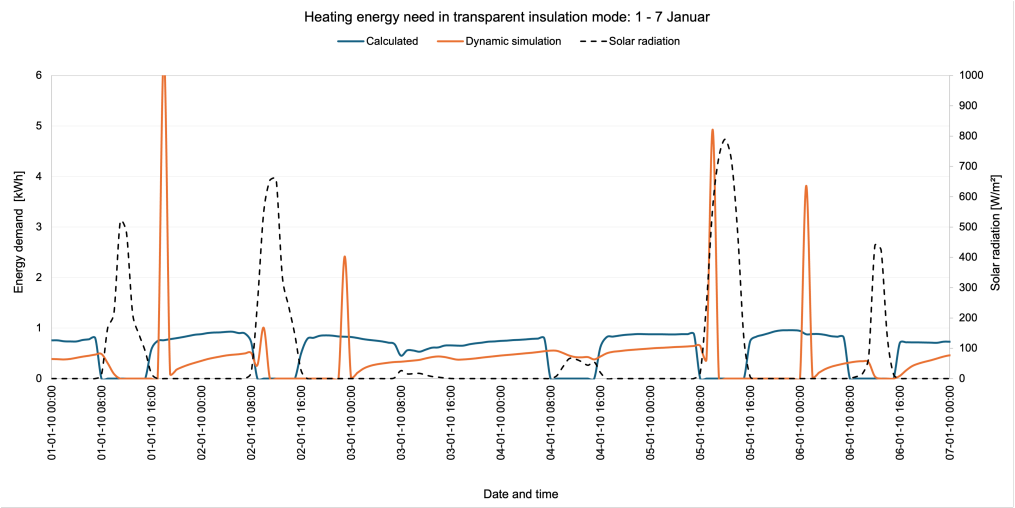

Figure 4.39: Detail of heating energy need for transparent insulation mode, 4-7 January. SCM-TI versus IDA-ICE dynamic simulation reference.

A detailed view of mean cavity temperature for the full month of January is shown in Figure 4.40, with a further detailed view of 1-7 January shown in Figure 4.41. When solar radiation is below approximately 100 W/m² the framework cavity temperature almost aligns with the reference, following the same pattern closely. When solar radiation is high the framework produces unrealistic temperature peaks while the reference stays well below. The detail view of 4-7 January shows this pattern clearly at hourly resolution, on days with high solar radiation the framework cav-

ity spikes unrealistically while on cloudy days and nights both models track each other closely.

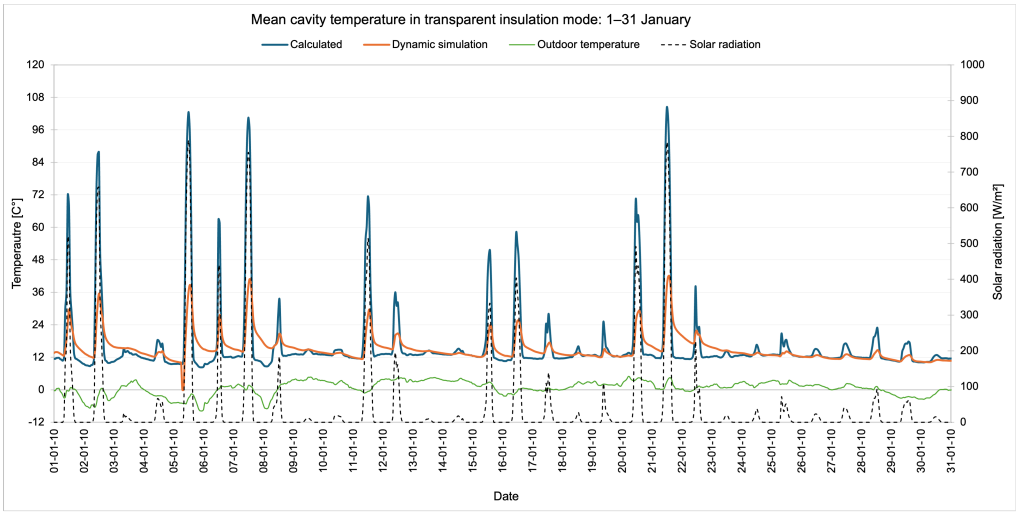

Figure 4.40: Mean cavity temperature for transparent insulation mode, January. SCM-TI compared to IDA-ICE dynamic simulation reference.

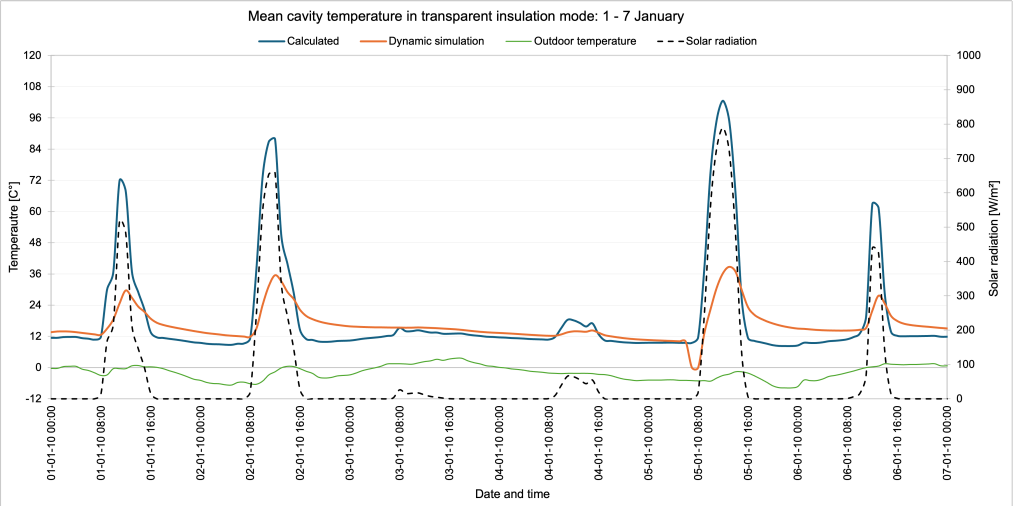

Figure 4.41: Detail of mean cavity temperature for transparent insulation mode, 4-7 January. SCM-TI versus IDA-ICE dynamic simulation reference.

The hourly scatter plots for mean cavity temperature and heating energy need are shown in Figure 4.42, with the IDA-ICE reference on the horizontal axis and the framework on the vertical axis. The dashed line shows perfect agreement.

The calculated model has weak agreement with the dynamic simulation for mean

cavity temperature in transparent insulation mode. It performs reasonably near lower temperatures, but at higher temperatures it becomes much less reliable, with frequent large deviations and many overpredicted temperature values.

For heating energy most points cluster near the perfect agreement line at low demand values. Markers on the vertical axis represent summer hours where the reference calculates zero heating demand, while the framework calculates positive values. Markers on the horizontal axis represent hours where the reference produces large heating demand spikes while the framework calculates near zero, corresponding to high solar radiation hours where the framework cavity temperature spikes unrealistically and heating demand drops to zero.

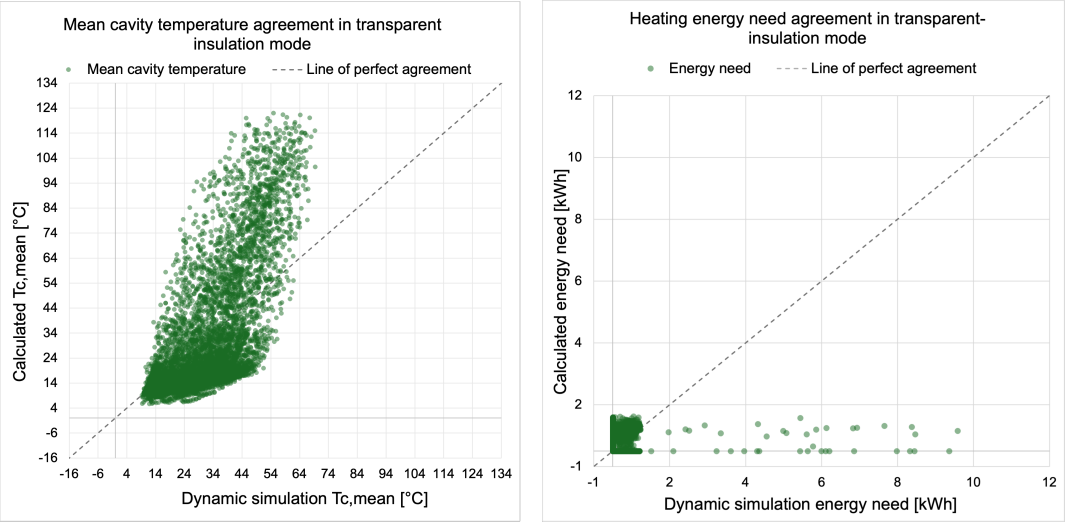

Figure 4.42: Scatter plots of hourly mean cavity temperature (a) and heating energy need (b) for transparent insulation mode. SCM-TI compared to IDA-ICE dynamic simulation reference.

Transparent insulation mode exhibits the largest deviations among the three operating modes. The total heating energy overestimation of 146.5% partially reflects a fundamental limitation of the sealed cavity formulation when thermal mass is not included.

In a sealed cavity without ventilation solar heat has no effective pathway for removal. The framework calculates cavity temperature instantaneously from the current solar radiation and outdoor temperature. When solar radiation is high the solar input drives the calculated cavity temperature to unrealistically high values within a single timestep. The peak cavity temperature overestimation of 52.63°C is a direct consequence of this limitation.

However, when solar radiation remains below approximately 100 W/m^2 the framework cavity temperature is in close agreement with the reference model, indicating that the main limitations are concentrated during periods of peak solar radiation.

In real I-DIFFER operation, transparent insulation mode runs without mechanical ventilation and without internal gains, operating during unoccupied hours on weekdays during winter when solar radiation is typically lower than during peak solar periods. The overestimation of cavity temperature therefore can mainly be concentrated during weekend days when solar radiation peaks occur without ventilation moderating the cavity response.

Furthermore, the reported heating energy overestimation of 146.5% is partly a consequence of the single-mode validation setup rather than a direct indication of expected behaviour under realistic transparent insulation mode operation.

Chapter 5

Case Scenario

5.1 Case study building

The case study used to apply and demonstrate the simplified hourly framework is a south-facing classroom in a semi-exposed one-storey school building from the 1960s. The building is located in Denmark and is representative of a large share of the Danish school building stock, where classrooms typically suffer from poor indoor air quality, insufficient ventilation, and high energy consumption due to ageing envelope components and outdated ventilation systems. The case study building and its geometric and thermal characteristics follow those defined in (Bugenings et al., 2022), to whom the reader is referred for a complete description of the building geometry, window details, and construction properties.

The classroom has a floor area of 50 m^2, a ceiling height of 2.70 m, and a total room volume of 135 m^3. The south-facing facade is made up of an opaque wall area of 10.6 m^2 and a window area of 12.54 m^2, giving a total south facade area of 23.14 m^2. The north side connects to a hallway, and both east and west walls are shared with neighbouring classrooms. All three non-south surfaces are treated as interior thermal boundaries with no heat transfer to the outdoor environment. The roof has an outdoor-facing area of 50 m^2, and the ground temperature is kept constant at 10°C throughout the calculations. The floor plan and cross-section of the classroom are shown in Figure 5.1.

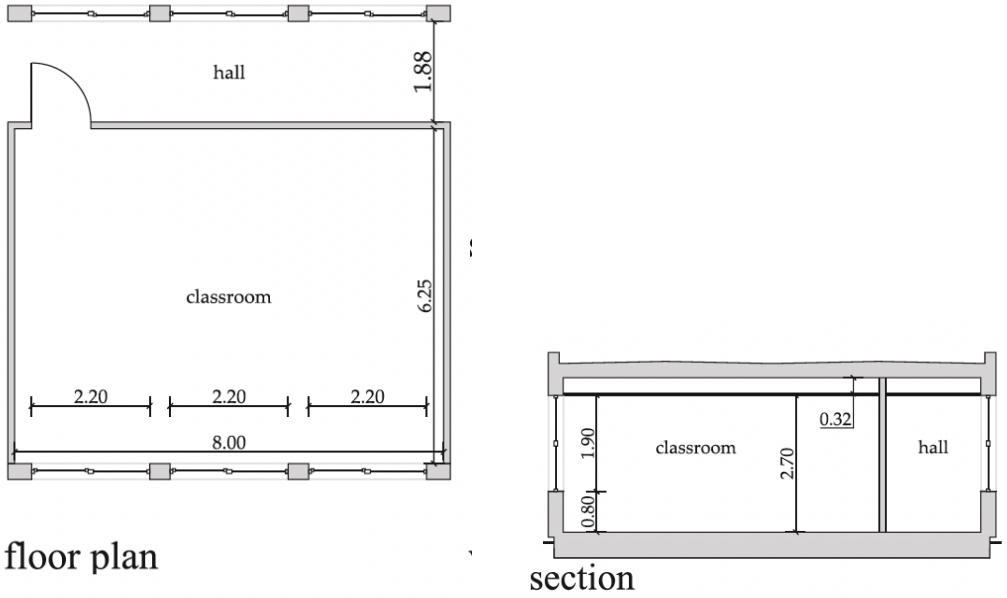

(a) Floor plan **(b)** Cross-section

Figure 5.1: Floor plan (a) and section (b) of the case study classroom. Adapted from (Bugenings et al., 2022).

The unrenovated envelope has a south-facing opaque wall combining aerated concrete infill panels at 0.50 W/(m^{2}K), representing 62% of the opaque area, and structural concrete columns at 0.92 W/(m^{2}K). The original windows have U_g=2.7 W/(m^{2}K), g=0.74, and τ=0.80. The roof has U=0.45 W/(m^{2}K), and the floor has U=0.43 W/(m^{2}K). Internal gains of 2500 W, equivalent to 50 W/m^2, are generated by 21 occupants and equipment during weekdays from 08:00 to 16:00, following (Bugenings et al., 2022). The heating setpoint is 20°C. All input parameters are summarised in Table 5.1.

The climate data used consist of measured hourly weather data for Copenhagen, Denmark, provided by Aalborg University. This dataset differs from the DRY2010 reference year used in (Bugenings et al., 2022). The case scenario uses the same building geometry, envelope properties, and system specifications defined in (Bugenings et al., 2022) as input data for the framework. The results are not validated against (Bugenings et al., 2022), because the study differs in both climate data and modelling approach, but are examined to assess whether the framework produces physically reasonable energy demand values consistent with the expected behaviour of the three renovation scenarios.

5.2 Renovation scenarios

Three scenarios are defined and compared using the simplified hourly framework. The first scenario represents the unrenovated building and serves as the baseline reference. The second scenario represents a conventional traditional renovation approach. The third scenario represents the I-DIFFER concept, which is an integrated solution combining a double-skin facade with diffuse ceiling ventilation. All three scenarios are evaluated under the same climatic basis, room geometry, occupancy schedule, internal gains, and heating setpoint. The sensitivity of results to control assumptions is assessed in Section 5.4 before the case scenario results are presented in Chapter 6.

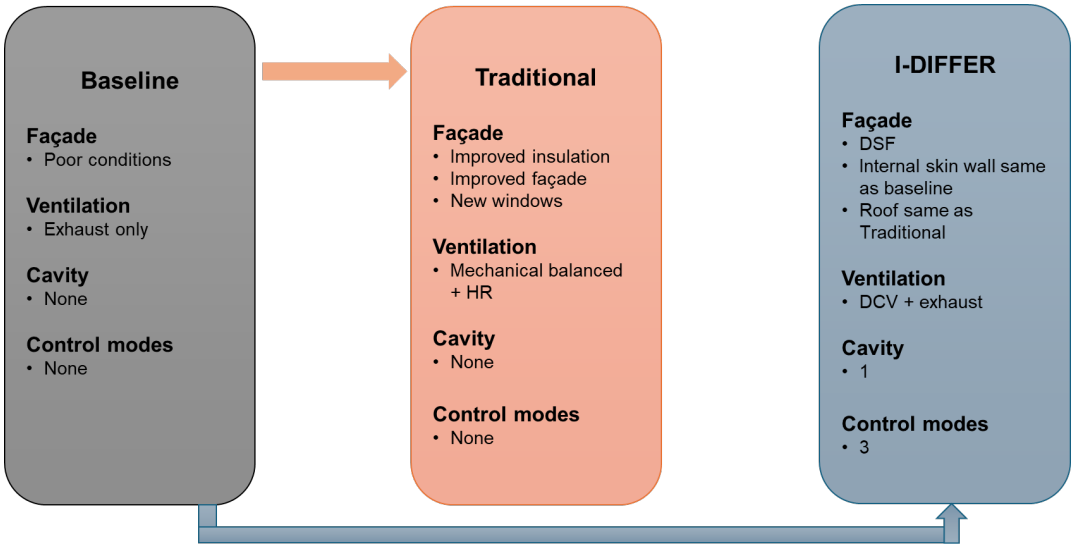

Figure 5.2: Key scenarios aspects

5.2.1 Baseline-unrenovated building

The baseline scenario represents the classroom in its unrenovated state as described in (Bugenings et al., 2022). The building is equipped with an exhaust-only ventilation system, where a mechanical fan extracts indoor air from the room, creating a slight negative pressure that draws outdoor air passively through gaps and cracks in the building envelope at outdoor temperature, without any preheating or heat recovery. The ventilation airflow rate is 18 $m^3/(h \cdot m^2)$, equivalent to 900 m^3/h for the 50 m^2 classroom, during occupied hours, and 1.26 $m^3/(h \cdot m^2)$, equivalent to 63 m^3/h, during unoccupied hours, consistent with (DS/EN 16798, 2019). No solar shading is installed.

Infiltration is calculated using a pressurisation test value of q_{50}=3.6 $m^3/(h \cdot m^2)$ at

50 Pa following (DS/EN ISO 13789, 2017), consistent with (Bugenings et al., 2022). A reduction factor of 1/20 is applied to represent real operating conditions at approximately 4 Pa, giving an infiltration airflow of 13.17 m^3/h distributed across the exterior wall of 23.14 m^2 and the roof of 50 m^2, totalling 73.14 m^2. The resulting infiltration heat transfer coefficient is H_{inf}=4.41 W/K.

5.2.2 Traditional renovation

The traditional renovation adheres to the minimum requirements of BR18 and the construction details in (Bugenings et al., 2022). The exterior wall is insulated to U=0.18 W/(m^2K), and the roof is insulated to U=0.12 W/(m^2K). The original windows are replaced with D-C1 double glazing from (Bugenings et al., 2022), with U_g=1.1 W/(m^2K), g=0.71, and τ=0.83. The floor remains unchanged at U=0.43 W/(m^2K).

A balanced mechanical ventilation system with 73% heat recovery is installed, meeting the minimum BR18 (Danish Building Regulations, 2018) requirement for a fully replaced ventilation system. Ventilation rates follow (DS/EN 16798, 2019).

External venetian blinds with reflective slats are installed according to the shading control logic described in (Bugenings et al., 2022), as described by (Karlsen et al., 2016). Shading activates when solar irradiation on the facade exceeds 150 W/m^2, reducing the effective g-value from 0.71 to 0.10. This value corresponds to the boundary between Class 3 and Class 4 solar shading performance, as defined in (DS/EN 14501, 2021), where Class 4 is defined by g_{tot}<0.10. The infiltration coefficient stays at H_{inf}=4.41 W/K.

In addition to the primary D-C1 configuration, the T-C1 triple glazing from (Bugenings et al., 2022), with U_g=0.5 W/(m^2K), g=0.60, and τ=0.77, is tested in Chapter 6 to represent the best-performing traditional renovation option and provide the most competitive reference for the I-DIFFER comparison.

5.2.3 I-DIFFER concept

The I-DIFFER scenario integrates a double-skin facade with diffuse ceiling ventilation as an alternative renovation strategy for the same classroom. The concept was originally proposed and analysed in (Bugenings et al., 2022) and forms the basis for the case scenario examined in this thesis. Rather than insulating the existing facade wall, the I-DIFFER approach adds a transparent outer glazing layer in front of the existing south-facing facade, creating a DSF cavity of 0.32 m depth. The outer glazing uses the D-C1 double-glazed configuration from (Bugenings et al., 2022), Table 5, with U_g=1.1 W/(m^2K), g=0.71, and τ=0.83. The inner facade, including the original windows, remains unchanged, with U_g=2.7 W/(m^2K) and g=0.74. The

roof is insulated to U=0.12 W/(m^2K), consistent with BR18 requirements. The floor construction remains unchanged.

The DSF cavity is constrained by bottom inlet and top outlet openings, which are multi-leaf dampers with heights of 0.3 m and 0.15 m, respectively, following the specifications in (Bugenings et al., 2022). Venetian blinds with reflective slats are positioned on the inner side of the outer DSF glazing, inside the cavity, following (Bugenings et al., 2022). The airflow through the cavity is mechanically driven in pre-heating mode and buoyancy-driven in cooling mode.

The bypass pathway above the DSF cavity allows direct outdoor air entry to the plenum without passing through the cavity. (Bugenings et al., 2022) modelled this bypass as a leakage component with a known mechanical flow rate, without specifying explicit geometric dimensions. In the simplified framework, the thermal effect of the bypass in cooling mode is represented by assuming that supply air enters the room at outdoor temperature.

The diffuse ceiling ventilation system supplies air uniformly through air-permeable wood-wool-cement ceiling panels across the full ceiling area at low velocity. The ventilation airflow rate is 18 $m^3/(h \cdot m^2)$ during occupied hours and 1.26 $m^3/(h \cdot m^2)$ during unoccupied hours, consistent with (DS/EN 16798, 2019).

5.3 Framework input parameters

The input parameters applied in the simplified hourly framework for each scenario are summarised in Table 5.1.

Table 5.1: Framework input parameters for all three scenarios

Parameter	Unit	I-DIFFER	Traditional	Baseline
Room geometry and boundary conditions				
Floor area	m^2		50	
Ceiling height	m		2.70	
Room volume	m^3		135	
Orientation	–		South	
Heating setpoint	°C		20	
Ground temperature	°C		10	
Climate	–		Copenhagen measured, Denmark	
Envelope properties				
Opaque facade area	m^2	10.6	10.6	10.6
Opaque facade U-value	$W/(m^2K)$	0.50	0.18	0.50
Roof U-value	$W/(m^2K)$	0.12	0.12	0.45
Floor U-value	$W/(m^2K)$	0.43	0.43	0.43
Infiltration H_{inf}	W/K	4.41	4.41	4.41
Window and glazing properties				
Inner window area	m^2	12.54	12.54	12.54
Inner window U_g	$W/(m^2K)$	2.7	1.1 (D-C1)	2.7
Inner window g-value	–	0.74	0.71 (D-C1)	0.74
Inner window τ	–	0.80	0.83 (D-C1)	0.80
DSF properties (I-DIFFER only)				
Outer DSF glazing type	–	D-C1	–	–
Outer DSF glazing area	m^2	20.5	–	–
Outer DSF U_g	$W/(m^2K)$	1.1	–	–
Outer DSF g-value	–	0.71	–	–
Outer DSF τ	–	0.83	–	–
Cavity depth	m	0.32	–	–
Bottom inlet height	m	0.30	–	–
Top outlet height	m	0.15	–	–
Solar shading				
Shading type	–	Cavity venetian blind	External venetian blind	–
Shading activation	W/m^2	>150 (cooling)	>150	–
g-value shaded	–	0.10	0.10	–
Ventilation and internal gains				
Ventilation system	–	Exhaust + DCV	Balanced + HRV	Exhaust only
Heat recovery efficiency	%	0	73	0
Ventilation rate occupied	$m^3/(h{\cdot}m^2)$	18	18	18
Ventilation rate unoccupied	$m^3/(h{\cdot}m^2)$	1.26	1.26	1.26
Internal gains occupied	W	2500	2500	2500
Occupancy schedule	h	Weekdays 08:00–16:00	Weekdays 08:00–16:00	Weekdays 08:00–16:00

5.4 Operating mode assumptions - I-DIFFER

The I-DIFFER scenario operates in three modes depending on the season and occupancy state. The seasonal boundary is defined by the 30-day outdoor running mean temperature (ORM30), calculated as the arithmetic mean of hourly outdoor temperatures over the preceding 30 days, as a simplification of the exponentially weighted daily formulation defined in (DS/EN 16798, 2019). A threshold of 10°C is applied to the ORM30 value at each hour. This threshold follows the same criterion used by (Bugenings et al., 2022) to switch the heating system off; in the simplified framework, it is applied to switch between operating modes rather than to control the heating system directly. When ORM30 is below 10°C the heating season is active and either pre-heating or transparent insulation mode runs depending on occupancy. When ORM30 reaches or exceeds 10°C, cooling mode activates for all hours. Applied to the measured hourly weather data, Copenhagen, Denmark, this transition occurs on 23 May at 22:00 in spring and 29 October at 18:00 in autumn, giving a cooling season of 3813 hours and a heating season of 4947 hours. The mode assignment is summarised in Table 5.2 and the hourly operating mode and shading control logic is illustrated in Figure 5.4. The monthly mean ORM30 values and seasonal boundaries are shown in Figure 5.3.

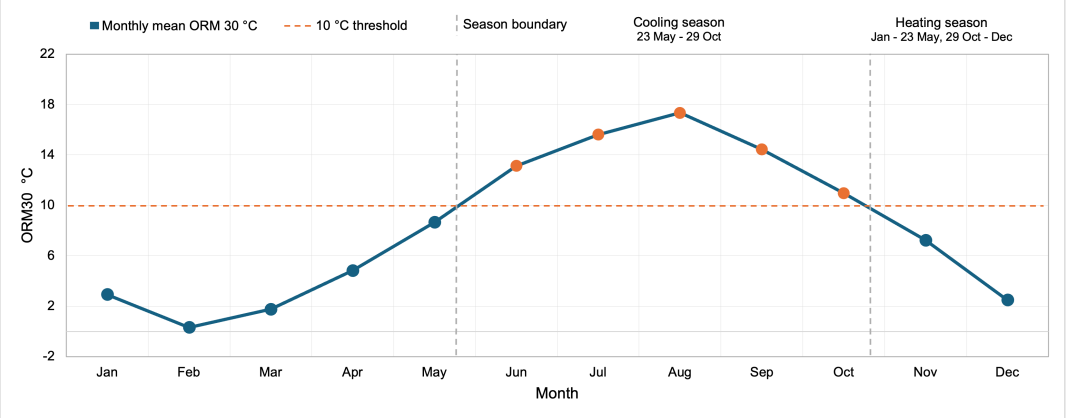

Figure 5.3: Monthly mean ORM30 and cooling season boundaries for measured hourly weather data, Copenhagen, Denmark.

Table 5.2: I-DIFFER mode operation logic

ORM30	Occupancy	Active Mode	Approximate Period
Below 10°C	Weekdays 08:00–16:00	Pre-heating	1 Jan–23 May, 29 Oct–31 Dec
Below 10°C	Unoccupied	Transparent insulation	1 Jan–23 May, 29 Oct–31 Dec
At or above 10°C	All hours	Cooling	23 May–29 Oct

Note: The approximate periods shown apply to the ORM30 seasonal switching configuration using measured hourly weather data, Copenhagen, Denmark. In the instantaneous energy-based switching configuration all three modes operate throughout the full year based on the hourly energy comparison and occupancy schedule.

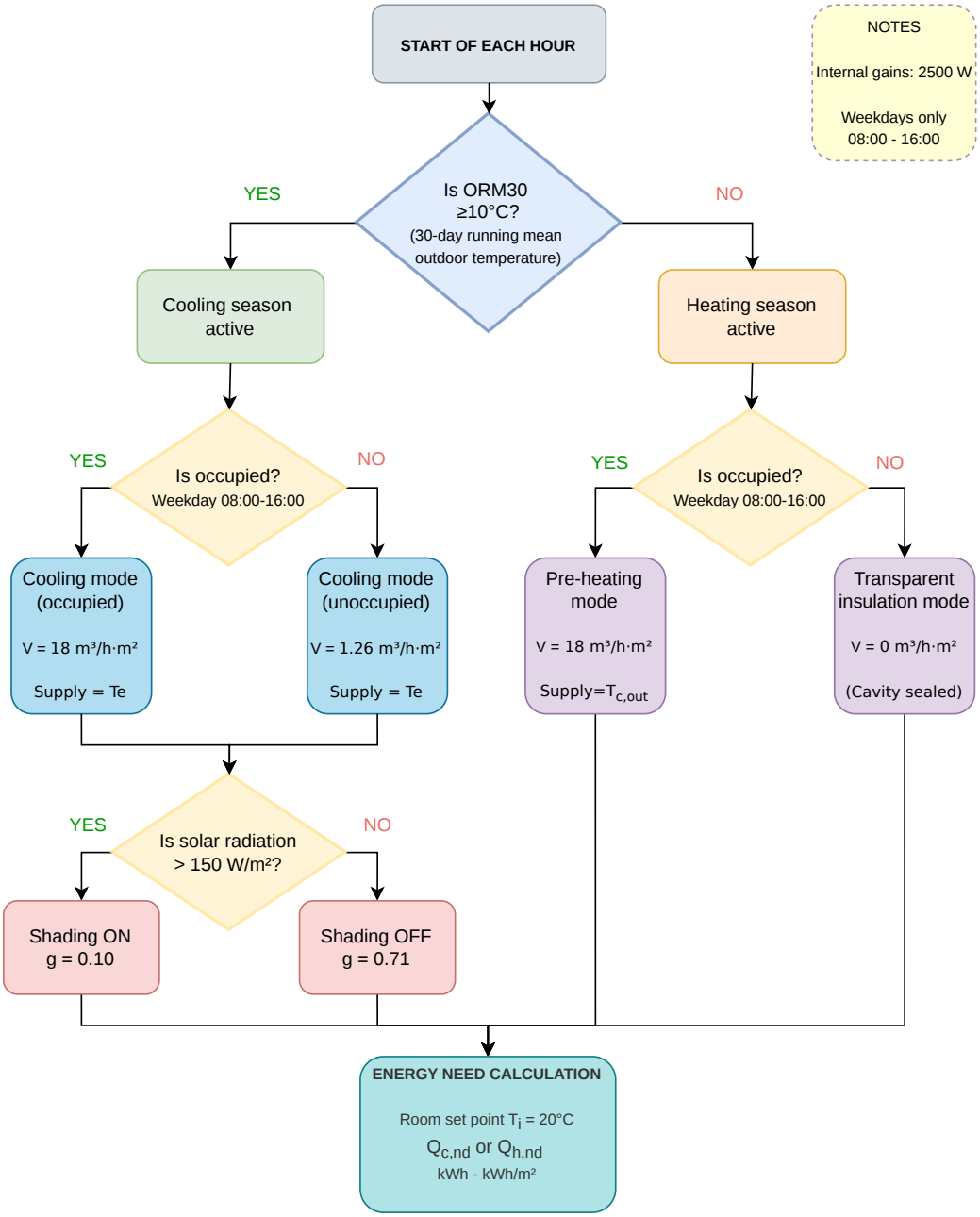

Figure 5.4: Hourly operating mode and shading control logic for the I-DIFFER framework.

5.4.1 Pre-heating mode

Pre-heating mode is active during occupied hours in the heating season, specifically on weekdays from 08:00 to 16:00 when ORM30 is below 10°C. In this mode, mechanically driven ventilation air enters the DSF cavity at the bottom inlet, is heated by solar gains and heat exchange with the inner facade, and exits at the top outlet into the diffuse ceiling plenum before being distributed to the room through air-permeable ceiling panels. The outlet temperature of the cavity is calculated following the (BESTFACADE, 2007) simplified calculation method as described in Chapter 3. The cavity outlet temperature is used directly as the supply air temperature entering the room through the diffuse ceiling panels. Solar shading is never activated in pre-heating mode, consistent with (Bugenings et al., 2022), in order to maximise solar-assisted preheating of the supply air.

5.4.2 Transparent insulation mode

Transparent insulation mode runs during unoccupied hours when ORM30 is below 10°C. Both cavity openings are closed, and the cavity acts as a sealed thermal buffer. The mean cavity temperature is calculated following the (BESTFACADE, 2007) simplified calculation method as described in Chapter 3. No mechanical ventilation flows through the cavity in this mode.

Shading is not activated in transparent insulation mode. (Bugenings et al., 2022) activate shading at low solar irradiation levels in this mode to reduce thermal radiation losses, which requires modelling of long-wave radiation exchange between cavity surfaces, which the simplified framework does not include.

5.4.3 Cooling mode

Cooling mode runs for all hours when ORM30 is at or above 10°C, from approximately 23 May to 29 October in the measured Copenhagen weather data. Both cavity openings are fully open, allowing outdoor air to flow through the cavity by buoyancy and remove heat from the cavity. Supply air enters the room through the bypass pathway above the cavity at outdoor temperature and is mechanically driven. The mean cavity temperature is calculated using the Hellström buoyancy formulation following (BESTFACADE, 2007) described in Chapter 3. Supply air is assumed to enter the room at outdoor temperature through the bypass pathway, consistent with the bypass operation described in (Bugenings et al., 2022).

Shading activates in cooling mode when solar irradiation exceeds 150 W/m^2, following the control logic described in (Bugenings et al., 2022) based on (Karlsen et al., 2016). When active, the effective g-value is reduced from 0.71 to 0.10, corresponding to the boundary between Class 3 and Class 4 solar shading performance

in (DS/EN 14501, 2021), where Class 4 is defined as g_{tot} below 0.10.

5.5 Control parameter selection

The framework includes two user-adjustable control parameters that determine how operating modes are assigned at each hour and whether solar shading is active. The two mode-switching approaches and the two shading states are described in detail in Chapter 3. This section summarises the four configurations tested in the sensitivity analysis, presents the results, and justifies the selection of the final configuration used throughout Chapter 6.

5.5.1 Sensitivity configurations

Two mode-switching approaches are compared, ORM30 seasonal switching and instantaneous energy-based switching, each combined with two shading states: active and inactive. This gives four configurations as summarised in Table 5.3. Each parameter is assessed independently by comparing configurations in which only that parameter changes, while the others remain fixed.

Table 5.3: Sensitivity analysis configurations for mode-switching logic and solar shading

Configuration	Switching	Shading
ORM30 + shading ON	ORM30	ON
ORM30 + shading OFF	ORM30	OFF
Instantaneous + shading ON	Energy comparison	ON
Instantaneous + shading OFF	Energy comparison	OFF

ORM30

ORM30 switching uses the 30-day outdoor running mean temperature as described in Section 5.4, giving a cooling season of 3813 hours and a heating season of 4947 hours in the Copenhagen measured climate.

Instantaneous

Instantaneous energy-based switching applies no fixed seasonal boundary. At each hour the framework calculates the total energy need for each available mode and assigns the mode that requires the least energy to keep the room at 20°C. Occupied hours compare pre-heating against cooling mode. Unoccupied hours compare transparent insulation against cooling mode. All three modes can operate throughout the full year based on the hourly energy comparison and occupancy schedule.

Shading ON

Shading ON means venetian blinds activate in cooling mode when solar radiation exceeds 150 W/m², reducing the effective solar heat gain coefficient from g = 0.71 to g = 0.10, consistent with Class 4 solar shading performance as defined in (DS/EN 14501, 2021). Shading is never activated in pre-heating or transparent insulation mode.

Shading OFF

Shading OFF means no shading is applied in any mode. Solar radiation enters the room at the full unshaded g-value of 0.71 throughout the year.

5.5.2 Sensitivity results

This subsection presents the annual energy results for all four configurations and analyses the effect of each control parameter independently and in combination. The four configurations and their annual energy results are shown in Table 5.4. The monthly heating and cooling energy distributions for all four configurations are shown in Figure 5.5.

Table 5.4: Sensitivity analysis of seasonal switching and shading assumptions

Parameter	ORM30		Instantaneous	
	Shading ON	**Shading OFF**	**Shading ON**	**Shading OFF**
Energy				
Heating kWh/m^2	104.14	98.55	111.74	96.63
Cooling kWh/m^2	26.88	62.96	42.76	88.73
Total kWh/m^2	131.02	161.51	154.50	185.36
vs ORM30 + shading ON	–	+23.3%	+17.9%	+41.5%
Mode hours				
Pre-heating hours	1168	1168	669	623
Cooling hours	3813	3813	2542	2618
Transparent ins. hours	3779	3779	5549	5519
Heating energy share				
Pre-heating %	21%	22%	38%	38%
Transparent insulation %	39%	41%	41%	44%
Cooling mode %	40%	37%	21%	19%
Cooling energy share				
Pre-heating %	0%	0%	32%	22%
Transparent insulation %	0%	0%	4%	6%
Cooling mode %	100%	100%	64%	72%

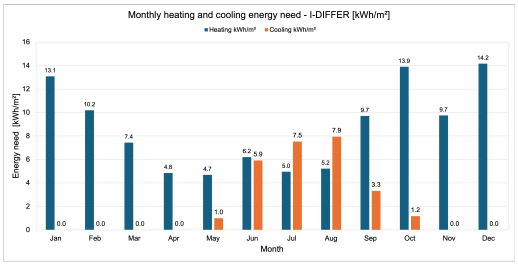

(a) Final: ORM30 + shading ON

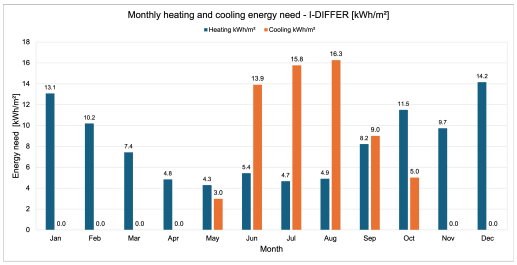

(b) ORM30 + shading OFF

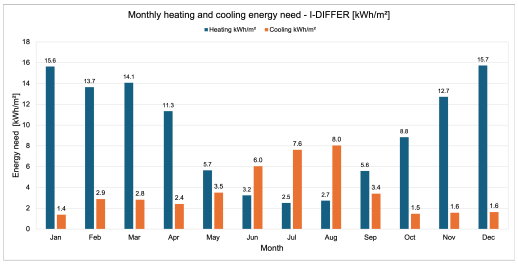

(c) Instantaneous + shading ON

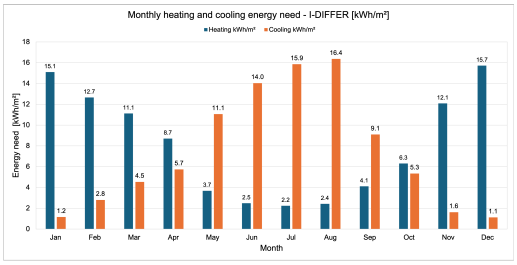

(d) Instantaneous + shading OFF

Figure 5.5: Monthly heating and cooling energy distribution for all four sensitivity configurations. (a): ORM30 + shading ON. (b): ORM30 + shading OFF. (c): instantaneous + shading ON. (d): instantaneous + shading OFF.

Shading effect

Removing shading while keeping ORM30 switching increases total energy demand by 23.3% from 131.02 to 161.51 kWh/m². Cooling demand increases by 134% from 26.88 to 62.96 kWh/m² while heating decreases slightly from 104.14 to 98.55 kWh/m² because, without shading, more solar radiation enters the room during cooling season hours, reducing the temperature difference that drives heating demand in adjacent hours. Shading is active only in cooling mode above 150 W/m². In transparent insulation mode and in pre-heating mode, shading is never activated, since the purpose of pre-heating is to capture solar gains to heat the supply air. The mode-hour distribution is unchanged in both ORM30 configurations: 1168 pre-heating hours, 3813 cooling hours, and 3779 transparent insulation hours, confirming that shading affects the energy share calculated in each mode. The cooling energy share remains 100% from cooling mode in both ORM30 configurations, regardless of shading status.

Removing shading while keeping instantaneous switching increases total energy demand by 19.9% from 154.50 to 185.36 kWh/m². Cooling demand increases by 107% from 42.76 to 88.73 kWh/m². The shading effect is slightly smaller under

instantaneous switching than under ORM30 because cooling energy is distributed across all three modes, and the shading impact is spread differently across the year. The pre-heating cooling share changes from 32% with shading to 22% without shading. This drop occurs because without shading, the total cooling demand increases substantially, and a larger share of the additional cooling is generated in cooling mode rather than in pre-heating hours, reducing the relative pre-heating contribution even though the absolute pre-heating cooling energy increases.

Mode selection effect

Replacing ORM30 with instantaneous energy-based switching while keeping shading active increases total energy demand by 17.9% from 131.02 to 154.50 kWh/m². Pre-heating hours drop from 1168 to 669, and transparent insulation hours increase from 3779 to 5549 as the energy comparison redistributes hours across all seasons without a fixed seasonal boundary.

The most important difference is the cooling energy distribution. In the ORM30 configuration 100% of cooling energy comes from cooling mode, the open cavity removing solar heat by natural ventilation. In the instantaneous configuration 32% comes from pre-heating hours where mechanical ventilation delivers supply air warmer than the room, generating cooling demand through ventilation heat gain.

Replacing ORM30 with instantaneous switching, while removing shading increases total energy demand by 14.8% from 161.51 to 185.36 kWh/m². The effect is slightly smaller without shading because the energy comparison more frequently selects cooling mode reducing the difference between the two switching methods. Without shading, more solar radiation enters the room in all hours across all seasons. This means gains exceed losses more frequently, the energy comparison in the instantaneous configuration more often selects cooling mode as the most efficient option. The instantaneous configuration therefore produces more cooling hours and fewer transparent insulation and pre-heating hours when shading is off.

Combined effect

Moving from the best configuration, ORM30 with shading, to the worst case, instantaneous with no shading, increases total energy demand by 41.5% from 131.02 to 185.36 kWh/m². This increase comes from two independent contributions: first removing shading adds 23.3%, and changing the switching method adds 17.9%. Both parameters individually have a significant effect on total energy demand, but removing both together produces the largest increase, confirming that each control assumption is essential to the framework's performance.

5.5.3 Final configuration selection

The sensitivity results show that the choice of switching method significantly affects not only total energy demand but, more importantly, the physical consistency of cooling energy assignment across the three operating modes. The ORM30 configuration produces the lowest total energy demand of the four configurations at 131.0 kWh/m² and is considered the most physically consistent choice based on the sensitivity results. In the ORM30 configuration 100% of cooling energy comes from cooling mode during the summer season, with the open cavity removing solar heat by natural ventilation before it reaches the room. In the instantaneous configuration 32% of cooling energy comes from pre-heating hours, a mode where the cavity is configured to deliver warm supply air to the room, not to remove heat from it, meaning cooling demand in pre-heating hours has no physical removal mechanism. It is also important to note that (Bugenings et al., 2022) do not include a mechanical cooling system; the cooling mode activates the open DSF cavity and natural ventilation, but no mechanical cooling energy is consumed. Without ORM30 switching, the simplified framework would calculate cooling energy on sunny winter days when gains exceed losses, and activate cooling mode. In a seasonal climate like Denmark, outdoor temperature during the heating season can be as low as 7°C during occupied hours. If instantaneous switching were used and solar radiation drives high heat gains, the energy comparison might select cooling mode, meaning the room receives cold outdoor supply air instead of the warmer preheated air that pre-heating mode would deliver, causing a significant difference in thermal comfort and heating energy demand.

Both configurations are available as input parameters in the framework, and the user can select the most appropriate option for their specific climate and operating strategy. In this case, ORM30 was chosen because it captures seasonal climate transitions and restricts cooling energy calculations to the summer season, where they are physically meaningful. The ORM30 configuration with shading active is therefore used as the final configuration for all results presented in Chapter 6.

5.6 Comparison indicators

This section outlines the method used to compare the annual energy performance of the three scenarios on an hourly basis. It also defines the key performance indicators and highlights the operational differences in how heating and cooling demands are calculated, particularly for the I-DIFFER system.

The framework calculates hourly heating and cooling energy needs for all three scenarios across all 8760 hours of the year. Results are expressed per unit floor area in kWh/m^2 to allow comparison between scenarios independently of room

size.

- Annual heating energy need [kWh/m^2] is the total energy delivered by the heating system over the year to keep the room at or above the setpoint temperature of 20°C, divided by 50 m^2.
- Annual cooling energy need [kWh/m^2] is the total energy removed to prevent the room from exceeding the setpoint temperature, divided by 50 m^2.
- Total annual energy need [kWh/m^2] is the sum of the two values above.
- Total energy reduction [%] is the percentage reduction in total kWh/m^2 compared to the unrenovated baseline.

An important operational difference between the scenarios is that baseline and traditional renovation calculate cooling all year whenever gains exceed losses, while I-DIFFER only calculates cooling during the ORM30-defined cooling season from 23 May to 29 October. In winter, I-DIFFER redirects solar gains into pre-heating rather than treating them as an overheating problem. This difference is discussed further in Chapter 6.

5.7 Framework simplifications

The simplified framework does not include several aspects of the full I-DIFFER system reported by (Bugenings et al., 2022). These simplifications are relevant when interpreting the results.

- **Thermal mass of cavity is not modelled.** All heat gains and losses are assumed to affect the room temperature instantaneously. The most visible consequence is in transparent insulation mode, where the sealed cavity reaches a calculated maximum of 108.9°C, compared to 63.6°C in the simplified reference model from the validation study. Since the cavity has no thermal mass in the framework, it cannot store heat between hours and reacts instantly to outdoor conditions and solar radiation at each timestep.
- **The control logic is simplified.** (Bugenings et al., 2022) report that the I-DIFFER system uses operative temperature thresholds with hysteresis bands. The simplified framework assigns modes based on ORM30 or instantaneous energy comparison, occupancy status, and shading only.
- **Energy uses.** Ventilation fan electricity and lighting are not included. The framework calculates only heating and cooling energy need expressed as final energy.
- **Weather data.** The measured hourly weather data for Copenhagen, Denmark,

differ from the Danish Design Reference Year DRY2010 used by (Bugenings et al., 2022). Since the goal is to produce reliable results using the building geometry, envelope properties, and system specifications from (Bugenings et al., 2022), rather than to reproduce their reported outputs, this difference is accepted and stated throughout.

Chapter 6

Results

6.1 Overview

This chapter presents the results of the simplified hourly framework applied to the three scenarios defined in Chapter 5: the unrenovated baseline, the traditional renovation, and the I-DIFFER concept. All results are calculated using measured hourly weather data, Copenhagen, Denmark, provided by Aalborg University. The primary comparison indicators are annual heating and cooling energy need expressed in kWh and kWh/m^2 of floor area, and the percentage reduction in total annual energy need relative to the unrenovated baseline.

The main purpose of the chapter is to compare the energy performance of the traditional renovation and the I-DIFFER concept using the unrenovated baseline as a reference point, and to further analyse the behaviour of I-DIFFER through its operating mode distribution, cooling season hourly demand distribution, cavity temperature behaviour, and sensitivity to glazing properties, cavity depth, and facade orientation.

Previous work by Bugenings et al. (2022) does not include a mechanical cooling system and does not calculate cooling energy demand. The simplified framework calculates the cooling energy demand needed to maintain the room at the setpoint temperature throughout the year. The relationship between the framework results and the findings of (Bugenings et al., 2022)is discussed in Chapter **??**.

Three percentage-based indicators are used consistently throughout this chapter. The first is the percentage reduction of a renovation scenario relative to the unrenovated baseline:

$$\frac{E_{\text{base}} - E_{\text{scen}}}{E_{\text{base}}} \times 100 \tag{6.1}$$

where E_{base} is the total annual energy demand of the baseline in kWh/m^2 and E_{scen} is the total annual energy demand of the renovation scenario in kWh/m^2. This indicator is used in Tables 6.1 and 6.9 to show how much each renovation saves compared to doing nothing.

The second is the percentage difference between two renovation scenarios:

$$\frac{E_{\text{ref}} - E_{\text{scen}}}{E_{\text{ref}}} \times 100 \tag{6.2}$$

where E_{ref} is the total annual energy demand of the reference scenario in kWh/m^2. A positive result means the compared scenario uses less energy than the reference. A negative result means more energy. This indicator is used in Table 6.2 and throughout the text when comparing renovation approaches directly.

The third is the absolute energy difference between two scenarios:

$$\Delta E = E_{\text{scen}} - E_{\text{ref}} \tag{6.3}$$

A negative value indicates lower energy demand than the reference and a positive value indicates higher energy demand. This indicator is used in Table 6.2 to show the heating and cooling differences separately, making it possible to see both the heating increase and cooling reduction of I-DIFFER at the same time.

All energy values are expressed per unit floor area in kWh/m^2 by dividing total annual energy in kWh by the floor area of 50 m^2. All percentages are rounded to one decimal place.

6.2 Annual energy demand - south orientation

For all three scenarios, the annual heating and cooling energy needs on the primary south-facing orientation are summarised in Table 6.1.

Table 6.1: Annual heating and cooling energy demand - south orientation

Scenario	Heating kWh	Heating kWh/m^2	Cooling kWh	Cooling kWh/m^2	Total kWh	Total kWh/m^2	Reduction %
Baseline	11075	221.5	6072	121.4	17147	342.9	–
Traditional D-C1 shading OFF	3633	72.7	8107	162.1	11740	234.8	31.5%
Traditional D-C1 shading ON	3905	78.1	3960	79.2	7865	157.3	54.1%
Traditional T-C1 shading ON	3291	65.8	3990	79.8	7281	145.6	57.5%
Traditional T-C1 shading OFF	3083	61.7	7405	148.1	10488	209.8	38.8%
I-DIFFER D-C1 shading OFF	4927	98.5	3149	63.0	8077	161.5	52.9%
I-DIFFER D-C1 shading ON	5207	104.1	1344	26.9	6552	131.0	61.8%

Highlighted rows represent the primary comparison scenarios used throughout Chapter 6.

The unrenovated baseline shows the highest total annual energy demand at 342.9 kWh/m^2. This reflects the combination of large transmission losses through the poorly insulated envelope, high ventilation losses from the exhaust-only system without heat recovery, and large solar gains through the unshaded original glazing, resulting in increased cooling demand on sunny, occupied days throughout the year.

The traditional renovation with D-C1 double glazing and solar shading achieves a 54.1% total reduction, mainly driven by a 64.7% drop in heating demand from improved insulation and heat recovery. An unexpected result appears when shading is removed from the traditional renovation: cooling demand rises to 8107 kWh, which is actually higher than the baseline cooling demand of 6072 kWh, despite the building being much better insulated. This happens because better insulation and heat recovery reduce transmission and ventilation losses so effectively that solar and internal gains can no longer be offset by those losses, meaning nearly all solar gain must be removed by cooling. This shows that shading is not only a comfort measure, but a fundamental part of the energy strategy for well-insulated buildings, consistent with the design approach of (Bugenings et al., 2022), who include external venetian blinds as a standard component of the traditional renovation. Shading reduces traditional D-C1 cooling demand by 4147 kWh, corresponding to 51.1%, and total energy demand by 3875 kWh, corresponding to 33.0%.

The traditional renovation with T-C1 triple glazing and shading gives a total annual energy demand of 145.6 kWh/m^2, which is 7.4% lower than D-C1 with shading. The improvement comes primarily from the much better thermal insulation of triple glazing, with U_g=0.5 W/(m^{2}K) compared to 1.1 W/(m^{2}K). Without shading, T-C1 produces 209.8 kWh/m^2, confirming that shading is essential regardless of glazing type.

The I-DIFFER scenario achieves the best total result at 131.0 kWh/m^2, corresponding to a 61.8% reduction from the baseline. Its heating demand of 104.1 kWh/m^2

is higher than both traditional renovation options, because the inner facade is left unrenovated and retains its original high transmission losses. However, the cooling demand of 26.9 kWh/m^2 is 66.1% lower than traditional D-C1 with shading, confirming that the combination of natural DSF cavity ventilation and cavity venetian blind shading is highly effective at preventing solar heat from entering the room during the cooling season.

When shading is removed from I-DIFFER, the total energy demand rises to 161.5 kWh/m^2, which is nearly identical to the traditional renovation without shading (162.1 kWh/m^2). This shows that, without shading, the two renovation approaches perform almost the same. The solar gains that enter the cavity through the high g-value outer glazing are beneficial in winter for preheating, but in summer, without shading, they increase cooling demand to a level comparable to the traditional renovation. This means that shading is not just an additional feature for I-DIFFER; it is what makes the system effective. If it is removed, the energy advantage over the traditional renovation disappears.

The annual heating and cooling energy demand for all scenarios is shown visually in Figure 6.1.

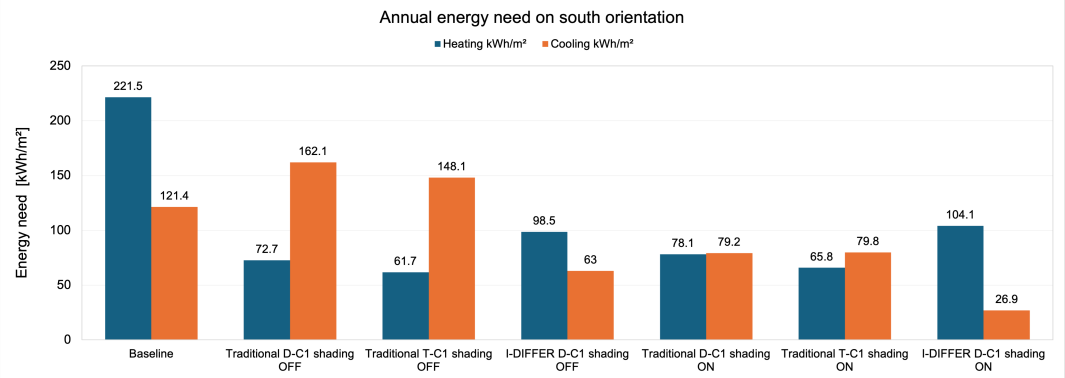

Figure 6.1: Annual heating and cooling energy demand for all scenarios on south orientation.

Note: Traditional renovation with D-C1 double glazing and shading ON is the primary traditional renovation configuration following (Bugenings et al., 2022). Traditional renovation with T-C1 triple glazing and shading ON represents the best-performing alternative traditional renovation configuration. Shading ON refers to venetian blind shading activated above 150 W/m^2. Shading OFF refers to no shading applied. I-DIFFER results use D-C1 outer glazing throughout.

6.3 Scenario comparison - south orientation

Table 6.2 summarises the direct comparisons between all scenarios. Negative values indicate a reduction relative to the reference scenario, while positive values indicate an increase relative to the reference scenario.

Table 6.2: Direct comparison between scenarios

Comparison	Heating kWh/m^2	Cooling kWh/m^2	Total kWh/m^2	Reduction %
Traditional D-C1 vs Baseline	-143.4	-42.2	-185.6	54.1%
I-DIFFER D-C1 vs Baseline	-117.4	-94.6	-211.9	61.8%
I-DIFFER D-C1 vs Traditional D-C1	+26.0	-52.3	-26.3	16.7%
Traditional T-C1 vs Baseline	-155.7	-41.6	-197.3	57.5%
I-DIFFER D-C1 vs Traditional T-C1	+38.3	-52.9	-14.6	10.0%

Highlighted rows represent the primary comparison scenarios used throughout Chapter 6.

I-DIFFER achieves 16.7% lower total energy demand than traditional renovation with D-C1 glazing and 10.0% lower than traditional renovation with T-C1 triple glazing. The comparison against T-C1 is the most relevant because it represents the most energy-efficient conventional renovation option. The heating increase of I-DIFFER relative to D-C1 is 26.0 kWh/m^2, attributable to the unrenovated inner facade. This is more than offset by the cooling reduction of 52.3 kWh/m^2, giving a total energy advantage of 26.3 kWh/m^2 for I-DIFFER. Against T-C1, the heating increase grows to 38.3 kWh/m^2 because triple glazing provides better winter insulation, while the cooling reduction stays at a similar level of 52.9 kWh/m^2.

An important operational difference between the scenarios is that baseline and traditional renovation cooling is calculated all year whenever gains exceed losses, while I-DIFFER cooling is restricted to the ORM30-defined summer season from 23 May to 29 October. In winter, I-DIFFER redirects solar gains into pre-heating mode rather than triggering cooling mode. This operational difference is important to the I-DIFFER concept and is discussed further in Section 6.5.

6.3.1 Sensitivity of scenario comparison to control assumptions

The scenario comparison presented in Table 6.2 reflects the final framework configuration with ORM30 seasonal switching and venetian blind shading active. To assess how robust the I-DIFFER advantage over traditional renovation is to changes in these two control assumptions Table 6.3 extends the comparison across all four sensitivity configurations. The traditional renovation results are unchanged across all configurations, ORM30 switching and shading only affect the I-DIFFER framework. The baseline is included as a fixed reference point.

Table 6.3: Sensitivity of scenario comparison to control assumptions

Configuration	Baseline	Trad OFF	Trad ON	I-DIFFER	vs Baseline	vs Trad OFF	vs Trad ON
ORM30 + shading ON	342.9	234.8	157.3	131.0	-61.8%	-44.2%	-16.7%
ORM30 + shading OFF	342.9	234.8	157.3	161.5	-52.9%	-31.2%	+2.7%
Instantaneous + shading ON	342.9	234.8	157.3	154.5	-54.9%	-34.2%	-1.8%
Instantaneous + shading OFF	342.9	234.8	157.3	185.4	-45.9%	-21.1%	+17.8%

Note: Baseline, Trad OFF, Trad ON, and I-DIFFER values are given in kWh/m^2. Trad OFF refers to traditional renovation with shading OFF, while Trad ON refers to traditional renovation with shading ON. Percentage columns show the relative difference between I-DIFFER and the corresponding reference case.

The total annual energy need for all scenarios across all four configurations is shown in Figure 6.2. The I-DIFFER heating and cooling split is shown in Figure 6.3.

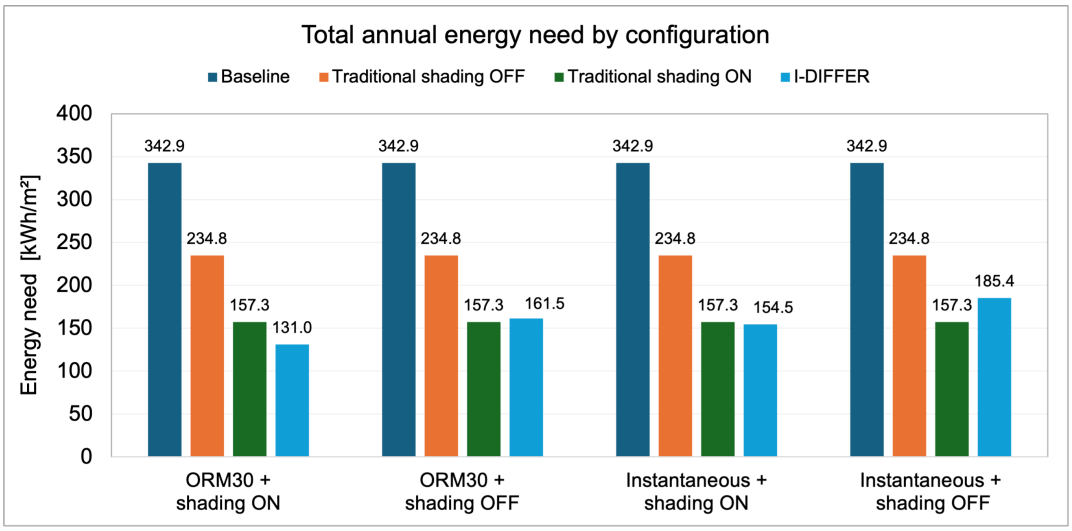

Figure 6.2: Total annual energy need for baseline, traditional renovation without shading, traditional renovation with shading, and I-DIFFER across four sensitivity configurations.

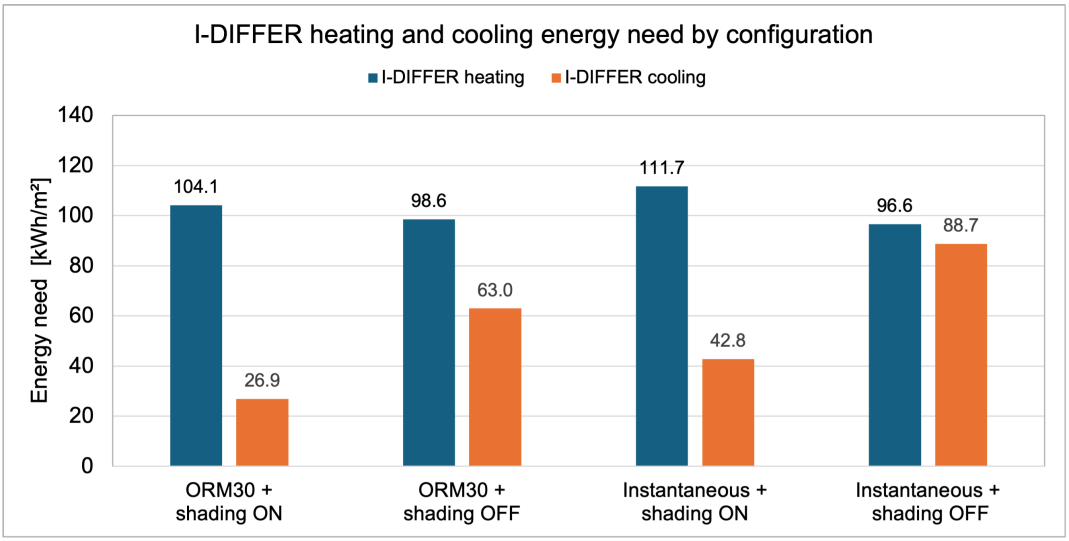

Figure 6.3: Annual heating and cooling energy need for I-DIFFER across four sensitivity configurations.

The I-DIFFER advantage over traditional renovation with shading depends on both control assumptions being active. With ORM30 switching and shading active I-DIFFER achieves 16.7% lower total energy than traditional renovation with shading. Removing shading reverses this advantage, and I-DIFFER becomes 2.7% worse than traditional renovation with shading as cooling demand rises from 26.9 to 63.0 kWh/m². Replacing ORM30 with instantaneous switching reduces the advantage to only 1.8%, and the two renovation strategies produce almost identical total energy demand. In the worst case, instantaneous switching with no shading, I-DIFFER is 17.8% worse than traditional renovation with shading.

However, in all four configurations, I-DIFFER remains substantially below the unrenovated baseline, ranging from 45.9% to 61.8% reduction, and performs better than traditional renovation without shading, ranging from 21.1% to 44.2% improvement. This shows that I-DIFFER provides energy benefits across all configurations tested. The choice of control parameters affects whether I-DIFFER outperforms traditional renovation with shading, but does not change the direction of improvement relative to the unrenovated baseline.

Figure 6.3 confirms that heating demand is relatively stable across all four configurations, ranging from 96.6 to 117.1 kWh/m², while cooling demand varies widely from 26.9 to 112.7 kWh/m². ORM30 switching and shading together produce the lowest total energy demand of the four configurations tested and are the control assumptions used throughout the case scenario results presented in Chapter 6.

6.4 Monthly energy distribution

The monthly heating and cooling energy demand for all three scenarios shows distinct seasonal patterns consistent with the measured hourly weather data for Copenhagen, Denmark.

For the baseline, heating demand peaks in January and December, reflecting the high transmission and ventilation losses of the unrenovated envelope combined with low outdoor temperatures. Cooling demand is present throughout most of the year, including winter months, because the unshaded original glazing allows large solar gains that frequently exceed transmission losses on sunny days.

For the traditional renovation, heating demand is dramatically reduced across all months due to improved insulation and 73% heat recovery. Cooling demand continues throughout the year, including January and February, because the reduced losses mean that solar and internal gains can exceed losses on sunny occupied days regardless of season.

For I-DIFFER, the monthly pattern shows a two-part character. During the heating season from January through May and October through December, cooling demand is absent. This is a direct consequence of the ORM30 mode switching logic, which redirects solar gains into pre-heating rather than triggering cooling mode. During the cooling season from late May through October, both heating and cooling demand appear in the same months, reflecting the cool Copenhagen climate, where many nights and weekends during the official cooling season still require heating.

The monthly distribution of heating and cooling energy demand for all three scenarios is shown in Figure 6.4.

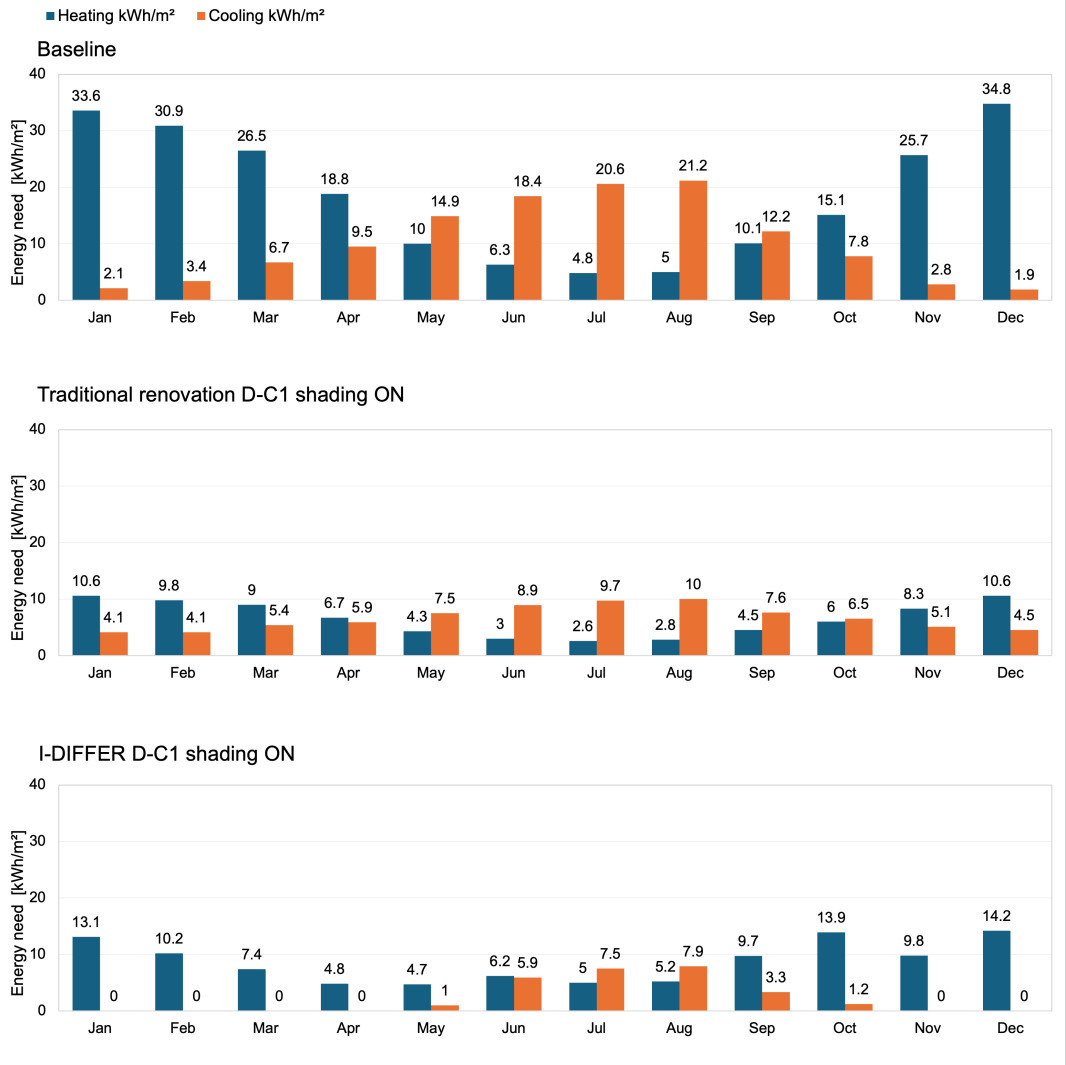

Figure 6.4: Monthly heating and cooling energy demand for baseline, traditional renovation D-C1 with shading, and I-DIFFER on south orientation.

The absence of cooling demand in I-DIFFER during winter months is clearly visible, confirming that the ORM30 mode switching logic successfully redirects winter solar gains into pre-heating rather than triggering cooling demand.

6.5 I-DIFFER operating mode analysis

Table 6.4 shows how the 8760 annual hours are distributed between the three I-DIFFER operating modes and the heating and cooling energy contribution from each mode.

Table 6.4: I-DIFFER operating mode energy distribution - south orientation

Mode	Hours	% year	Heating kWh	Heating kWh/m^2	% heating	Cooling kWh	Cooling kWh/m^2
Pre-heating	1168	13.3%	1070	21.4	20.5%	0	0
Transparent insulation	3779	43.1%	2044	40.9	39.3%	0	0
Cooling	3813	43.5%	2094	41.9	40.2%	1344	26.9
Total	8760	100%	5207	104.1	100%	1344	26.9

The annual hour distribution and heating energy contribution across the three modes are shown in Figure 6.2.

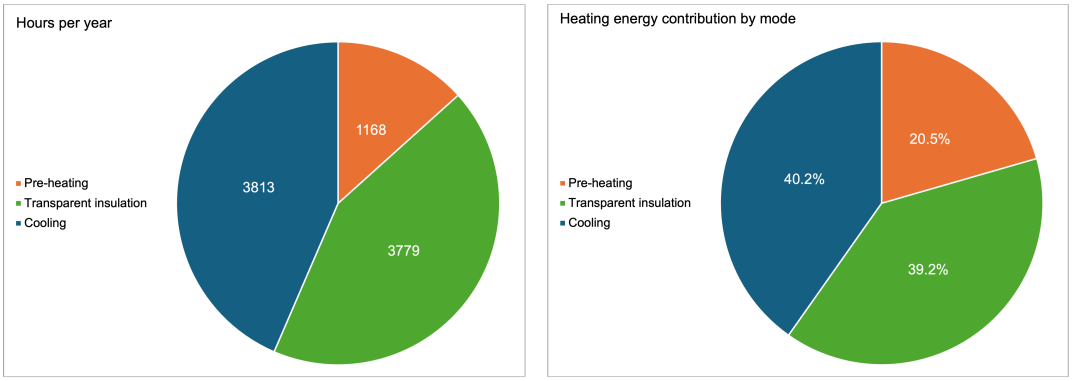

(a) **(b)**

Figure 6.5: I-DIFFER operating mode distribution by annual hours (a) and heating energy contribution (b) on south orientation.

Transparent insulation mode runs for the largest proportion of hours, at 43.1%, and contributes 39.3% of annual heating demand. This covers all unoccupied heating season hours, including nights, weekends, and school holidays. Despite the sealed cavity providing some thermal buffering, the unrenovated inner facade still loses significant heat during these long unoccupied periods. During unoccupied hours on winter weekdays, the cavity receives little or no solar radiation, since most unoccupied time falls at night and early morning. On winter weekends, however, the cavity operates in transparent insulation mode throughout the full day, allowing solar radiation to contribute to cavity heating during daylight hours. The framework reacts instantaneously to outdoor conditions and solar radiation at each hour without accounting for the thermal mass of the cavity construction, meaning that

temperature oscillations between solar radiation periods and cold nights are not moderated as they would be in a real building.

Pre-heating mode is active for 13.3% of hours and contributes 20.5% of annual heating. An analysis of the pre-heating outlet temperature shows that during 750 of the 1168 pre-heating occupied hours, corresponding to 64.2%, the DSF cavity outlet temperature falls below the room setpoint of 20°C, with a mean outlet temperature of 11.7°C during those hours. During these periods, the mechanically driven ventilation air enters the room cooler than the setpoint, contributing to heating demand despite operating in pre-heating mode. The total ventilation energy balance in pre-heating mode shows a loss of 407.0 kWh per year, made up of 1438.9 kWh of ventilation gain during the 418 effective pre-heating hours, offset by 1845.9 kWh of ventilation loss during the 750 insufficient pre-heating hours. Even during these hours, the cavity provides partial preheating, reducing ventilation losses compared to the baseline, where supply air enters directly at outdoor temperature.

Cooling mode accounts for 43.5% of hours and 40.2% of annual heating demand, in addition to all cooling demand. The heating demand within the cooling season arises from cool summer nights and weekends in the Copenhagen climate, where outdoor temperatures frequently drop below 20°C even during the official cooling season.

6.6 Cooling season thermal analysis

The analysis in this section applies specifically to the final framework configuration with both ORM30 switching and summer-only cooling active. The cooling season runs for 3813 hours from 23 May at 22:00 to 29 October at 18:00, as defined by the ORM30 threshold transition in the measured hourly weather data for Copenhagen, Denmark. Table 6.5 shows these hours divided by outdoor temperature relative to the 20°C room setpoint.

Table 6.5: Cooling season hourly demand distribution

Parameter	Total	T_e below 20°C	T_e above 20°C	Unit
Hours	3813	3531	282	h
% of cooling season	100.0%	92.6%	7.4%	%
Mean T_e	14.0	13.4	22.1	°C
Hours heating above 0.1 kWh	2778	2748	30	h
Hours cooling above 0.1 kWh	894	679	215	h
% hours heating	72.9%	77.8%	10.6%	%
% hours cooling	23.5%	19.2%	76.2%	%
Hours neither	141	104	37	h
% hours neither	3.7%	2.9%	13.1%	%

A notable finding from Table 6.5 is how cool the Copenhagen cooling season actually is. Of the 3813 cooling season hours 3531 (92.6%) have outdoor temperatures

below 20°C, with a mean of only 13.4°C. Heating demand occurs in 77.8% of these cool hours, mostly at night and on weekends when internal gains are zero and the room loses heat through the inner facade. However 19.2% of these cool hours still produce cooling demand, which happens mainly on occupied weekday afternoons when solar gains and internal gains together push the room above the setpoint even though outdoor temperature is well below 20°C.

The hours with outdoor temperature at or above 20°C make up only 7.4% of the cooling season (282 hours) with a mean of 22.1°C. During these hours cooling demand appears in 76.2% of cases. A further 141 hours (3.7%) show neither significant heating nor cooling demand. These thermally neutral hours occur when outdoor temperature is close to 20°C and solar and internal gains are small, leaving the room close to thermal equilibrium without requiring active energy input.

The distribution of hours with heating demand, cooling demand, and neither within each outdoor temperature group is shown in Figure 6.6.

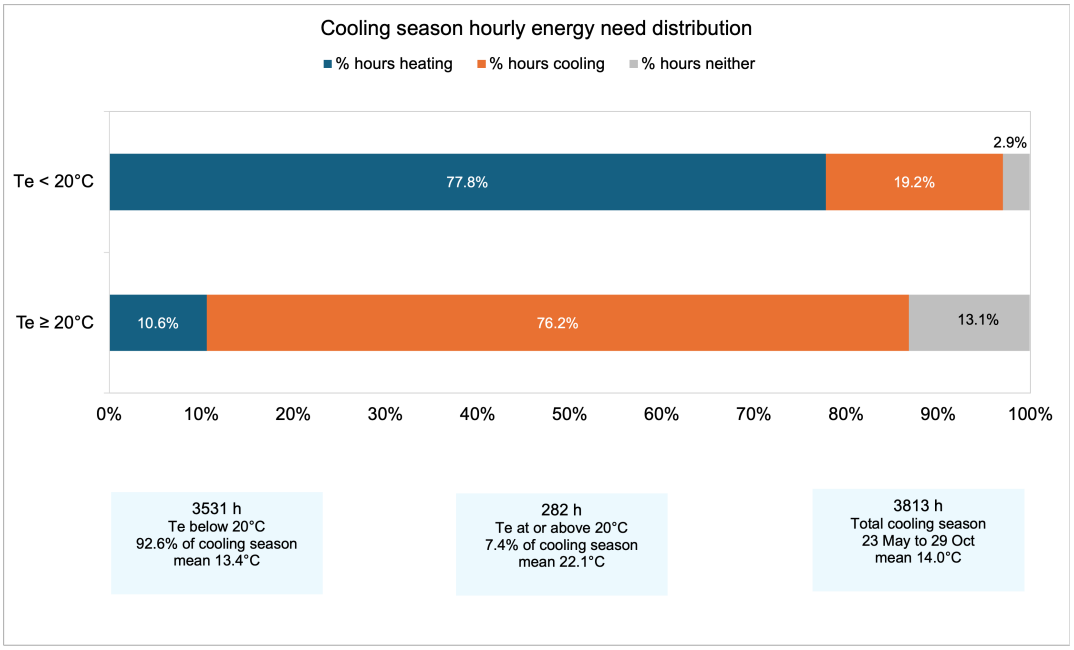

Figure 6.6: Cooling season hourly demand distribution by outdoor temperature

6.7 Cavity temperature behaviour

Table 6.6 shows the cavity temperature statistics for each operating mode under the measured hourly weather data for Copenhagen, Denmark. Since the climate data used here differ from the reference year used in the validation study in Chap-

ter 4, direct numerical comparison with the validation reference values is not appropriate. The statistics are reported to characterise how the DSF cavity behaves thermally under the case scenario conditions.

Table 6.6: DSF cavity temperatures by operating mode

Parameter	Pre-heating mode	Pre-heating outlet	Transparent ins. mode	Cooling mode
Mean [°C]	11.9	18.8	17.6	15.4
Maximum [°C]	33.9	50.7	108.9	30.6
Minimum [°C]	-2.9	0.9	7.7	1.0
Active hours	1168	1168	3779	3813
Occupancy	Occupied	Occupied	Unoccupied	All hours

In pre-heating mode, the mean cavity temperature of 11.9°C and mean outlet temperature of 18.8°C confirm that the cavity provides meaningful solar-assisted preheating of ventilation air, with supply air entering the room close to the 20°C setpoint on average. The minimum cavity temperature of -2.9°C occurs on very cold occupied mornings before solar radiation has had time to warm the cavity.

In transparent insulation mode, the mean temperature of 17.6°C shows that the sealed cavity remains above outdoor temperature due to solar gains during daylight hours. The maximum temperature of 108.9°C is a direct consequence of the high solar radiation during weekend days.

In cooling mode, the mean cavity temperature of 15.4°C is close to the mean outdoor temperature of 14.0°C during the cooling season. This shows that buoyancy-driven natural ventilation through the open cavity effectively removes solar heat within the cavity. The maximum temperature of 30.6°C shows that, even under peak solar radiation conditions, the open cavity stays within physically reasonable temperature limits.

6.8 Sensitivity analysis - DSF glazing properties and cavity depth

To assess the sensitivity of I-DIFFER results to the outer DSF glazing properties, all ten configurations from (Bugenings et al., 2022), Table 5.1 were tested under the final framework configuration for the south orientation. The results are summarised in Table 6.7.

Table 6.7: DSF outer glazing sensitivity - south orientation

Glazing	Type	U_g W/(m^{2}K)	g	τ	Shading ON kWh/m^2	Shading OFF kWh/m^2	Shading benefit kWh/m^2
S-A1	Single	5.8	0.88	0.91	127.5	162.2	34.7
D-D1	Double	2.7	0.80	0.83	128.7	159.4	30.7
S-B1	Single	5.7	0.70	0.67	130.4	153.2	22.8
D-C1	Double	1.1	0.71	0.83	131.0	162.0	31.0
D-C2	Double	1.4	0.71	0.83	131.0	161.5	30.5
D-B1	Double	1.0	0.62	0.82	133.8	163.6	29.8
D-B2	Double	1.2	0.62	0.82	133.8	163.6	29.8
S-C1	Single	5.8	0.57	0.51	133.7	148.9	15.2
S-D1	Single	5.8	0.44	0.37	138.3	147.3	9.0
D-E1	Double	1.0	0.33	0.70	148.0	171.2	23.2

The results show a clear pattern when shading is active; higher g-value outer glazing leads to lower total annual energy demand. S-A1 with g = 0.88 gives the lowest total of 127.5 kWh/m^2, while D-E1 with g = 0.33 gives the highest at 148.0 kWh/m^2, a difference of 20.5 kWh/m^2. This behaviour is physically consistent. Higher g-value glazing allows more solar radiation into the cavity, increasing the preheating effect in winter and reducing transmission losses through the inner facade in transparent insulation mode. Lower g-value glazing blocks more solar radiation and therefore reduces this effect, leading to higher heating demand. This result is consistent with (Bugenings et al., 2022), who identify glazing properties as an important factor for I-DIFFER performance.

The relationship between the glazing g-value and total annual energy demand is shown in Figure 6.7 for both shading active and inactive.

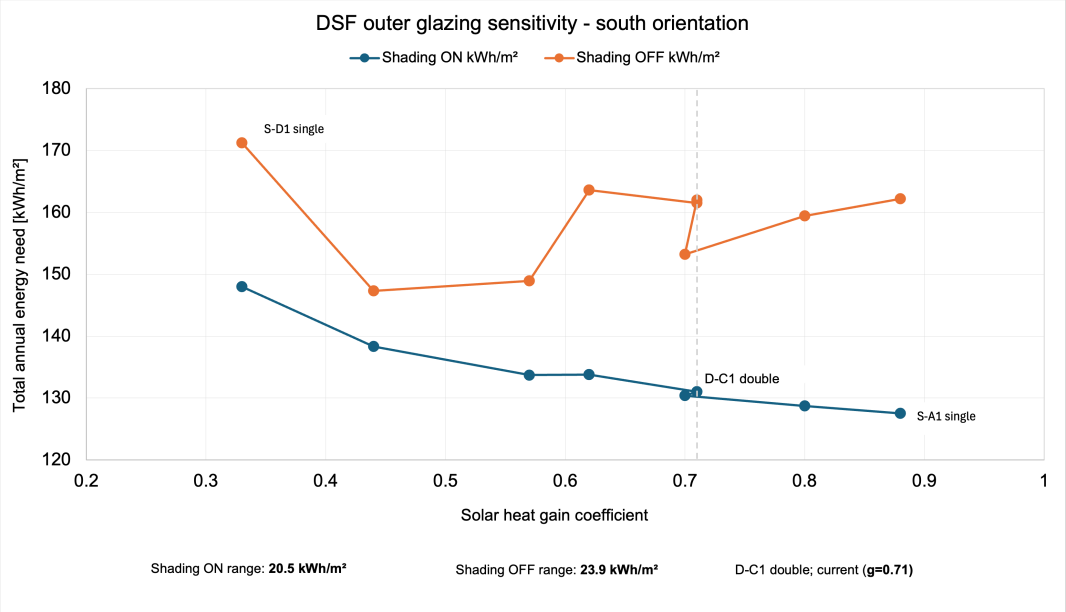

Figure 6.7: Total annual energy demand for ten outer DSF glazing configurations on south orientation plotted against solar heat gain coefficient g.

The downward trend of the shading ON line confirms that higher g-value outer glazing gives lower total energy demand due to better solar preheating in winter. The shading OFF line shows a different pattern where low g-value glazing performs better by blocking summer solar gains.

The simplified framework calculates each hour completely independently. At 10:00 on 14 January with solar radiation of 149.25 W/m^2 on the south facade, D-C1 glazing with g = 0.71 produces a mean cavity temperature of 7.18°C while S-D1 with g = 0.44 produces 5.15°C, as shown in Table 6.7. This difference of 2.03°C at a single hour illustrates how glazing g-value directly affects how much solar radiation heats the cavity air.

Table 6.8: DSF mean cavity temperature in pre-heating mode at 10:00 on 14 January - solar radiation 149.25 W/m^2

Glazing	Type	U_g W/(m^{2}K)	g	τ	Cavity temperature °C
D-C1	Double	1.1	0.71	0.83	7.18
S-D1	Single	5.8	0.44	0.37	5.15
Difference	–	–	–	–	2.03

At 11:00, however, the calculation starts again, and the cavity has no memory of

what happened one hour earlier. Any difference between the two glazing types therefore disappears at each new timestep.

In a real building, the cavity glass surfaces and the inner facade wall have physical mass. They absorb solar heat during the day and release it slowly over the following hours. A cavity with high g-value glazing can therefore stay warmer through the evening and into the next morning compared with one with low g-value glazing. Over an entire winter, this small daily difference builds up. The simplified framework cannot calculate this because it has no heat storage between hours. This is most likely why (Bugenings et al., 2022) found glazing properties to have a superior influence on I-DIFFER performance, since dynamic simulation accounts for thermal mass and therefore captures the cumulative effect of glazing choice over the heating season.

When shading is removed, the pattern changes. Total energy ranges from 147.3 to 171.2 kWh/m^2, a spread of 23.9 kWh/m^2. Without shading, high g-value glazing allows more solar radiation through both the outer and inner glazing into the room during summer, significantly increasing cooling demand. S-A1 with g = 0.88 gains 34.7 kWh/m^2 from having shading active, while S-D1 with g = 0.44 gains only 9.0 kWh/m^2. This shows clearly that the higher the g-value, the more important shading becomes for controlling summer cooling demand. It is also notable that without shading the ranking changes. S-D1, with the lowest g-value, gives the lowest total energy without shading at 147.3 kWh/m^2 because it blocks most solar gain in summer, while S-A1, with the highest g-value, gives the second highest total at 162.2 kWh/m^2 because it allows the most uncontrolled solar gain into the room.

A supplementary test was carried out to assess the sensitivity of I-DIFFER results to DSF cavity depth, testing depths of 0.20 m, 0.32 m, and 0.50 m under the final framework configuration for the south orientation. The results are shown in Table 6.9.

Table 6.9: DSF cavity depth sensitivity - south orientation

Cavity depth m	Heating kWh/m^2	Cooling kWh/m^2	Total kWh/m^2
0.20	103.8	26.7	130.5
0.32	104.1	26.9	131.0
0.50	104.8	27.0	131.8

Total annual energy demand varies by only 1.3 kWh/m^2 across the three cavity depths, from 130.5 to 131.8 kWh/m^2. This is smaller than the glazing sensitivity of 20.5 kWh/m^2 found across the ten glazing configurations, confirming the finding of (Bugenings et al., 2022) that glazing properties have a stronger influence on

I-DIFFER performance than cavity thickness.

6.9 Orientation sensitivity - east facade

To assess the sensitivity of the framework results to facade orientation, all three scenarios were also run for an east-facing classroom, representing a common classroom orientation in school buildings. On an east-facing facade, solar radiation in the morning hours is higher than on a south-facing facade at the same time, meaning that solar gains at the start of occupancy at 08:00 can be larger on the east facade than on the south facade. However, the south-facing orientation receives more solar radiation overall during the day, particularly around midday when the sun is at its highest. Tables 6.10 and 6.11 show the east orientation results and the comparison with the south orientation.

Table 6.10: Annual energy demand - east orientation

Scenario	Heating kWh	Heating kWh/m^2	Cooling kWh	Cooling kWh/m^2	Total kWh	Total kWh/m^2	Reduction %
Baseline	11681	233.6	4184	83.7	15865	317.3	–
Traditional D-C1 shading ON	3911	78.2	3937	78.7	7848	157.0	50.5%
Traditional D-C1 shading OFF	3747	74.9	6008	120.2	9755	195.1	38.5%
I-DIFFER shading ON	6385	127.7	1316	26.3	7702	154.0	51.4%
I-DIFFER shading OFF	6098	122.0	3100	62.0	9197	183.9	42.0%

Table 6.11: South vs east orientation comparison

Scenario	South kWh/m^2	East kWh/m^2	Difference kWh/m^2	Change %
Baseline total	342.9	317.3	-25.6	-7.5%
Traditional D-C1 shading ON	157.3	157.0	-0.3	-0.2%
Traditional D-C1 shading OFF	234.8	195.1	-39.7	-16.9%
I-DIFFER shading ON	131.0	154.0	+23.0	+17.6%
I-DIFFER shading OFF	161.5	183.9	+22.4	+13.9%
I-DIFFER vs Traditional - south	131.0 vs 157.3	–	-26.3	-16.7%
I-DIFFER vs Traditional - east	–	154.0 vs 157.0	-3.0	-1.9%

The heating and cooling energy demand for all scenarios on both orientations is shown in Figure 6.8.

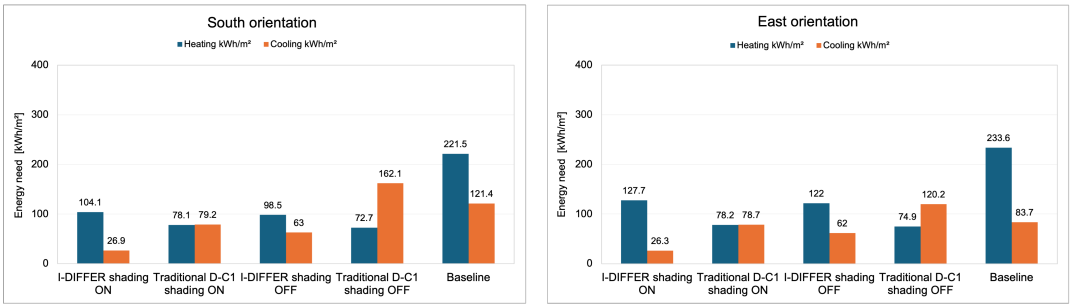

(a) **(b)**

Figure 6.8: Heating and cooling energy demand for south (a) and east (b) orientation, all scenarios with and without shading.

The significant increase in I-DIFFER heating demand on east orientation is clearly visible, while cooling demand stays similar on both orientations. The traditional renovation bars are almost identical on both orientations confirming its orientation independence.

The baseline results show that east orientation results in 7.5% lower total energy than south orientation. This mainly comes from lower cooling demand on the east (83.7 vs 121.4 kWh/m^2), since the east facade receives less solar radiation throughout the day than the south facade. For the traditional renovation with shading, the orientation makes almost no difference, at only 0.2%, which is expected because the main energy reductions from insulation and heat recovery apply regardless of the facade's orientation. Removing shadings from the traditional renovation shows a bigger orientation effect. Performance is for 16.9% better on the east than on the south because lower afternoon solar radiation significantly reduces uncontrolled solar gains, whereas midday sun in the south drives very high cooling demand without shading.

The interesting result is for I-DIFFER. Replacing the south with the east site increases total energy demand by 17.6%, from 131.0 to 154.0 kWh/m^2. The cooling demand remains very similar between the two orientations (26.9 vs 26.3 kWh/m^2), but the heating demand rises significantly from 104.1 to 127.7 kWh/m^2. The reason is simply that the east facade receives much less solar radiation during the winter heating season, which means the DSF cavity in pre-heating mode cannot warm the supply air as effectively, and the sealed cavity in transparent insulation mode offers less thermal buffering, meaning the cavity air temperature stays closer to outdoor temperature, reducing the insulation benefit between the cold outdoor environment and the inner facade. Despite morning solar on the east aligning with occupancy starting at 08:00, the total daily winter solar on the south is higher, which drives a better annual pre-heating performance on the south. As a result,

the I-DIFFER advantage over traditional renovation drops from 16.7% on south to only 1.9% on east. This is a significant finding, suggesting that I-DIFFER is strongly orientation-dependent and performs best when oriented south, where total winter solar radiation is maximised.

The east orientation results also confirm that shading remains important regardless of orientation. Without shading on east orientation, I-DIFFER total energy increases to 183.9 kWh/m^2, an increase of 29.9 kWh/m^2 compared to the shaded case, very similar to the south orientation shading benefit of 30.5 kWh/m^2. This shows that the shading benefit is largely independent of orientation; it is driven by summer solar radiation, which significantly affects both east and south facades during the cooling season.

(Bugenings et al., 2022) noted in their conclusions that the applicability of I-DIFFER for other orientations should be analysed in future work, expecting that primary energy consumption would increase due to reduced solar radiation. The east orientation results from the simplified framework confirms this expectation. Total energy increases by 17.6% on the east compared to the south, and the I-DIFFER advantage over traditional renovation basically disappears.

Chapter 7

Discussion

7.1 Framework suitability for early-stage comparison

The research question asked how a simplified hourly calculation framework can be developed for early-stage comparison of heating and cooling energy needs between traditional renovation solutions and the I-DIFFER concept. The framework was assessed in two validation stages. First, cavity temperatures and energy-related outputs were compared against measured data from the full-scale DSF test facility at Aalborg University for pre-heating and cooling mode. Second, the framework was compared with a modified IDA-ICE reference model based on (Bugenings et al., 2022) for all three operating modes using the DRY10 climate dataset. This validation covered cavity temperature and heating energy need over a full 8760-hour period.

The dynamic validation showed that cooling mode and pre-heating mode produce results that are sufficiently close to the reference for early-stage comparative use, with total heating energy differences of 2.2% and 3.8%, respectively. Transparent insulation mode shows a much larger difference in heating energy need of 146.5%. This result should be interpreted with caution, since the validation setup represents each mode as a single constant mode operating throughout the full year. In transparent insulation mode, this means that the cavity remains sealed for the entire year.

The main reason for the larger deviation in transparent insulation mode is the simplified representation of thermal storage. The room heat balance includes the effect of building thermal mass only in simplified form following (BESTFACADE, 2007) through the (DS/EN ISO 13790, 2008) utilisation factor and room time constant. However, the framework does not reproduce the full dynamic thermal mass

behaviour of the reference simulation, and the DSF cavity does not include an equivalent heat storage. As a result, the cavity temperature reacts instantaneously to changes in solar radiation and outdoor temperature. When solar radiation is no longer available, the calculated cavity temperature can drop too quickly instead of remaining warmer due to heat stored in the glazing, cavity surfaces, and facade construction. This effect is strongest in transparent insulation mode.

The large heating energy deviation in transparent insulation mode should therefore be interpreted mainly as a consequence of the simplified thermal storage representation and the full-year single-mode validation setup, rather than as evidence that the transparent insulation principle itself is invalid. Other simplifications also affect the absolute results. The framework does not include detailed window frame losses or linear thermal bridges in the envelope. These simplifications are consistent with the early-stage purpose of the framework, but they must be considered when interpreting the results.

Therefore, the framework may support early-stage comparison, provided that its simplified assumptions and limitations are recognised. The results are most useful for comparing relative performance trends between design options, while detailed dynamic simulation remains necessary for final design decisions, comfort assessment, and detailed system sizing.

7.2 Heating and cooling trade-off

An important insight from the results is that renovation strategy affects both the size and balance of heating and cooling demand. The traditional renovation scenario without solar shading results in a cooling demand of 162.14 kWh/m², which is higher than the unrenovated baseline value of 121.44 kWh/m², despite the improved insulation level.

This apparent contradiction can be explained by reduced heat losses. In the unrenovated case, high transmission and ventilation losses partly remove solar and internal gains. After insulation and heat recovery are improved, less heat is lost to the exterior, so solar gains during sunny occupied periods are more likely to increase cooling demand.

This shows that solar shading is not only a comfort measure, but also an important energy measure in well-insulated buildings. Without shading, improved insulation may reduce heating demand while increasing cooling demand. This interpretation is consistent with (Bugenings et al., 2022), who include external venetian blinds in the traditional renovation scenario.

The I-DIFFER concept manages this heating-cooling trade-off differently. Rather

than simply blocking solar gains, it uses different operating modes to redirect them. During the heating season, solar gains can be used through pre-heating mode, while during the cooling season excess heat can be removed through natural cavity ventilation.

As a result, I-DIFFER has a heating demand of 104.04 kWh/m², compared with 78.10 kWh/m² for the best traditional renovation configuration. This represents an additional heating demand of 25.94 kWh/m², mainly due to the unrenovated inner facade.

However, this additional heating demand is offset by a cooling benefit of 52.16 kWh/m². Overall, this gives I-DIFFER a net total energy advantage of 26.22 kWh/m² for the south-facing orientation. The result indicates that the main advantage of I-DIFFER is not lower heating demand, but its ability to reduce cooling demand while keeping the additional heating demand moderate.

7.3 Role of solar shading

The sensitivity analysis shows that solar shading is the most influential single parameter in the framework. Removing shading from cooling mode increases cooling demand by 133%, from 27.04 kWh/m² to 62.98 kWh/m², and increases total energy demand by 23.2%.

The effectiveness of shading depends strongly on the solar transmittance of the glazing. For example, configuration S-A1, with single glazing and g = 0.88, achieves a shading benefit of 34.36 kWh/m². In contrast, configuration S-D1, with g = 0.44, achieves a smaller benefit of 9.56 kWh/m². This is physically expected because high-transmittance glazing allows more solar radiation to enter the cavity and room. Therefore, shading has a greater effect when solar transmittance is high.

A notable finding is the limited sensitivity of total energy demand to the outer DSF glazing properties when shading is active. Across all ten configurations, the difference in total energy demand is only 2.34 kWh/m². This suggests that active shading reduces the influence of outer glazing properties on the total energy balance.

7.4 Orientation sensitivity

The orientation analysis shows that I-DIFFER performance depends strongly on facade orientation. Moving from a south-facing to an east-facing facade increases total I-DIFFER energy demand by 17.9%, from 131.08 kWh/m² to 154.54 kWh/m².

In contrast, the traditional renovation scenario shows almost no orientation effect, with only a 0.2% difference.

As a result, the energy advantage of I-DIFFER over traditional renovation decreases from 16.7% for the south-facing orientation to only 1.5% for the east-facing orientation. The cooling benefit remains almost identical for both orientations, at 27.04 kWh/m². This suggests that natural cavity ventilation can remove solar heat effectively in both cases.

The main difference occurs in heating demand. The additional heating demand of I-DIFFER compared with traditional renovation increases from 25.94 kWh/m² on the south-facing facade to 49.28 kWh/m² on the east-facing facade. This is mainly because the east-facing facade receives less useful winter solar radiation, which reduces the effectiveness of pre-heating and transparent insulation thermal buffering.

This finding has direct practical implications. The I-DIFFER concept appears most effective on south-facing facades, where winter solar radiation can be used more effectively for cavity pre-heating. On east-facing facades, the concept still provides a similar cooling benefit, but this is offset by a much larger additional heating demand. As a result, the total energy balance becomes only slightly better than traditional renovation.

Therefore, facade orientation should be carefully assessed when considering I-DIFFER as a renovation strategy.

7.5 Delimitation

The framework was developed within a defined scope, and several simplifications were intentionally adopted to maintain transparency and suitability for early-stage use. Cavity thermal mass is not modelled. The DSF cavity temperature is calculated instantaneously at each timestep without heat storage between hours. This is most critical in the sealed transparent insulation mode, where peak cavity temperatures reach 108.9°C in the case scenario compared with 63.6°C in the validation reference. The limitation is less significant in cooling mode, where the naturally ventilated cavity results in only a slight underestimation of cavity temperature. Cooling demand is not calculated during the heating season when ORM30 seasonal switching is active. When ORM30 falls below 10°C, the cooling energy is set to zero, regardless of whether room gains exceed losses in that hour. On sunny winter days, this may lead to a slight underestimation of total cooling demand, as such occurrences are not captured. Window frame heat losses, linear thermal bridges, and excess heat from shading blind reflection in the DSF cavity are not included in the framework.

Chapter 8

Conclusion

This thesis developed a simplified hourly calculation framework for early-stage comparison of heating and cooling energy needs between traditional renovation solutions and the I-DIFFER concept. The framework was applied to an unrenovated baseline, traditional renovation scenarios, and the I-DIFFER concept under the same climate, geometry, and boundary conditions, enabling consistent comparison.

The main contribution of the thesis is a transparent, spreadsheet-based framework that links facade behaviour, ventilation effects, and seasonal operating logic within a single, simplified hourly calculation structure. The results suggest that the framework may provide a useful basis for early-stage comparison of renovation strategies, provided that its simplified assumptions and limitations are recognised.

The analysis also showed that I-DIFFER performance depends strongly on operating conditions. Solar shading is important for limiting cooling demand, and ORM30 seasonal switching prevents the cooling mode from operating during winter.

Orientation is also important. When the facade is rotated from south to east, the I-DIFFER advantage over traditional renovation decreases because reduced winter solar radiation limits the effectiveness of pre-heating and transparent insulation mode.

For the south-facing case, I-DIFFER achieved lower total energy demand than both the unrenovated baseline and the traditional renovation cases. Compared with the traditional D-C1 renovation, I-DIFFER reduced total energy demand by 16.7%, while compared with the better-performing T-C1 traditional renovation, the reduction was 10.0%. This indicates that the main benefit of I-DIFFER is its ability to

reduce cooling demand, although its heating demand is higher than in the traditional renovation case.

The main limitation of the framework is the overprediction of cavity temperature in transparent insulation mode during periods of high solar radiation. Because the sealed cavity has no ventilation path and the framework responds directly to hourly solar gains, strong solar radiation can produce unrealistically high cavity temperatures within a single timestep. This limitation mainly affects transparent insulation mode and should be considered when interpreting the results.

Future improvements should focus on reducing the overprediction of cavity temperature in transparent insulation. Future weather data should also be used to assess how the energy performance of each renovation scenario may change under anticipated climate conditions. As summers in northern Europe are expected to become warmer, the relative cooling benefit of I-DIFFER may increase, making this analysis relevant to long-term renovation decision-making.

Overall, the framework provides a transparent and structured basis for comparing renovation strategies at an early design stage. It should not replace detailed dynamic simulation, but it may help identify the main heating and cooling trade-offs, the role of solar shading, and the influence of facade orientation before more detailed modelling is carried out.

Bibliography

Attia, S., Gratia, E., De Herde, A., & Hensen, J. L. (2012). Simulation-based decision support tool for early stages of zero-energy building design. *Energy and Buildings*, *49*, 2–15. https://doi.org/10.1016/j.enbuild.2012.01.028

BESTFACADE. (2007, June). *BESTFAÇADE Best Practice for Double Skin Façades EIE/04/135/S07.38652 WP 4 Report "Simple calculation method"* (tech. rep.). Fraunhofer-Institute for Building Physics (IB. Stuttgart. chrome-extension://efaidnbmnnnibpcajpcglclefindmkaj/https://www.bestfacade.com/pdf/downloads/Bestfacade_WP4-Report_26_07_07.pdf

Bugenings, L. A., Schaffer, M., Larsen, O. K., & Zhang, C. (2022). A novel solution for school renovations: Combining diffuse ceiling ventilation with double skin facade. *Journal of Building Engineering*, *49*. https://doi.org/10.1016/j.jobe.2022.104026

Catto Lucchino, E., Gelesz, A., Skeie, K., Gennaro, G., Reith, A., Serra, V., & Goia, F. (2021). Modelling double skin façades (DSFs) in whole-building energy simulation tools: Validation and inter-software comparison of a mechanically ventilated single-story DSF. *Building and Environment*, *199*, 107906. https://doi.org/10.1016/j.buildenv.2021.107906

Danish Building Regulations. (2018). BR18. https://www.bygningsreglementet.dk/

DS EN ISO 13790. (2008). *Bygningers energieffektivitet-Beregning af energiforbrug til rumopvarmning og-køling Energy performance of buildings-Calculation of energy use for space heating and cooling* (tech. rep.).

DS/EN 14501. (2021). DS/EN 14501. https://sd.ds.dk/Viewer?ProjectNr=M390799&Status=90.20&Inline=true&Page=1&VariantID=

DS/EN 16798. (2019). DS/EN 16798-1:2019. https://sd.ds.dk/Viewer?ProjectNr=M297459&Status=60.61&Inline=true&Page=1&VariantID=41

DS/EN ISO 13789. (2017). DS/EN ISO 13789. https://sd.ds.dk/Viewer?ProjectNr=M289830&Status=60.60&Inline=true&Page=1&VariantID=41

DS/EN ISO 13790. (2008). DS/EN ISO 13790. https://sd.ds.dk/Viewer?ProjectNr=M204448&Status=99.60&Inline=true&Page=1&VariantID=

European Commission. (2020). EUR-Lex - 52020DC0662 - EN - EUR-Lex. https://eur-lex.europa.eu/legal-content/EN/TXT/?uri=celex%3A52020DC0662&utm_source=chatgpt.com

Gennaro, G., Catto Lucchino, E., Goia, F., & Favoino, F. (2023). Modelling double skin façades (DSFs) in whole-building energy simulation tools: Validation and inter-software comparison of naturally ventilated single-story DSFs. *Building and Environment*, *231*, 110002. https://doi.org/10.1016/j.buildenv.2023.110002

Gratia, E., & De Herde, A. (2004a). Natural cooling strategies efficiency in an office building with a double-skin façade. *Energy and Buildings*, *36*(11), 1139–1152. https://doi.org/10.1016/j.enbuild.2004.05.004

Gratia, E., & De Herde, A. (2004b). Natural ventilation in a double-skin facade. *Energy and Buildings*, *36*(2), 137–146. https://doi.org/10.1016/j.enbuild.2003.10.008

Gratia, E., & De Herde, A. (2007). The most efficient position of shading devices in a double-skin facade. *Energy and Buildings*, *39*(3), 364–373. https://doi.org/10.1016/J.ENBUILD.2006.09.001

Hu, Y., Larsen, O. K., Zhang, C., & Larsen, T. S. (2023). Energyplus model of double skin façade and diffuse ceiling ventilation. *Journal of Physics: Conference Series*, *2600*(6). https://doi.org/10.1088/1742-6596/2600/6/062003

IEA. (2023). Buildings - Energy System - IEA. https://www.iea.org/energy-system/buildings

Jankovic, A., & Goia, F. (2021). Impact of double skin facade constructional features on heat transfer and fluid dynamic behaviour. *Building and Environment*, *196*, 107796. https://doi.org/10.1016/j.buildenv.2021.107796

Jensen, P. A., Maslesa, E., Berg, J. B., & Thuesen, C. (2018). 10 questions concerning sustainable building renovation. *Building and Environment*, *143*(2), 130–137. https://doi.org/https://doi.org/10.1016/j.buildenv.2018.06.051

Kalema, T., Jhannesson, G., Pylsy, P., & Hagengran, P. (2008). Accuracy of energy analysis of buildings: A comparison of a monthly energy balance method and simulation methods in calculating the energy consumption and the effect of thermal mass. *Journal of Building Physics*, *32*(2), 101–130. https://doi.org/10.1177/1744259108093920

Kalyanova, O. (2008). Double-Skin Facade: Modelling and Experimental Investigations of Thermal Performance. https://vbn.aau.dk/en/publications/double-skin-facade-modelling-and-experimental-investigations-of-t/

Kalyanova, O., & Lund, R. (2014a). *Aalborg Universitet Experimental data and boundary conditions for a Double-Skin Facade building in external air curtain mode* (tech. rep.).

Kalyanova, O., & Lund, R. (2014b). *Aalborg Universitet Experimental data and boundary conditions for a Double-Skin Facade building in preheating mode* (tech. rep.).

Karlsen, L., Heiselberg, P., Bryn, I., & Johra, H. (2016). Solar shading control strategy for office buildings in cold climate. *Energy and Buildings*, *118*, 316–328. https://doi.org/10.1016/J.ENBUILD.2016.03.014

Marszal, A. J., Thomas, S. J., Larsen, O. K., & Heiselberg, P. (2009). Empirical Validation of Simple Calculation Method for Assessment of Energy Performance in Double-Skin Façade Building. https://vbn.aau.dk/en/publications/empirical-validation-of-simple-calculation-method-for-assessment-/

Negendahl, K., & Nielsen, T. R. (2015). Building energy optimization in the early design stages: A simplified method. *Energy and Buildings*, *105*(3), 88–99. https://doi.org/10.1016/j.enbuild.2015.06.087

Nielsen, A. N., Jensen, R. L., Larsen, T. S., & Nissen, S. B. (2016). Early stage decision support for sustainable building renovation – A review. *Building and Environment*, *103*(6), 165–181. https://doi.org/10.1016/j.buildenv.2016.04.009

Pelletier, K., Wood, C., Calautit, J., & Wu, Y. (2023). The viability of double-skin façade systems in the 21st century: A systematic review and meta-analysis of the nexus of factors affecting ventilation and thermal performance, and building integration. *Building and Environment*, *228*(2), 109870. https://doi.org/10.1016/j.buildenv.2022.109870

Poirazis, H. (2006). *Double Skin Façades A Literature Review A report of IEA SHC Task 34 ECBCS Annex 43* (tech. rep.). IEA ECBCS Annex 43, Task 34. chrome-extension://efaidnbmnnnibpcajpcglclefindmkaj/https://annex53.iea-ebc.org/Data/publications/EBC_Annex_43_Task34-Double_Skin_Facades_A_Literature_Review.pdf

Preet, S., Mathur, J., & Mathur, S. (2022). Influence of geometric design parameters of double skin façade on its thermal and fluid dynamics behavior: A comprehensive review. *Solar Energy*, *236*, 249–279. https://doi.org/https://doi.org/10.1016/j.solener.2022.02.055

Saelens, D., Carmeliet, J., & Hens, H. (2003). Energy performance assessment of multiple-skin facades. *HVAC and R Research*, *9*(2), 167–185. https://doi.org/10.1080/10789669.2003.10391063

Saelens, D., Roels, S., & Hens, H. (2008). Strategies to improve the energy performance of multiple-skin facades. *Building and Environment*, *43*(4), 638–650. https://doi.org/10.1016/J.BUILDENV.2006.06.024

Schaffer, M., Bugenings, L. A., Larsen, O. K., & Zhang, C. (2023). Exploring the potential of combining diffuse ceiling and double-skin facade for school renovations. *Building and Environment*, *235*. https://doi.org/10.1016/j.buildenv.2023.110199

Thuvander, L., Femenías, P., Mjörnell, K., & Meiling, P. (2012). Unveiling the Process of Sustainable Renovation. *Sustainability 2012, Vol. 4, Pages 1188-1213*, *4*(6), 1188–1213. https://doi.org/10.3390/su4061188

Zhang, C. (2016). (PDF) Diffuse Ceiling Ventilation: design guide. https://doi.org/10.13140/RG.2.2.25455.43684

Zhang, C., Heiselberg, P., & Nielsen, P. V. (2014). Diffuse ceiling ventilation - A review. *International Journal of Ventilation*, *13*(1), 49–63. https://doi.org/10.1080/14733315.2014.11684036

Zhang, C., Larsen, O. K., Hu, Y., Mikkelsen, A. K., Pedersen, L. L., Nyborg, V. Ø., & Larsen, T. S. (2023). Experimental investigation of an integrated renovation solution combining diffuse ceiling ventilation and double skin façade. *Building and Environment*, *246*. https://doi.org/10.1016/j.buildenv.2023.111000

Appendix A

Supplementary experimental validation summary tables

Table A.1: Summary values for measured and calculated variables in pre-heating mode

Variable	Calc. average	Meas. average	Calc. min	Meas. min	Calc. max	Meas. max
Mean cavity temperature [°C]	9.99	9.30	3.28	3.46	26.07	20.32
Outlet cavity temperature [°C]	12.47	12.95	5.78	9.98	41.04	26.66
Heating energy need [kWh]	0.95	1.13	0.00	0.00	1.59	1.69
Cooling energy need [kWh]	0.15	0.08	0.00	0.00	3.93	2.73

Table A.2: Summary values for measured and calculated variables in cooling mode

Variable	Calc. average	Meas. average	Calc. min	Meas. min	Calc. max	Meas. max
Mean cavity temperature [°C]	13.15	14.26	5.37	9.23	21.00	26.73
Outlet cavity temperature [°C]	13.80	15.36	5.82	7.84	22.77	27.69
Heating energy need [kWh]	0.36	0.27	0.00	0.00	0.76	0.76
Cooling energy need [kWh]	0.75	0.40	0.00	0.00	4.94	4.00
Airflow [m^3/h]	1864.51	1328.23	1196.21	299.38	3516.53	3754.19

Appendix B

Calculation equations used in the simplified framework

This appendix summarises the main equations used in the simplified hourly calculation framework. The equations are based on the simple calculation method developed in the BESTFACADE project, which includes calculation principles from EN ISO 13790, EN ISO 13789, DIN V 18599, and the detailed Hellström approach for approximating natural ventilation in double-skin façade cavities. The purpose of this appendix is to provide a compact overview of the calculation basis used for estimating transmission heat transfer, ventilation heat transfer, natural cavity ventilation, solar gains, DSF cavity temperature, and heating and cooling energy needs.

B.1 Transmission heat transfer

The transmission heat transfer coefficient is calculated from the area and thermal transmittance of each relevant envelope element:

$$H_T = \sum_i A_i U_i \tag{B.1}$$

where H_T is the transmission heat transfer coefficient [W/K], A_i is the area of element i [m^2], and U_i is the thermal transmittance of element i [W/(m^{2}K)].

For a given hourly timestep, the corresponding transmission heat transfer is calculated as:

$$Q_{tr} = H_T \left(T_i - T_e\right) t \tag{B.2}$$

where Q_{tr} is the transmission heat transfer [Wh], T_i is the indoor air temperature [°C], T_e is the outdoor air temperature [°C], and t is the timestep duration [h].

B.2 Ventilation heat transfer

The general ventilation heat transfer coefficient is calculated as:

$$H_v = \rho_a c_a q_v \tag{B.3}$$

where H_v is the ventilation heat transfer coefficient [W/K], ρ_a is the air density [kg/m^3], c_a is the specific heat capacity of air [J/(kgK)], and q_v is the ventilation airflow rate [m^3/s].

The ventilation-related heat transfer for one timestep is calculated as:

$$Q_v = H_v \left(T_i - T_e\right) t \tag{B.4}$$

where Q_v is the ventilation-related heat transfer [Wh].

B.3 Natural ventilation in the DSF cavity

In cooling mode, the DSF cavity ventilation is represented using the detailed Hellström approach from the BESTFACADE simple calculation method. In this approach, the cavity is treated as an unheated intermediate zone, and the ventilation heat transfer coefficient between the cavity and the outdoor environment depends on the temperature difference between the mean cavity temperature and the outdoor air temperature. This allows buoyancy-driven heat removal in the naturally ventilated cavity to be represented in simplified form.

The ventilation heat transfer coefficient between the cavity and the outdoor environment is calculated as:

$$H_{V,ue} = h_v \left|T_{c,mean} - T_e\right|^{0.5} \tag{B.5}$$

where $H_{V,ue}$ is the ventilation heat transfer coefficient between the cavity and outdoor air [W/K], h_v is the Hellström ventilation coefficient [W/(K$^{1.5}$)], $T_{c,mean}$ is the mean cavity temperature [°C], and T_e is the outdoor air temperature [°C].

The Hellström ventilation coefficient is calculated as:

$$h_v = \left(\frac{2gH_{cav}}{T_{e,abs}\xi_{tot}} \right)^{0.5} \rho_u c_p \Delta T_{rel} A_{cav} \tag{B.6}$$

where g is the gravitational acceleration [m/s^2], H_{cav} is the cavity height [m], $T_{e,abs}$ is the absolute outdoor air temperature [K], ξ_{tot} is the total pressure-loss coefficient [-], ρ_u is the air density in the cavity [kg/m^3], c_p is the specific heat capacity of air [J/(kgK)], ΔT_{rel} is the relative temperature rise [-], and A_{cav} is the characteristic cavity flow area [m^2].

The relative temperature rise is calculated as:

$$\Delta T_{rel} = \frac{T_{c,out} - T_e}{T_{c,mean} - T_e} \tag{B.7}$$

where $T_{c,out}$ is the cavity outlet temperature [°C].

A key simplification in the Hellström approach is that ventilation heat transfer between the room and the façade cavity is assumed to be zero:

$$H_{V,iu} = 0 \tag{B.8}$$

For the condition $T_{c,mean} - T_e > 0$, the relationship between the cavity excess temperature, transmission heat transfer, solar gains, and natural ventilation can be expressed as:

$$h_v \left(T_{c,mean} - T_e\right)^{1.5} + \left(H_t^{r-c} + H_t^{c-o}\right)\left(T_{c,mean} - T_e\right) - \left[H_t^{r-c}\left(T_i - T_e\right) + \phi_s^c\right] = 0 \tag{B.9}$$

where H_t^{r-c} is the transmission heat transfer coefficient between the room and the cavity [W/K], H_t^{c-o} is the transmission heat transfer coefficient between the cavity and the outdoor environment [W/K], T_i is the indoor air temperature [°C], and ϕ_s^c is the heat flow affecting the DSF cavity [W].

B.4 Infiltration heat transfer

Infiltration describes air leakage through the building envelope. The infiltration airflow rate is estimated from the air permeability at 50 Pa:

$$\dot{V}_{inf} = \frac{q_{50}}{20} A_{env} \tag{B.10}$$

where $\dot{V}_{inf}$ is the infiltration airflow rate [m^3/s], q_{50} is the air permeability at 50 Pa [$m^3/(h\ m^2)$], and A_{env} is the exposed envelope area [m^2].

The corresponding infiltration heat transfer coefficient is calculated as:

$$H_{inf} = \rho_a c_a \dot{V}_{inf} \tag{B.11}$$

where H_{inf} is the infiltration heat transfer coefficient [W/K].

B.5 Heat recovery in mechanical ventilation

For the traditional renovation scenario, heat recovery is included in the balanced mechanical ventilation system. The effective ventilation heat transfer coefficient after heat recovery is calculated as:

$$H_{v,eff} = \rho_a c_a q_v \left(1 - \eta_{hr}\right) \tag{B.12}$$

where $H_{v,eff}$ is the effective ventilation heat transfer coefficient after heat recovery [W/K], q_v is the ventilation airflow rate [m^3/s], and η_{hr} is the heat recovery efficiency [-].

B.6 Total heat losses

The total heat losses are calculated as the sum of transmission and ventilation-related losses:

$$Q_{ls} = Q_{tr} + Q_v \tag{B.13}$$

where Q_{ls} is the total heat losses [W or Wh], Q_{tr} is the transmission losses [W or Wh], and Q_v is the ventilation-related losses [W or Wh].

B.7 Solar radiation entering the DSF cavity

The total solar radiation entering the DSF through the external glazing is calculated as:

$$\phi_s^{total} = F_{F,ue} A_{ue} g_{eff,ue} I_s \tag{B.14}$$

where ϕ_s^{total} is the total solar radiation entering the DSF [W], $F_{F,ue}$ is the frame correction factor for the external glazing [-], A_{ue} is the external glazed area [m^2], $g_{eff,ue}$ is the effective solar transmittance of the external transparent component [-], and I_s is the solar radiation [W/m^2].

B.8 Direct solar gains to the room

The direct solar heat gains transmitted through the DSF into the room are calculated as:

$$\phi_s^{room} = F_{F,iu} A_{iu} g_{eff,iu} F_{F,ue} \tau_{e,ue} I_s t \tag{B.15}$$

where ϕ_s^{room} is the direct solar heat gain to the room [Wh], $F_{F,iu}$ is the frame correction factor for the internal glazing [-], A_{iu} is the area of the internal transparent component separating the room from the DSF cavity [m^2], $g_{eff,iu}$ is the effective solar transmittance of the internal transparent component [-], $F_{F,ue}$ is the frame correction factor for the external glazing [-], $\tau_{e,ue}$ is the solar transmittance of external glazing [-], I_s is the solar radiation [W/m^2], and t is the timestep duration [h].

When solar shading is active, the direct solar heat gain is reduced using the shading coefficient:

$$\phi_{s,sh}^{room} = F_{F,iu} A_{iu} g_{eff,iu} F_{F,ue} \tau_{e,ue} I_s t SC \tag{B.16}$$

where SC is the shading coefficient [-].

B.9 Heat gains affecting the DSF cavity

The heat flow affecting the cavity is calculated as the solar radiation entering the DSF minus the part transmitted directly to the room, together with any internal gains assigned to the cavity:

$$\phi_s^c = \sum \phi_s^{total} - \frac{\sum \phi_s^{room}}{t} + \sum \phi_h^c \tag{B.17}$$

where ϕ_s^c is the heat flow affecting the cavity [W], ϕ_s^{total} is the total solar radiation entering the DSF [W], ϕ_s^{room} is the direct solar heat gain to the room [Wh], t is the timestep duration [h], and ϕ_h^c represents internal gains assigned to the cavity [W].

B.10 Mean DSF cavity temperature

The mean temperature in the DSF cavity is calculated by representing the cavity as an intermediate unheated zone between the room and the outdoor environment:

$$T_{c,mean} = \frac{\phi_s^c + T_i \left(H_t^{r-c} + H_v^{r-c} + H_i^{r-c}\right) + T_e \left(H_t^{c-o} + H_v^{c-o} + H_i^{c-o}\right)}{H_t^{r-c} + H_v^{r-c} + H_i^{r-c} + H_t^{c-o} + H_v^{c-o} + H_i^{c-o}} \tag{B.18}$$

where $T_{c,mean}$ is the mean cavity temperature [°C], ϕ_s^c is the heat flow affecting the cavity [W], T_i is the indoor air temperature [°C], T_e is the outdoor air temperature [°C], H_t^{r-c} is the transmission heat transfer coefficient between room and cavity [W/K], H_v^{r-c} is the ventilation heat transfer coefficient between room and cavity [W/K], H_i^{r-c} is the additional heat transfer coefficient between room and cavity [W/K], H_t^{c-o} is the transmission heat transfer coefficient between cavity and outdoor environment [W/K], H_v^{c-o} is the ventilation heat transfer coefficient between cavity and outdoor environment [W/K], and H_i^{c-o} is the additional heat transfer coefficient between cavity and outdoor environment [W/K].

B.11 Outlet temperature from the DSF cavity

The outlet temperature from the DSF cavity is calculated from the mean cavity temperature and inlet temperature:

$$T_{c,out} = 2T_{c,mean} - T_{c,in} \tag{B.19}$$

where $T_{c,out}$ is the cavity outlet temperature [°C], $T_{c,mean}$ is the mean cavity temperature [°C], and $T_{c,in}$ is the cavity inlet temperature [°C].

In cooling mode, where the inlet air is assumed to be outdoor air, this can also be written as:

$$T_{c,out} = T_e + 2\left(T_{c,mean} - T_e\right) \tag{B.20}$$

B.12 Total heat gains

The total heat gains are calculated as the sum of internal and solar heat gains:

$$Q_{gn} = Q_{int} + Q_{sol} \tag{B.21}$$

where Q_{gn} is the total heat gains [W or Wh], Q_{int} is the internal gains [W or Wh], and Q_{sol} is the solar gains [W or Wh].

B.13 Heating energy need

The heating energy need is calculated using the EN ISO 13790 utilisation factor approach:

$$Q_{h,nd} = Q_{h,ls} - \eta_{h,gn} Q_{h,gn} \tag{B.22}$$

where $Q_{h,nd}$ is the heating energy need [kWh], $Q_{h,ls}$ is the total heat losses for heating [kWh], $Q_{h,gn}$ is the total heat gains for heating [kWh], and $\eta_{h,gn}$ is the gain utilisation factor for heating [-].

The gain-to-loss ratio for heating is calculated as:

$$\gamma_h = \frac{Q_{h,gn}}{Q_{h,ls}} \tag{B.23}$$

For $\gamma_h \neq 1$, the heating gain utilisation factor is calculated as:

$$\eta_{h,gn} = \frac{1 - \gamma_h^{a_h}}{1 - \gamma_h^{a_h+1}} \tag{B.24}$$

For $\gamma_h = 1$, the heating gain utilisation factor is calculated as:

$$\eta_{h,gn} = \frac{a_h}{a_h + 1} \tag{B.25}$$

The numerical parameter a_h is calculated as:

$$a_h = a_{0,h} + \frac{\tau}{\tau_{0,h}} \tag{B.26}$$

where $a_{0,h}$ is the reference numerical parameter [-], τ is the building or zone time constant [h], and $\tau_{0,h}$ is the reference time constant [h].

B.14 Cooling energy need

The cooling energy need is calculated using the EN ISO 13790 utilisation factor approach:

$$Q_{c,nd} = Q_{c,gn} - \eta_{c,ls} Q_{c,ls} \tag{B.27}$$

where $Q_{c,nd}$ is the cooling energy need [kWh], $Q_{c,gn}$ is the total heat gains for cooling [kWh], $Q_{c,ls}$ is the total heat losses for cooling [kWh], and $\eta_{c,ls}$ is the loss utilisation factor for cooling [-].

The gain-to-loss ratio for cooling is calculated as:

$$\lambda_c = \frac{Q_{c,gn}}{Q_{c,ls}} \tag{B.28}$$

For $\lambda_c \neq 1$ and $\lambda_c > 0$, the cooling loss utilisation factor is calculated as:

$$\eta_{c,ls} = \frac{1 - \lambda_c^{-a_c}}{1 - \lambda_c^{-(a_c+1)}} \tag{B.29}$$

For $\lambda_c = 1$, the cooling loss utilisation factor is calculated as:

$$\eta_{c,ls} = \frac{a_c}{a_c + 1} \tag{B.30}$$

For $\lambda_c < 0$, the cooling loss utilisation factor is set to:

$$\eta_{c,ls} = 1 \tag{B.31}$$

The numerical parameter a_c is calculated as:

$$a_c = a_{0,c} + \frac{\tau}{\tau_{0,c}} \tag{B.32}$$

where $a_{0,c}$ is the reference numerical parameter [-], τ is the building or zone time constant [h], and $\tau_{0,c}$ is the reference time constant [h].

B.15 Building time constant

The time constant of the building or building zone is calculated as:

$$\tau = \frac{C_m}{3.6 H_m} \tag{B.33}$$

where τ is the time constant [h], C_m is the effective internal heat capacity [J/K], and H_m is the total heat loss coefficient [W/K].

The effective internal heat capacity is calculated as:

$$C_m = \sum_j \sum_i \rho_{ij} c_{ij} d_{ij} A_j \tag{B.34}$$

where C_m is the effective internal heat capacity [J/K], ρ_{ij} is the density of material layer i in element j [kg/m^3], c_{ij} is the specific heat capacity of material layer i in element j [J/(kgK)], d_{ij} is the effective thickness of material layer i in element j [m], and A_j is the area of element j [m^2].

B.16 Annual energy indicators

Hourly heating and cooling energy needs are summed over the year to obtain the annual energy need:

$$Q_{h,annual} = \sum_{t=1}^{8760} Q_{h,nd,t} \tag{B.35}$$

$$Q_{c,annual} = \sum_{t=1}^{8760} Q_{c,nd,t} \tag{B.36}$$

The total annual energy need is calculated as:

$$Q_{tot,annual} = Q_{h,annual} + Q_{c,annual} \tag{B.37}$$

The area-normalised annual energy need is calculated as:

$$E_{annual} = \frac{Q_{tot,annual}}{A_{floor}} \tag{B.38}$$

where E_{annual} is the area-normalised annual energy need [kWh/m^2], $Q_{tot,annual}$ is the total annual energy need [kWh], and A_{floor} is the floor area [m^2].

The energy difference between scenarios is calculated as:

$$\Delta E = E_{scen} - E_{ref} \tag{B.39}$$

where ΔE is the energy difference between scenarios [kWh/m^2], E_{scen} is the total annual energy demand of the evaluated scenario [kWh/m^2], and E_{ref} is the total annual energy demand of the reference scenario [kWh/m^2].

The relative difference between two scenarios is calculated as:

$$\Delta E_{rel} = \frac{E_{scen} - E_{ref}}{E_{ref}} \cdot 100 \tag{B.40}$$

where ΔE_{rel} is the relative difference between scenarios [%].

Appendix C

Detail input parameters for all scenarios

This appendix provides a detailed overview of the input parameters used to define the three analyzed scenarios: the baseline , the traditional renovation, and the I-DIFFER concept. These parameters include climatic data like hourly outdoor temperature and solar radiation, geometric characteristics of the modeled space, façade properties such as thermal transmittance, glazing characteristics, and ventilation parameters including airflow rates and heat recovery efficiency, and internal heat gains.

Internal Temp T_i	20
T_{soil}	10

Room Specification		
D	6,25	m
W	8	m
H	2,7	m
A_{room}	50,000	m^2
V_{room}	135,000	m^3

Internal Loads 1h period		
Lights	0	W
Equipment	0	W
People	pcs	W
Adults	1	2500
Children	0	0
η	0	%
$q_{air\ flow\ rate}$	900	m3/h
q_{inf}	0,18	m^3/hm^2

Room Schedule			
1	☐	13	☑
2	☐	14	☑
3	☐	15	☑
4	☐	16	☑
5	☐	17	☐
6	☐	18	☐
7	☐	19	☐
8	☐	20	☐
9	☑	21	☐
10	☑	22	☐
11	☑	23	☐
12	☑	24	☐

heat loss coefficient calculation				
	A [m^2]	U [W/m^2K]	Ht[W/K]	ΣH_{lh} [W/K]
Facade infill-south	6,05	0,5	3,025	**82,472**
Facade column-south	3,7	0,92	3,404	
Window glazing	10,2	2,7	27,54	
Window frame	2,37	1,9	4,503	
Roof	50	0,45	22,5	
Floor	50	0,43	21,5	

internal heat capacity calculation					
	d [m]	ρ [kg/m^3]	c [kJ/kgK]	A [m^2]	ΣCm [kJ/K]
South wall column	0,1	600	1	6,05	**27342,02**
South wall	0,1	1800	0,84	3,7	
East wall	0,1	850	1,09	17,44	
West wall	0,1	850	1,09	17,44	
North wall	0,1	850	1,09	22,32	
Roof	0,1	2400	0,88	50	
Floor	0,1	2400	0,88	50	

		Wall 1		Wall 2	Wall 3	Wall 4	Ceiling	Floor
Envelope Characteristics	Wall Orientation	South		East	West	North	-	-
	A_{wall} [m^2]	6,570	4,028	16,200	16,200	21,600	50,000	50,000
	U-value $_{wall}$ [W/m^2K]	0,5	0,920	0	0	0	0,45	0,43
	A_{window} [m^2]	12,54	0,000	0	0	0	0	-
	U-value $_{window}$ [W/m^2K]	2,7	0,000	0	0	0	0	-
	F_F	0,70	0,000	0,00	0,00	0,00	0,00	-
	Heated / Unheated	Unheated		Heated	Heated	Heated	Unheated	Soil
	g_{eff}	**0,800**	-	**0,479**	**0,479**	**0,479**	**0,479**	-
	g	0,8	-	0,63	0,63	0,63	0,63	-
	f_g	1	-	0,8	0,8	0,8	0,8	-
	$f_{shading}$	1	-	1	1	1	1	-
	f_{shadow}	1	-	1	1	1	1	-
	f_{dirt}	1	-	0,95	0,95	0,95	0,95	-
	$\tau_{e,int}$	0,8	-	0,84	0,84	0,84	0,84	-
	t [h]	1	-	1	1	1	1	-

Figure C.1: Baseline inputs

Room Specification		
D	6,25	m
W	8	m
H	2,7	m
A_{room}	50,000	m^2
V_{room}	135,000	m^3

Internal Loads 1h period		
Lights	0	W
Equipment	0	W
People	pcs	W
Adults	1	2500
Children	0	0
η	0,73	%
$q_{air\ flow\ rate}$	900	m^3/h
q_{inf}	0,18	m^3/hm^2

Room Schedule			
1	☐	13	☑
2	☐	14	☑
3	☐	15	☑
4	☐	16	☑
5	☐	17	☐
6	☐	18	☐
7	☐	19	☐
8	☐	20	☐
9	☑	21	☐
10	☑	22	☐
11	☑	23	☐
12	☑	24	☐

heat loss coefficient calculation				
	A [m^2]	U [W/m^2K]	Ht[W/K]	ΣH_{lh} [W/K]
Facade infill-south	6,05	0,5	3,025	**82,472**
Facade column-south	3,7	0,92	3,404	
Window glazing	10,2	2,7	27,54	
Window frame	2,37	1,9	4,503	
Roof	50	0,45	22,5	
Floor	50	0,43	21,5	

internal heat capacity calculation					
	d [m]	ρ [kg/m^3]	c [kJ/kgK]	A [m^2]	ΣCm [kJ/K]
South wall column	0,1	600	1	6,05	**27342,02**
South wall	0,1	1800	0,84	3,7	
East wall	0,1	850	1,09	17,44	
West wall	0,1	850	1,09	17,44	
North wall	0,1	850	1,09	22,32	
Roof	0,1	2400	0,88	50	
Floor	0,1	2400	0,88	50	

Envelope Characteristics		Wall 1		Wall 2	Wall 3	Wall 4	Ceiling	Floor
	Wall Orientation	South		East	West	North	-	-
	A_{wall} [m^2]	6,570	4,028	16,200	16,200	21,600	50,000	50,000
	U-value $_{wall}$ [W/m^2K]	0,18	0,180	0	0	0	0,12	0,43
	A_{window} [m^2]	12,54	0,000	0	0	0	0	-
	U-value $_{window}$ [W/m^2K]	1,1	0,000	0	0	0	0	-
	F_F	0,70	0,000	0,00	0,00	0,00	0,00	-
	Heated / Unheated	Unheated		Heated	Heated	Heated	Unheated	Soil
	g_{gl}	**0,710**	-	**0,479**	**0,479**	**0,479**	**0,479**	-
	g	0,71	-	0,63	0,63	0,63	0,63	-
	f_{fr}	1	-	0,8	0,8	0,8	0,8	-
	$f_{shading}$	1	-	1	1	1	1	-
	f_{shadow}	1	-	1	1	1	1	-
	f_{curt}	1	-	0,95	0,95	0,95	0,95	-
	$\tau_{e,wk}$	0,.83	-	0,84	0,84	0,84	0,84	-
	t[h]	1	-	1	1	1	1	-

SHADING	150	**W/M2**	**(K39)**

Figure C.2: Traditional inputs

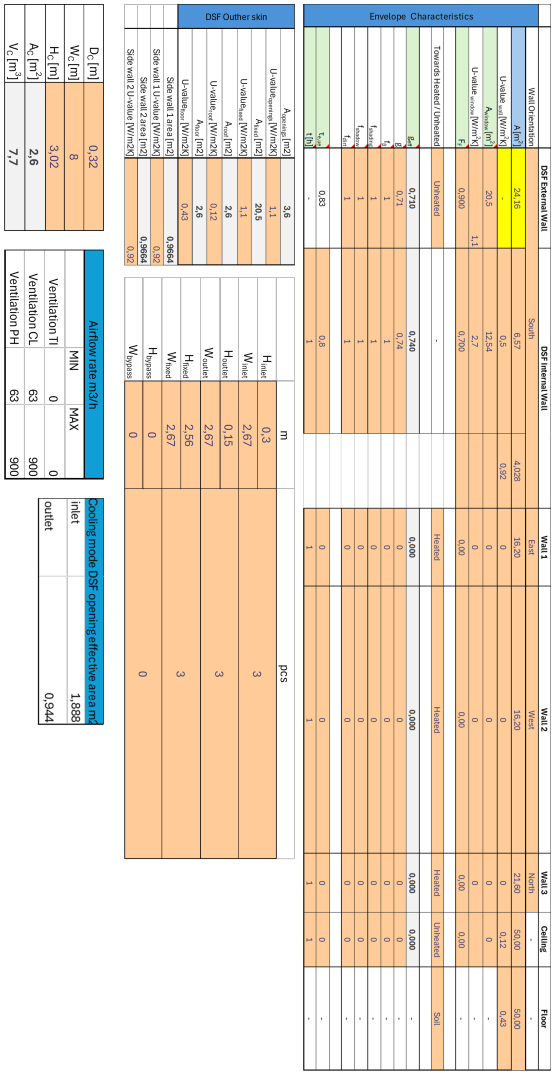

Figure C.3: I-DIFFER inputs

internal heat capacity calculation

	d [m]	ρ [kg/m^3]	c [kJ/kgK]	A [m^2]
Facade infill-south	0,1	600	1	6,05
Facade column-south	0,1	1800	0,84	3,7
East wall	0,1	850	1,09	17,44
West wall	0,1	850	1,09	17,44
North wall	0,1	850	1,09	22,32
Roof	0,1	2400	0,88	50
Floor	0,1	2400	0,88	50

ΣCm [kJ/K]
27342,02

heat loss coefficient calculation

	A [m^2]	U [W/m^{2}K]	Ht[W/K]	ΣH_{in} [W/K]
Facade infill-south	6,05	0,5	3,025	**82,472**
Facade column-south	3,7	0,92	3,404	
Window glazing	10,2	2,7	27,54	
Window frame	2,37	1,9	4,503	
Roof	50	0,45	22,5	
Floor	50	0,43	21,5	

room's time constant	τ [h]
	92,1

	SHADING CONTROL	
	MODE	VALUE
M40	TRANSPARENT	9999 W/m2
M41	COOLING	150 W/m2

	SHADING CONTROL	
	MODE	VALUE
M40	TRANSPARENT	9999 W/m2
M41	COOLING	150 W/m2

Figure C.4: I-DIFFER inputs


STUDENT REPORT
AALBORG UNIVERSITY